# Analysis of Asphalt Mixtures Using Alternative Aggregate in SMA and Superpave

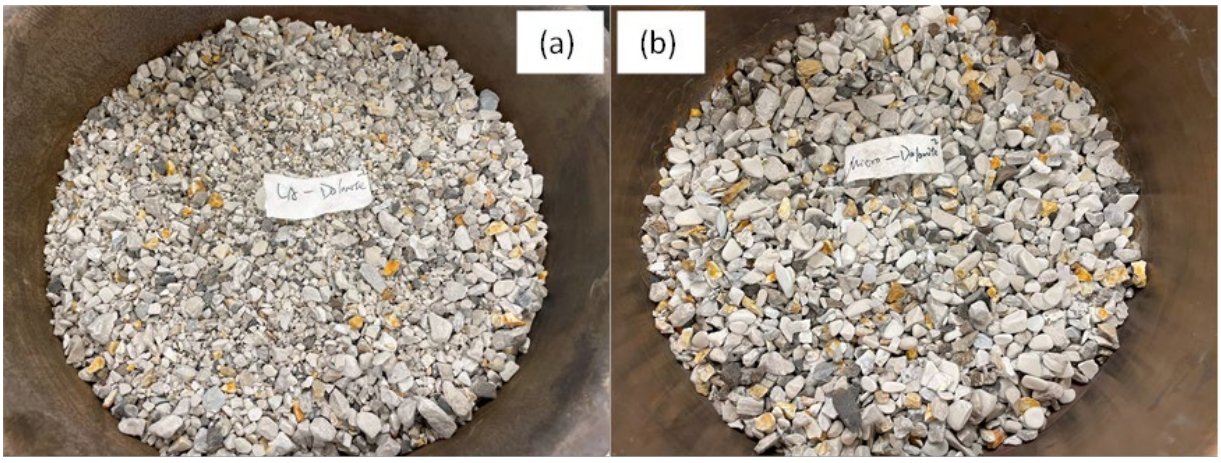


August 2024
Final Report

Project number TR202205
MoDOT Research Report number cmr 24-014

**PREPARED BY:**

Jenny Liu

Emad Kassem

Yizhuang David Wang

Bo Lin

Missouri University of Science and Technology

**PREPARED FOR:**

Missouri Department of Transportation

Construction and Materials Division, Research Section

# Technical Report Documentation Page

| | | |
|---|---|---|
| **1. Report No.**<br>CMR 24-014 | **2. Government Accession No.** | **3. Recipient's Catalog No.** |
| **4. Title and Subtitle**<br>Analysis of Asphalt Mixtures Using Alternative Aggregate in SMA and Superpave | | **5. Report Date**<br>May 2024<br>Published: August 2024<br>**6. Performing Organization Code** |
| **7. Author(s)**<br>Jenny Liu<br>Emad Kassem<br>Yizhuang David Wang<br>Bo Lin | | **8. Performing Organization Report No.** |
| **9. Performing Organization Name and Address**<br>Department of Civil, Architectural and Environmental Engineering<br>Missouri University of Science and Technology<br>1401 N. Pine St.<br>Rolla, MO 65409 | | **10. Work Unit No. (TRAIS)**<br>**11. Contract or Grant No.**<br>MoDOT project # TR202205 |
| **12. Sponsoring Agency Name and Address**<br>Missouri Department of Transportation (SPR-B)<br>Construction and Materials Division<br>P.O. Box 270<br>Jefferson City, MO 65102 | | **13. Type of Report and Period Covered**<br>Final Report (May 2022-August 2024)<br>**14. Sponsoring Agency Code** |

**15. Supplementary Notes**
Conducted in cooperation with the U.S. Department of Transportation, Federal Highway Administration. MoDOT research reports are available in the Innovation Library at https://www.modot.org/research-publications.


**16. Abstract**
To identify locally available, cost-effective, and durable crushed coarse aggregates for Stone Matrix Asphalt (SMA) and high-level Hot Mix Asphalt (HMA) mixes, multiple well-distributed aggregates have been evaluated in this study as candidate aggregates, including traprock (control), chat, gravels, steel slag, limestone, and dolomite. Aggregate screening and durability evaluations were conducted to eliminate unqualified candidates. Subsequently, SMA and HMA mixtures were designed with qualified candidate aggregates following AASHTO R 46 and R 35, respectively. Performance verification included Hamburg Wheel Tracker rutting test (HWTT) and IDEAL-CT cracking test to finalize the mix designs, and balanced mix design methods (BMD) were used to complete the designs if the volumetric optimum designs failed to meet the performance requirements. The testing results showed that while the SMA and HMA mixes with traprock and gravel could satisfy both volumetric and performance thresholds. SMA and HMA mixes with blended aggregates (i.e., limestone and chat, and dolomite and chat) passed volumetric limits as well. For SMA and HMA mixtures with steel slag, the binder contents from the volumetric designs had to be increased to meet the cracking resistance requirements. Additional performance tests including fatigue and rutting on the Asphalt Mixture Performance Tester (AMPT), low-temperature Indirect Tensile (IDT) tests, and the Accelerated Friction Tests (AFT) were conducted to fully evaluate the mixtures' performance and durability. Analyses on both the material and pavement structural levels were performed, and cost-effective analysis for projects with mixtures using different aggregates were also used in this study. The results indicated that mixes with alternative aggregates performed comparably to those with control aggregates.


| | |
|---|---|
| **17. Key Words**<br>Stone matrix asphalt; Alternative local aggregate; Cracking; Balanced mix design; Fatigue cracking; Rutting; Accelerating friction testing; Structural performance simulation; Cost-effective analysis | **18. Distribution Statement**<br>No restrictions. This document is available through the National Technical Information Service, Springfield, VA 22161. |

| | | | |
|---|---|---|---|
| **19. Security Classification (of this report)**<br>Unclassified | **20. Security Classification (of this page)**<br>Unclassified | **21. No. of Pages**<br>163 | **22. Price** |

Form DOT F 1700.7 (8-72) Reproduction of completed page authorized

# Analysis of Asphalt Mixtures Using Alternative Aggregate in SMA and Superpave

*By*
Jenny Liu, Ph.D., P.E.,
Emad Kassem, Ph.D., P.E.,
Yizhuang David Wang, Ph.D.,
Bo Lin

Department of Civil, Architectural and Environmental Engineering
Missouri University of Science and Technology

Prepared for
Missouri Department of Transportation

May 31, 2024

**Final Report**

# Copyright

Authors herein are responsible for the authenticity of their materials and for obtaining written permissions from publishers or individuals who own the copyright to any previously published or copyrighted material used herein.

# Disclaimer

The content of this report reflects the views of the authors, who are responsible for the facts and the accuracy of the data presented herein. The contents do not necessarily reflect the official view or policies of the Missouri Department of Transportation (MoDOT). This report does not constitute a standard, specification, or regulation.

# Acknowledgments

The authors are thankful for MoDOT's sponsorship of this research project. They wish to express their appreciation to all project advisory committee members. They would also like to thank all the quarries and asphalt plants who provided the test aggregates and other materials. Acknowledgement is also extended to Seyed Alireza Ghanoon, Ping Jiang, and Chuanjun Liu, who contributed to the laboratory testing in this study.

# TABLE OF CONTENTS

# LIST OF FIGURES

# LIST OF TABLES

# LIST OF EQUATIONS

# LIST OF ABBREVIATIONS AND ACRONYMS

AFT ..... Accelerated Friction Testing

AMPT ..... Asphalt Mixture Performance Tester

Blend H1 ..... Blended Limestone & Chat in HMA

Blend H2 ..... Blended Dolomite & Chat in HMA

Blend S1 ..... Blended Limestone & Chat in SMA

Blend S2 ..... Blended Dolomite & Chat in SMA

BMD ..... Balanced Mix Design

DOT ..... Department of Transportation

FPBF ..... Four-Point Beam Fatigue

HD ..... HMA with Dolomite

HDC ..... HMA with Dolomite & Chat

HG ..... HMA with Gravel

HL ..... HMA with Limestone

HLC ..... HMA with Limestone & Chat

HMA ..... Hot Mix Asphalt

HS ..... HMA with Steel Slag

HWTT ..... Hamburg Wheel Tracker Tests

IDEAL-CT ..... Ideal Cracking Test

IDT ..... Indirect Tensile

IFI ..... International Friction Index

LCCA ..... Life Cycle Cost Analysis

M.i.S.T ..... Moisture Induced Stress Tester

MTD ..... Mean Texture Depth

NMAS ..... Nominal Maximum Aggregate Size

NPV ..... Net Present Value

RAP ..... Reclaimed Asphalt Pavement

RCA ..... Recycled Concrete Aggregates

RRI ..... Rutting Resistance Index

RSI ..... Rutting Strain Index

RV ..... Rotational Viscometer

SD ..... SMA with Dolomite

SDC ..... SMA with Dolomite & Chat

SG ..... SMA with Gravel

SGC ..... Superpave Gyratory Compactor

SHAs ..... State Highway Agencies

SL ..... SMA with Limestone

SLC ..... SMA with Limestone & Chat

SMA ..... Stone Matrix Asphalt

SS ..... SMA with Steel Slag

SSR ..... Stress Sweep Rutting

ST ..... SMA with Traprock

TEMPS ..... Temperature Estimate Model for Pavement Structures

TSR ..... Tensile Strength Ratio

*VCA* ..... Voids in the Coarse Aggregate

$VCA_{DRC}$ ..... *VCA* in Dry-Rodded Condition

$VCA_{mix}$ ..... VCA of Compacted Mixture

*VFA* ..... Voids Filled with Asphalt

*VMA* ..... Voids in Mineral Aggregates

VECD ..... Viscoelastic Continuum Damage

JMFs ..... Job Mix Formulas

LTPP ..... Long-Term Pavement Performance

FHWA ..... Federal Highway Administration

AADT ..... Average Annual Daily Traffic

$G_{ca}$ ..... Bulk Specific Gravity of Coarse Aggregate

$G_{sb}$ ..... Bulk specific gravity of the total aggregate

$P_s$ ..... Percent of aggregate in the mixture by mass

$P_b$ ..... Percent of asphalt binder in the mixture by mass

$G_{mb}$ ..... Bulk specific gravity of the compacted mixture

*PCA* ..... Percent of coarse aggregate in the total mixture

$G_{mm}$ ..... Theoretical maximum density of the mixture

$G_{se}$ ..... Effective specific gravity of the combined aggregate

$P_{0.075}$ ..... Percent of aggregate passing the 0.075 $\mu m$

$P_{ba}$ ..... Percent of absorber binder

$P_{be}$ ..... Effective binder content

PFC ..... Porous Friction Course

# EXECUTIVE SUMMARY

Currently, most state highway agencies (SHAs), including Missouri Department of Transportation (MoDOT), require specific aggregates for Stone Matrix Asphalt (SMA) and high-level Hot Mix Asphalt (HMA) mixtures. For example, traprock, which can only be acquired from southeast Missouri, has been specified by MoDOT to be the major coarse aggregate for SMA to ensure a solid skeleton structure. Meanwhile, to reduce the cost and maintain mixtures' durability, SHAs have been trying to identify locally available, cost-effective, and durable alternative coarse aggregates for SMA and high-level HMA mixes. In this study, a systematic analysis was conducted to identify alterative coarse aggregates that are locally available and durable for SMA and high-level Superpave HMA in MoDOT.

Multiple well-distributed aggregate types were evaluated in this study as alternative coarse aggregate candidates, including traprock (control), chat, gravels, steel slag, limestone, and dolomite. A series of screening tests were conducted, including deleterious materials, Los Angeles (LA) abrasion, aggregate angularity, flat and elongated particles of aggregates, absorption, and sand equivalent. Additionally, the Micro-Deval abrasion test, post-compaction degradation assessment, and soundness tests were also undertaken to assess candidate resistance to polishing, degradation, and freeze-thaw damage, respectively. After the screening tests, SMA and HMA mixtures with qualified candidate aggregates were designed in accordance with the AASHTO R 46 and R 35, respectively. Following the volumetric design, performance tests, including the Hamburg Wheel Tracker rutting test (HWTT) and IDEAL-CT cracking tests, were conducted for performance verification. The design was finalized if it passed the performance requirements. Otherwise, the Balance Mix Design (BMD) method was applied to identify the performance optimum binder content that would enable the mixture to meet the performance requirements.

After the mix design was completed, to fully evaluate the mix performance with different aggregates, a series of performance tests were performed for all mixtures. Performance analysis on both the material and the structural levels was completed. On the material level, the fatigue index $S_{app}$ from the Asphalt Mixture Performance Tester (AMPT) tests and $CT_{Index}$ from IDEAL-CT tests were calculated to evaluate the intermediate-temperature cracking resistance. The cracking temperatures were also predicted from the results including creep compliance and tensile strength obtained from IDT tests at low temperatures. The Rutting Strain Index (RSI) values from the AMPT Stress Sweep Rutting (SSR) test and the Rutting Resistance Index (RRI) from the HWTT tests were calculated to evaluate the rutting resistance. The Tensile Strength Ratio (TSR) results after the Moisture Induced Stress Tester (M.i.S.T) conditioning were computed to compare the moisture susceptibility and the resistance to stripping of mixes with different aggregates. In addition, the International Friction Index (IFI) was calculated as a function of the measured coefficient of friction from Accelerated Friction Testing (AFT) to compare the skid resistance of mixtures with candidate aggregates. On the structural level, the %Damage and rut depth were predicted using the FlexPAVE™ program considering realistic data of climate, traffic volume, and typical pavement structure in Missouri. For the low-temperature cracking analysis, the temperature in pavement was predicted by

Temperature Estimate Model for Pavement Structures (TEMPS) software using Missouri climate data and pavement structures. The occurrence of low-temperature cracking in the pavement was predicted by comparing the critical cracking temperatures of mixtures and the pavement temperature profile. The Life Cycle Cost Analysis (LCCA) was also conducted to evaluate the cost effectiveness of the use of alternative aggregates in SMA and higher level Superpave mixtures.

This study found that gravel can be utilized as an alternative aggregate in both SMA and HMA, passing the aggregate durability and mixture performance criteria. Despite many trials, it's very difficult for both SMA and HMA mixtures with limestone or dolomite alone as the coarse aggregate to meet the Voids in Mineral Aggregates (VMA) requirement. To resolve this issue, new combinations by blending them with chat were created, which exhibited relatively fine gradation and excellent durability in the screening tests. The mixtures with chat & dolomite and chat & limestone achieved acceptable volumetric properties, satisfied moistures susceptibility and draindown percentage,and promising cracking and rutting resistance. While designing both SMA and HMA with steel slag, the mixtures passed volumetric and moisture susceptibility tests. However, they failed to meet the IDEAL-CT cracking threshold, triggering an adjustment in binder contents. With the adjusted performance optimum binder contents, the SMA and HMA mixtures with steel slag successfully met all requirements for volumetric properties, moisture susceptibility, draindown percentage, workability, and resistances to cracking and rutting. The test results highlighted the significance of incorporating performance tests in the mix design process.

Based on the BMD performance verification test results, in SMA mixtures, the control mixture, SMA with traprock, or ST, demonstrated the highest $CT_{Index}$, indicating superior resistance to intermediate-temperature cracking. The other SMA mixtures with candidate aggregates achieved results slightly below ST but still passed the threshold required in Missouri specifications. Among HMA mixtures, the HMA with steel slag, or HS, with adjusted binder content exhibited the highest $CT_{Index}$, while the remaining HMA mixtures with candidate aggregates showed results akin to the control mixture, HMA with limestone & chat, or HLC. Additionally, SMA with gravel, or SG, exhibited the highest RRI among SMA mixtures, indicating superior resistance to rutting.

Creep compliance *D(t)* results from IDT tests revealed that SLC exhibited the lowest creep compliance among SMA mixtures, while HLC showed the lowest among HMA mixtures. This indicated that SMA mixtures containing limestone with chat are comparatively stiffer than SMA mixtures with other candidate aggregates. Notably, SS (SMA with steel slag), SG, and SDC (SMA with dolomite and chat) in SMA mixtures, and HS (HMA with steel slag), HG (HMA with gravel), and HDC (HMA with dolomite and chat) in HMA mixtures, demonstrated comparable critical temperatures to their corresponding control mixtures.

Regarding moisture susceptibility, no significant disparity was noted in TSR value among various mixtures from AASHTO T 283 and M.i.S.T without adhesion cycle tests. Utilizing M.i.S.T without adhesion cycle test was recommended, due to its time efficiency, simplicity, and ability to

simulate dynamic vehicle loads. However, for areas with extremely heavy traffic in wet conditions, utilizing M.i.S.T test with adhesion cycles was suggested.

All candidate aggregates exhibited comparable dynamic modulus to the control in both SMA and HMA mixtures, suggesting a similar response under small loading amplitudes. SMA mixtures with candidate aggregates showed slightly lower $S_{app}$ values than ST, indicating comparable fatigue performance. All HMA mixtures with candidate aggregates demonstrated higher $S_{app}$ values than the control mixture HLC, implying enhanced resistance to fatigue cracking. Moreover, all mixtures with candidate aggregates in both SMA and HMA demonstrated similar rutting resistance to their respective control mixtures based on the result of RSI.

The friction evaluation results showed that SS had the highest friction followed by ST. SG, SLC and SDC had relatively comparable friction values but less than the control mixture ST; however, such difference is low at the terminal friction. The two HMA mixtures had lower friction compared to SMA mixtures and HLC had slightly higher friction compared to HG.

In terms of fatigue index and pavement structural simulation results, among SMA mixtures, the control mixture ST demonstrated the lowest fatigue damage value, at 15.6% after 20 years, indicating superior resistance to fatigue damage. For SMA mixtures with alternative aggregates, fatigue damage values range from 18.2% for SS to 22.1% for SG. All HMA mixtures with candidate aggregates exhibited predicted fatigue damage values similar to that of the control mixture SLC. Specifically, values ranged from 15.2% for HS to 16.9% for HG. Notably, the cracking temperatures of all candidate aggregates in SMA mixtures fell below the lowest predicted pavement temperature of the past 20 years, suggesting robust resistance to thermal cracking. Similarly, in HMA mixtures, mixtures HS and HG exhibited cracking temperatures slightly below the lowest recorded pavement temperature, indicating satisfactory resistance to thermal cracking. Additionally, HLC and HDC demonstrated relatively good resistance to thermal cracking during the coldest winter period.

The life cycle cost was estimated by factoring in both initial expenses and discounted future costs, including those for initial construction, future routine maintenance, and rehabilitation. The pavement fatigue index, %Damage, was utilized to predict the frequency of routine maintenance over the service life. Consequently, upon comparing the initial construction cost and net present value (NPV), integrating candidate aggregates as alternatives in SMA and high-quality HMA were considered more cost-effective, while offering comparable performance.

# CHAPTER 1 INTRODUCTION

## 1.1 Problem Statement

Innovative mix designs such as Stone Matrix Asphalt (SMA) and Superpave have been added in the Missouri Department of Transportation (MoDOT)'s hot mix asphalt (HMA) paving projects. SMA is a bituminous mixture with gap-graded aggregate and high asphalt binder content, relying on stone-to-stone contact of aggregates for improved structural capacity and stability. The Superpave mix design method consists of performance-graded asphalt binder specifications and volumetric mix design test procedures, tailored for better performance and longer life based on a geographical area's temperature extremes and traffic loads. For these two types of mixes, the strength and durability of the coarse aggregates are imperative. In accordance with the current MoDOT standard specification, most Missouri SMA mixtures use durable porphyry (Traprock) aggregate. However, its source is confined to the southeastern part of the State. Therefore, it is necessary to identify alternative durable crushed aggregates that are locally available and less expensive for SMA and Superpave mixes that can be used under high-volume traffic roads. Associated comprehensive study on materials characterization, mix design, and performance tests on aggregates and asphalt mixtures for both SMA and Superpave is needed.

## 1.2 Background

Several states have initiated research studies to identify locally available aggregates for SMA mixtures. The SMA mixtures prepared with local limestone in Kansas didn't pass the specification limit associated with the amount of degradation after compaction (Cross 1999). Celaya and Haddock (2006) developed testing methods to quantify aggregate qualities and evaluate local aggregates to be used in SMA for the Indiana Department of Transportation (InDOT). Among the tested materials, two dolomite aggregates experienced extensive degradation during compaction, and two SMA mixtures containing dolomite failed to meet the minimum requirements. Later, a follow-up research project suggested that some local polish-susceptible coarse aggregates (i.e., limestone) could be allowed to blend with steel or blast furnace slags or sandstones, and the combination could provide adequate friction (McDaniel and Shah 2012). The Illinois Department of Transportation (IDOT) is currently conducting a research project aiming to determine the applicability of local and relatively soft aggregates (e.g., limestone, dolomite, or gravel) in SMA mixtures. Studies have also been conducted to evaluate the applicability of other aggregate sources, such as novaculite and sandstone for the use in SMA mixtures (Mohammad et al. 1999, Polaczyk et al. 2022, Miao et al. 2022, Zhao et al. 2022). James et al. (2022) assessed the rutting resistance, moisture susceptibility, drain down, and cracking potential of mixtures using a high-loss granitic aggregate source in South Carolina, with varying performance metrics based on different nominal maximum aggregate sizes. Besides regulating the types of aggregate that can be used, Departments of Transportation (DOTs) have also specified physical aggregate properties and durability for SMA mixtures. These properties requirements involve a certain testing outcome from a wide variety of tests. The Los Angeles (LA) Abrasion, flat and elongated ratio, absorption, clay content, and soundness (NAPA 2002) tests are utilized. Degradation after compaction has also been considered as an

important durability index for the coarse aggregates in SMA (Cross 1999, NAPA 2002, Celaya and Haddock 2006). Additionally, the Micro-Deval Abrasion test was proposed to compliment the LA Abrasion test (Celaya and Haddock 2006), and researchers have also tested the polishing resistance of the coarse aggregates (McDaniel and Shah 2012, Miao et al. 2022). Performance tests of SMA mixtures with different aggregate sources have also been conducted for aggregate selection, among which the Hamburg Wheel Tracker rutting tests (HWTT) and Asphalt Mixture Performance Tester (AMPT) Flow Number (FN) were often used for rutting resistance evaluation (Mohammad et al. 1999, Apeagyei et al. 2013, Liu et al. 2019). Liu et al. (2019) performed the Taxes Overlay test to assess the cracking resistance of SMA mixtures with different aggregates. It was confirmed that more spherical (equant), angular, or better-crushed rough coarse aggregate particles in SMA mixtures would yield better cracking and rutting resistance. Ameli et al. (2020) conducted the HWTT, Four-Point Beam Fatigue (FPBF) tests, resilient modulus tests, and moisture susceptibility tests as per AASHTO T 283 and found that replacing a coarse portion of the aggregate skeleton with steel slag aggregate in SMA resulted in improved rutting resistance of mixtures but potentially decreased stripping and cracking resistance. The friction and resistance to polish were also investigated for alternative aggregate usages in SMA (Kowalski et al. 2010, McDaniel and Shah 2012). Kowalski et al. (2010) performed Accelerated Friction Tests (AFT), calculated the International Friction Index (IFI), and demonstrated that hard limestone or dolomite provides higher friction than soft limestone in mixtures. Steel slag and quartzite were also found to improve SMA frictional properties greatly.

Information from other states offers valuable insights, however, it is crucial to consider Missouri's unique factors, including local material resources, availability, and feasibility. The interest in utilizing local resources from MoDOT and other local engineers is currently facing an insufficient source of Missouri Specific resource data. To bridge this gap, there is a call for an associated comprehensive study encompassing material characterization, mix design, and performance evaluation of potential aggregate and asphalt mixtures that could serve as viable alternatives for traprock in SMA mixtures.

## 1.3 Objectives

The goal of this study is to identify and compare alternatives to Traprock (the current specified aggregate type for SMA in Missouri) for use in SMA and higher level Superpave mixes. To achieve this goal, the objectives of the study include the following elements:

- Review literature of current neighboring DOTs' practices and other research studies in selecting, evaluating, and using other available hard and durable aggregates for SMA and higher level Superpave mixtures

- Evaluate durability of a list of candidate aggregates and identification of alternative aggregates meeting MoDOT specification requirements

- Develop SMA and Superpave mix designs for mixtures with alternative aggregates in accordance with MoDOT current practice and specifications

- Evaluate performance of SMA and Superpave mixtures with alternative aggregates through a comprehensive laboratory testing and data analysis program

- Share findings and recommendations on the use of alternatives to Traprock in SMA and Superpave mixtures, including material selection, mix design, evaluation parameters, testing methods, and acceptance criteria for both aggregates and mixtures

## 1.4 Research Methodology

To achieve the objectives of this study, the following major tasks were completed:

- Task 1: Project Management
- Task 2: Literature Review
- Task 3: Aggregate Selection
- Task 4: Mix Design
- Task 5: Laboratory Testing and Data Analysis
- Task 6: Development of Draft Final Report, Research Summary, and Presentation

### 1.4.1 Task 1: Project Management

The primary investigator (PI) consulted with the research manager to establish the Technical Advisory Committee (TAC) of this project. The TAC provided the research team with guidance and technical feedback throughout this study. The work plan, scope, and schedule were reviewed in the kick-off meeting, and a protocol for regular ongoing communication and coordination with the team was established.

### 1.4.2 Task 2: Literature Review

Information and data from previous work conducted by MoDOT and neighboring states on this topic was gathered and reviewed. The research team conducted the literature review covering 1) state-of-the-art and state-of-the-practice testing, evaluating methods, and requirements of aggregates used and associated mix design methods for SMA and higher level Superpave mixes, and 2) benefits and concerns of use of alternative materials in terms of cost, availability/reliability of the source of material, durability testing records of alternatives, and performance of mixtures. The interim project report presents a full version of the comprehensive literature review.

### 1.4.3 Task 3: Aggregate Selection

All the information provided by MoDOT, quarry surveys, and literature regarding potential aggregates in Missouri has been compiled and listed in Appendix A. The research team developed a preliminary list of potential alternative aggregate for SMA and Superpave mixtures considering neighboring states' experience, documented research and literature, and the

availability of aggregate sources in Missouri. The list has been reviewed by the TAC, including traprock (as control), chat, gravel, steel slag, limestone, and dolomite. The research team also considered some blends of two studied aggregates.

Samples of candidate aggregates were collected. Fundamental physical properties, and a series of screening tests were evaluated on the aggregates. The list of candidate alternative aggregates that passed the requirements specified in this study along with the aggregate source, price, availability, and testing results with preliminary recommendations were provided to the TAC and finalized upon the TAC's review and approval.

### 1.4.4 Task 4: Mix Design

The research team acquired sufficient testing materials, including selected coarse aggregates, fine aggregates, mineral filler, cellulose fibers, and asphalt binder. Four Superpave and five SMA mixtures for each selected coarse aggregate, were developed using the existing typical Missouri Job Mix Formulas (JMFs) for both SMA and Superpave as baselines. Before finalizing the mix design, BMD performance tests, specifically the HWTT and ideal cracking test (IDEAL-CT) tests were conducted for performance verification. The candidate designs that met the threshold limits were finalized. For those unable to meet the limits, the binder content was adjusted to fulfill performance requirements. The Superpave mixture underwent a similar design process, but instead of using voids in the mineral aggregate (VMA) and voids in the coarse aggregate (VCA) concepts, it utilized volumetric parameters: VMA, voids filled with asphalt (VFA), and dust-to-binder ratio. Chapter 4 presents the results of final volumetric designs and BMD verification for SMA and HMA mixtures with alternative aggregates.

### 1.4.5 Task 5: Laboratory Testing and Data Analysis

The durability of alternative aggregates was assessed using the Micro-Deval abrasion test, the post-compaction degradation assessment, and soundness tests, which measured resistance to polishing, degradation, and freeze-thaw damage. Performance tests were then conducted on mixtures designed with these alternative aggregates. The collected laboratory data underwent thorough processing, followed by systematic statistical analyses at both materials and structural levels to evaluate the suitability of SMA and HMA mixtures incorporating alternative aggregates.

Additionally, a Life Cycle Cost Analysis (LCCA) was executed to determine the cost-effectiveness of utilizing alternative aggregates in SMA and higher-level Superpave mixtures. The outcomes of this analysis were synthesized to provide an overarching assessment of the viability of alternatives to traprock in SMA and higher-level Superpave mixtures, facilitating recommendations for their application.

### 1.4.6 Task 6: Development of Final Report

Quarterly reports to timely update project progress were submitted during the above tasks. The final report and an executive summary detailing the tasks completed during the project were developed. Findings from each task were documented including 1) summary of literature review; 2) procedures and results of aggregate selection and screening; 3) developed mix

designs for different aggregates; 4) testing and data analysis results from the comprehensive aggregate-level, mix-level, and structural-level testing and evaluation; and 5) final recommendations for the selection of the local alternative aggregates for SMA and higher level Superpave mixes.

## 1.5 Report Layout

The report consists of seven chapters. Chapter 1 introduces the study's background and research methodology. Chapter 2 outlines the sampling plan for candidate aggregates, mix design approach, and details of the experiments for both aggregates and mixtures. In Chapter 3, testing results for materials, final mix designs for candidate aggregates, and performance verification are presented. Chapter 4 delves into multiscale performance test results at the materials level and predictions at the structural level alongside a conducted cost analysis. Chapter 5 describes the evaluation of friction for the mixtures. Chapter 6 summarizes the conclusions and recommendations. Finally, the Appendix B provides a summary of the main findings from the literature.

# CHAPTER 2 MATERIALS AND EXPERIMENTS

## 2.1 Materials

### 2.1.1 Aggregate and Quarry Selection in Missouri

The locations of the quarries were considered as one of the factors during the selection of which aggregate would be chosen as testing samples. The initial roster of candidate aggregates in this study were traprock (control), chat, gravel, steel slag, limestone, and dolomite, which are well-distributed in Missouri. The locations of the quarries and the types of aggregates at those locations are presented in Figure 2.1. The list of candidate aggregates was reviewed and approved by MoDOT given the aggregate source, price, and availability. Table 2.1 presents the details of the proposed aggregate samples. The quarries corresponding to each candidate aggregate for sampling are indicated in Figure 2.1, while Figure 2.2 displays the sampled candidates.

**Table 2.1 Proposed Aggregate Samples for Preliminary Aggregate Testing**

| Sample # | Aggregate | Quarry | Ledge Description | Comment |
|---|---|---|---|---|
| **1** | Traprock (Control) | New Frontier, Iron Mountain Quarry-Porphyry | Porphyry | One of the three quarries with porphyry on the list; Traprock for SMA |
| **2** | Chat (Required) | Williams Divers Matl (WDM), Lawyer (Bingham #11) | Chat | Among the chat quarries, WDM Lawyer was the only one not marked with "best to avoid" |
| **3** | Gravel (Required) | Capital Sand #1, Wardsville (Osage Riv) | Gravel | Typical gravel in MO |
| **4** | Steel Slag (Required) | Nucor Steel Slag | Steel Slag | Only one quarry with steel slag |
| **5** | Limestone | New Frontier, Alton Weber #8 | Limestone | Already used in SMA; recommended by MoDOT |
| **6** | Dolomite | Capital Quarries #17, Sullivan | Potosi | Selected as a typical dolomite in MO |


**Figure 2.1 Distribution of quarries by aggregate type: (a) traprock, (b) steel slag, (c) gravel, (d) chat, (e) limestone, and (f) dolomite.**

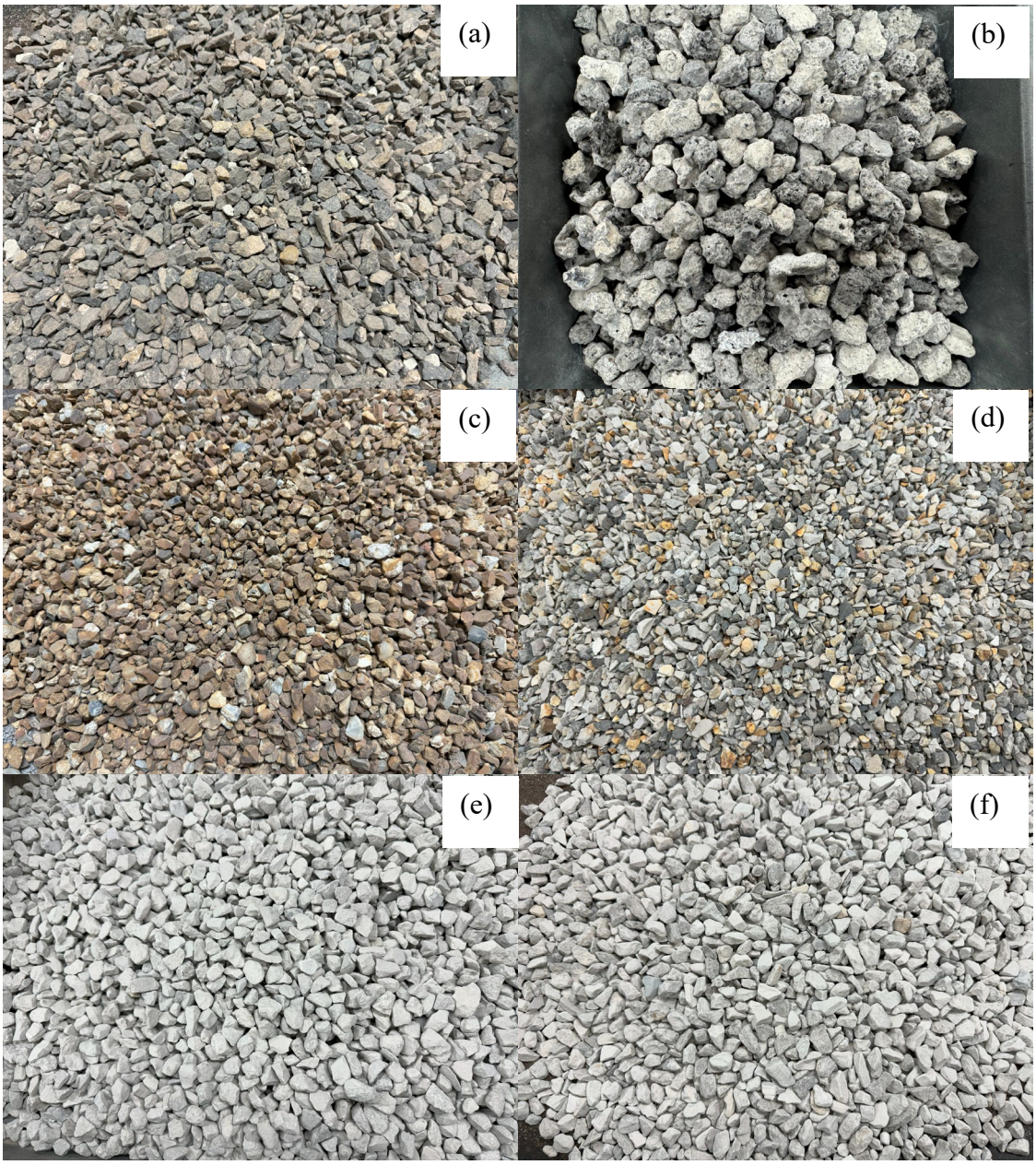


**Figure 2.2 Sampled candidate aggregates: (a) traprock, (b) steel slag, (c) gravel, (d) chat, (e) limestone, and (f) dolomite.**

In case mixes composed of a single type of coarse aggregate could not pass the design criteria, the research team also considered some blends of two aggregates. According to the current MoDOT standard specification (Sec. 403.3.3), coarse aggregates in SMA can be a combination of at least 40% of traprock by total weight (without the usage of steel slag) and other aggregates. In case that some of the selected aggregates cannot pass the preliminary aggregate screening tests when tested alone and blended with other aggregates, a list of potential substitute aggregates was prepared as presented in Figure 2.2.

**Table 2.2 Backup Plan of Potential Aggregate for Preliminary Aggregate Testing**

| Sample # | Aggregate | Quarry | Ledge Description | Comment |
|---|---|---|---|---|
| **7** | Chat | Flint Rock Products, Admiralty (Humble S&G) | Flint Chat | One Flint Chat for comparison |
| **8** | Gravel | Norris Quarries Savannah -Quarry-Breit | Gravel | Second source for Gravel, different location |
| **9** | Limestone | Bussen #3, Antire Quarry | Plattin | Different type of limestone |
| **10** | Limestone | Kerford Limestone Co., NE | Limestone | Different source for limestone |
| **11** | Dolomite | Lead Belt, Desloge Stone | Bonne Terre | Different type of dolomite |
| **12** | Granite | Martin Marietta (Mill Creek Quarry), OK | Troy Granite | Granite as potential aggregate candidate |

### 2.1.2 Aggregate Tests

Table 2.3 lists all the aggregate tests, and the corresponding limits for screening aggregates and finalizing the list of alternative aggregates to be tested. These tests include deleterious materials, LA abrasion, angularity, flat and elongated ratio, absorption, and clay content. Additionally, the Micro-Deval abrasion test, degradation after compaction, and soundness test were performed for durability evaluation. These tests do not have specified MoDOT requirements, but there are some limits suggested in other studies, as shown in Table 2.3.

**Table 2.3 Aggregate Durability Tests**

| Property | Testing Specification | Parameter | Limits From Other Studies |
|---|---|---|---|
| **Micro-Deval Abrasion** | ASTM D7428 | Max. percentage loss | 18%[a] |
| **Degradation After Compaction** | N/A | Increase on the #8 sieve | 4%[b] |
| **Soundness** | AASHTO T 104 | Percentage loss | N/A[c] |

a Liu et al. 2012; b Cross 1999; c No specific limit for surface layer of asphalt pavement.

### 2.1.3 Binders

In this study, PG 64-22V and PG 64-22 binders were used in SMA and HMA mixtures respectively. The binders were sampled from the asphalt plants that provided the JMFs and other materials for the control mixtures. After verification by the rotational viscometer (RV) test results as shown in Figure 2.3, the mixing and compaction temperatures were calculated and are presented in Table 2.4.

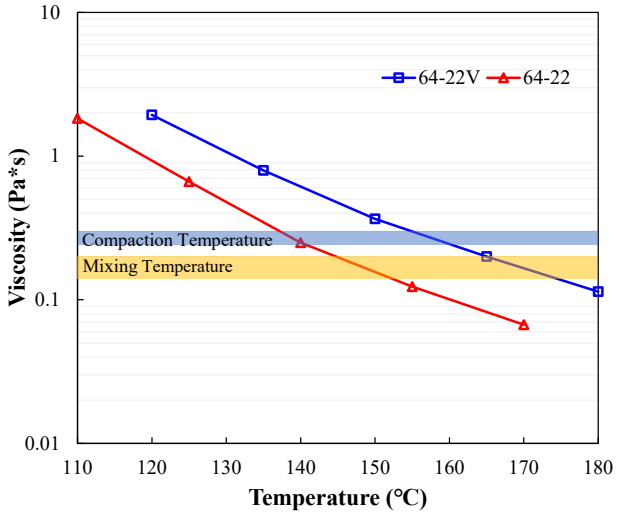


**Figure 2.3 Viscosity of binders for SMA and HMA mixtures.**

**Table 2.4 Table Mixing and Compaction Temperatures of Binders**

| Binder | Mixing Temp. (°C) (Viscosity 0.15~0.20 Pa*s) | Compaction Temp. (°C) (Viscosity 0.25~0.30 Pa*s) |
|---|---|---|
| **PG 64-22V** | 166~172 | 157~161 |
| **PG 64-22** | 148~154 | 141~144 |

### 2.1.4 Mixtures

The JMFs for SMA and HMA mixtures were provided by MoDOT as references. For SMA mixtures, traprock, PG 64-22V binder, and fiber were sampled from the Capital Quarries in Rolla. In this study, the traprock was replaced with other candidate aggregates while keeping the remaining components consistent across all SMA mixtures. For HMA mixtures, all aggregates, RAP, filler, and PG 64-22 binder were sourced from a local asphalt plant. Blended limestone with chat (Blend H1) was used in the original mix JMF and served as control coarse aggregates in this study. The candidate aggregates underwent revision following the aggregate screening tests and mix designs conducted with the initial roster.

Combinations of coarse aggregates were created since the sampled chat with a NMAS of #4 was too small to be used alone as a coarse stockpile and the mixtures with limestone or dolomite alone exhibited challenges to meeting the volumetric criteria (details are documented in Chapter 4). As results, the candidate aggregates included blended limestone with chat (Blend S1) and blended dolomite with chat (Blend S2) in SMA, and blended dolomite with chat (Blend H2) in HMA, as summarized in Table 2.5.

**Table 2.5 SMA and HMA Mixtures with Candidate Aggregates**

| Type of Mixture | Candidate Aggregates | Binder | Abbreviation for Mixtures |
|---|---|---|---|
| **SMA** | Traprock (Control) | PG 64-22V | ST |
| | Steel slag | | SS |
| | Gravel | | SG |
| | Limestone | | SL |
| | Dolomite | | SD |
| | Blend S1[a] | | SLC |
| | Blend S2[b] | | SDC |
| **HMA** | Blend H1 (Control)[c] | PG 64-22 | HLC |
| | Steel slag | | HS |
| | Gravel | | HG |
| | Limestone | | HL |
| | Dolomite | | HD |
| | Blend H2[d] | | HDC |

[a] Limestone & chat in SMA; [b] Dolomite & chat in SMA; [c] Limestone & chat in HMA; [d] Dolomite & chat in HMA.

## 2.2 Mix Design Method

### 2.2.1 Volumetric Mix Design

#### 2.2.1.1 SMA Volumetric Mix Design

This study involved developing SMA mixtures for each selected coarse aggregate while the typical Missouri JMF for SMA served as a baseline. Subsequently, volumetric parameters were calculated to ensure compliance with requirements such as *VMA*, $VCA_{DRC}$ and $VCA_{mix}$. $VCA_{mix}$ was required to be less than $VCA_{DRC}$ to ensure the integrity of the aggregate skeleton, as per AASHTO R 46 and MoDOT construction specifications. It also mandated a minimum of 17% *VMA* in SMA mixtures to ensure adequate space within the mixture for the proper coating and binding of asphalt binder to the aggregate particles. In cases where qualified *VMA* cannot be achieved in the typical mix design, primary adjustments focused on gradation until the *VMA* requirement was met. Binder content for new trial designs was calculated using the specific gravities of blended aggregates. Once SMA mixtures met all qualified parameters, draindown percentage was assessed at the anticipated plant-production temperature (162°C) according to AASHTO T 305. The draindown percentage should be no more than 0.3% according to AASHTO M 325. Then, moisture susceptibility of SMA mixtures was evaluated using TSR, with a minimum requirement of 0.8. IDT strength tests were conducted on samples conditioned by a freeze-thaw cycle following AASHTO T 283.

#### 2.2.1.2 HMA Volumetric Mix Design

Besides SMA, high-quality HMA mixtures were also developed for each selected coarse aggregate in this study. Volumetric parameters, including *VMA*, *VFA*, and the dust-to-binder

ratio, were evaluated in the trial mix designs. According to the MoDOT construction specification, the *VMA* for HMA should not be less than 14%, and the *VFA* should fall within the range of 65%-75%, corresponding to an optimal binder content in the asphalt mixture. Additionally, the dust-to-binder ratio was required to be within the range of 0.8-1.6 for proper distribution of asphalt binder throughout the mixture. Subsequently, the moisture susceptibility of HMA mixtures were evaluated using TSR following AASHTO T 283, with a minimum requirement of 0.8. IDT strength tests were also conducted on samples conditioned by a freeze-thaw cycle.

### 2.2.2 BMD Performance Verification

In this study, the BMD was also included in the mix design process to ensure the performance of the newly designed SMA mixtures. The design procedure flow is illustrated in Figure 2.4. This method uses the volumetric parameters including the $VCA_{DRC}$ and $VCA_{mix}$ to determine the initial gradation and binder content. The volumetric criteria are applied to ensure a stable skeleton structure and sufficient fine materials for a gap-graded mixture, and the draindown test is used to assure its constructability. The performance tests (highlighted in red in Figure 2.4) are included to ensure the mixture performance as a variety of components are used in the SMA design.

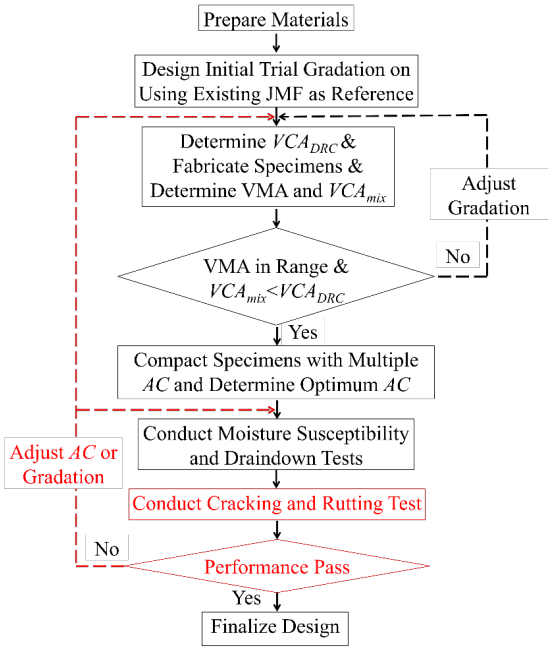


**Figure 2.4 Preliminary BMD design procedure for SMA mixtures.**

Upon completing the volumetric design, performance verification was ensured. Two performance tests, namely HWTT and IDEAL-CT, were employed to evaluate the resistance of SMA and HMA mixtures to rutting and cracking, respectively. The designs were finalized for those mixtures with candidate aggregates, utilizing the Superpave volumetric design method,

after passing the performance limits. Alternatively, adjustments were made to the binder content initially. Subsequently, additional performance tests were conducted for the SMA with different binder contents, and the balanced area for binder content was determined through comparing testing results with two performance limits. The SMA mixture with a binder content in this area can meet both cracking and rutting requirements. Then the optimum performance binder content was determined considering the variability, uncertainty, and cost in construction. Additionally, moisture susceptibility and draindown were re-evaluated, and the designs were finalized after meeting the requirements of both tests. Otherwise, a redesign involving adjustments to gradation and aggregate combination was initiated. The HMA mixtures were designed in the same way except that, instead of using the concepts of *VMA* and *VCA*, the volumetric parameters, *VMA* and VFA were applied.

## 2.3 Mixture Performance Tests

Table 2.6 outlines the performance tests conducted on the designed mixtures incorporating alternative aggregates. These tests were conducted to assess the durability of both SMA and HMA mixtures using the finalized mix designs from this study.

**Table 2.6 Proposed Mixture Performance Tests**

| Test | Performance | Parameters | Standard |
|---|---|---|---|
| **HWTT** | Moisture Susceptibility and Rutting Resistance | Number of passes at a certain rut depth | AASHTO T 324 |
| **IDEAL-CT** | Cracking Resistance | Cracking Tolerance Index ($CT_{Index}$) | ASTM D8225 |
| **IDT** | Low Temperature Cracking Resistance | Creep Compliance and Strength | AASHTO T 322 |
| **AMPT Cyclic Fatigue Test** | Cracking Resistance | $S_{app}$; material integrity vs. damage accumulation curve, $D^R$ fatigue damage criteria | AASHTO TP 133 |
| **AMPT Dynamic Modulus Test** | Dynamic Modulus | Dynamic modulus master curve, shift factors | AASHTO TP 132 |
| **AMPT Stress Sweep Rutting (SSR) Test** | Rutting Resistance | Rutting Strain Index (RSI); permanent deformation at different temperatures, loading frequencies, and amplitudes | AASHOT TP 134 |
| **M.i.S.T** | Moisture Susceptibility / Stripping | Material property changes due to moisture conditioning, e.g.;TSR | ASTM D7870 |
| **AFT** | Friction / Skid Resistance | Coefficient of Friction (COF) at different speeds; MTD; IFI | ASTM E1911 |

### 2.3.1 IDEAL-CT

The IDEAL-CT test is a rapid cracking test that is convenient to use in mix design and quality assurance (Liu et al. 2023). The testing procedures followed ASTM D8225 and are conducted at 25 ℃ with cylindrical specimens at a constant loading rate of 50mm/min, as shown in Figure 2.5. The test specimens had a diameter of 150 mm and a height of 62 mm, with air voids of 6±0.5% for SMA mixture and 7±0.5% for HMA mixture. The $CT_{Index}$ was calculated using Equation 2.1 (Zhou 2019). In accordance with MoDOT's specification (BMD Performance Testing for Job Mix Approval NJSP-21-08A), for SMA mixtures and HMA mixtures, $CT_{Index}$ should be no less than 135 and 45, respectively.

$$CT_{Index} = \frac{t}{62} * \frac{G_f}{|m_{75}|} * \left(\frac{l_{75}}{D}\right)$$

Where:

$t$ = the thickness of testing sample
$G_f$ = the fracture energy
$|m_{75}|$ = the post-peak slope of the load–displacement curve at 75% of the peak load
$D$ = the diameter of the testing sample
$l_{75}$ = the displacement at 75% of the peak load

**Equation 2.1 $CT_{Index}$ Calculation**

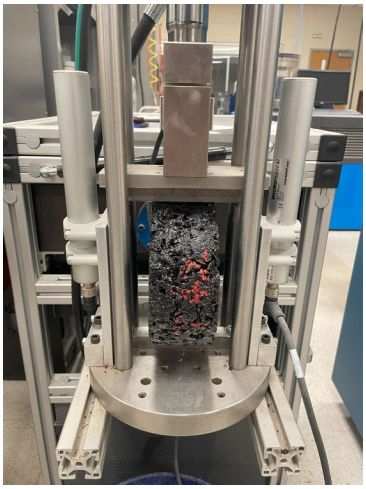

**Figure 2.5 IDEAL-CT equipment.**

To elucidate the impact of distinct aggregates on the IDEAL-CT of mixtures, Yin et al. (2023) conducted a thorough analysis for further evaluation. The analysis involved the construction of an interaction diagram, where the average $G_f$ (mixture toughness) was graphed on the y-axis against the average $l_{75}/m_{75}$ ratio (indicative of relative ductile-brittle behavior) on the x-axis. An elevation in both $G_f$ and $l_{75}/m_{75}$ contributes to a higher $CT_{Index}$ value according to the Equation

2.1. The interaction diagram comprises a series of $CT_{Index}$ contour curves, with each contour curve representing data points featuring the same $CT_{Index}$ value but differing $G_f$ and $l_{75}/m_{75}$ results.

### 2.3.2 HWTT

The HWTT can evaluate the mixture moisture susceptibility and rutting resistance simultaneously. The testing device is shown in Figure 2.6. The test specimens had a diameter of 150 mm and a height of 62 mm, with air voids of 6±0.5% for SMA mixture and 7±0.5% for HMA mixture. The testing procedures followed AASHTO T 324. In accordance with MoDOT's specification, for SMA and HMA mixtures, the rut depth should not exceed 12.5 mm under 20,000 passes as specified in NJSP-21-08. Additionally, the rutting resistance index (RRI), calculated using Equation 2.2 (Liu 2022), provides a comparative measure for tests completed at different loading cycles. The RRI parameter accounts for both the combined effect of the number of passes and the rut depth, addressing the nonlinear impact of loading passes on pavement rutting.

$$RRI = N^{0.3}\left(1 - \frac{RD}{25.4}\right)$$

Where:

*RRI* = rutting resistance index
*N* = 20,000 or number of passes reaching 12.5-mm rut depth
*RD* = rut depth at 20,000 passes or 12.5 mm for those reaching 12.5 mm rut depth before 20,000 passes

**Equation 2.2 RRI Calculation**


**Figure 2.6 HWTT equipment.**

### 2.3.3 IDT

The IDT tests were performed to evaluate the resistance of asphalt mixture to cracking at low temperature per AASHTO T 322. All samples for the IDT tests were cut down at least 6 mm on each side to provide a flat surface for setting up the LVDTs, as shown in Figure 2.7. The test specimens had a diameter of 150 mm and a height of 50 mm, with air voids of 6±0.5% for SMA mixture and 7±0.5% for HMA mixture. The device used for IDT tests in this study is a MTS 810 loading frame with a chamber MTS model 651.34, as shown in Figure 2.8. The loading system is computer-controlled, operating dynamically with closed-loop servo-hydraulic mechanisms. The chamber's temperature range spans from -30 to +100 ℃ with an accuracy of ±0.2 ℃.

**Figure 2.7 IDT samples before and after cutting.**

Considering the low-temperature grade of the binder (64-22V for SMA mixture, 64-22 for HMA mixture) employed in this study, testing temperatures of -20 ℃, -10 ℃, and 0 ℃ were selected. One of the fundamental materials properties obtained from the IDT test, namely the creep compliance *D(t)*, was utilized to compute thermal stress based on the specific coefficient of thermal expansion and an assumed cooling rate. Subsequently, the critical temperature of the asphalt mixture was forecasted by comparing the thermal stress with the results obtained from strength tests.

**Figure 2.8 MTS 810 loading frame with a chamber.**

#### 2.3.3.1 Creep Compliance Test

Creep compliance, as defined in AASHTO T 322, is the ratio of time-dependent strain to the applied stress. The cylindrical specimens are subjected to a static compressive load along a diametral axis for 100 seconds, under temperature-controlled conditions. The loads should be adjusted to maintain the average horizontal deformation between 0.00250 mm and 0.00900 mm across both specimen faces. Following trials on the SMA and HMA samples, the loads resulting in qualified horizontal deformation at various temperatures are summarized in Table 2.7. Throughout the loading period, vertical and horizontal deformations were measured using two extensometers per specimen face, as shown in Figure 2.9.

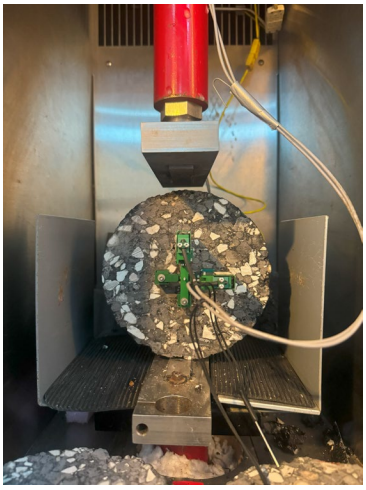

**Figure 2.9 Extensometers used for IDT creep tests.**

**Table 2.7 Loads for IDT Creep Compliance Tests**

| Mixture | Testing Temperature (℃) | Load (lb.) |
|---|---|---|
| SMA & HMA | -20 | 3000 |
| | -10 | 1800 |
| | 0 | 700 |

Since this testing method is non-destructive, specimens can be tested at various temperatures. It is recommended to conduct the tests from low to high temperatures to minimize any effects on the samples. The creep compliance was calculated using the Equations 2.3 and 2.4 below.

$$D(t) = \frac{\Delta X_{tm,t} \times D_{avg} \times b_{avg}}{P_{avg} \times GL} \times C_{cmpl}$$

Where:

$D(t)$ = creep compliance at time t (1/kPa)
$\Delta X_{tm,t}$ = trimmed mean of horizontal deformation
$D_{avg}$, $b_{avg}$, $P_{avg}$ = average thickness, diameter, and creep load of three replicate specimens
$GL$ = gauge length (38 mm for 150-mm-diameter specimens)

**Equation 2.3 Creep Compliance at Time t**

$$C_{cmpl} = 0.6354 \times \left(\frac{X}{Y}\right)^{-1} - 0.332$$

Where:

$X$ = horizontal deformation
$Y$ = vertical deformation

**Equation 2.4 Correction Factor $C_{cmpl}$**

#### 2.3.3.2 Strength Test

According to AASHTO T 322, the loading rate should be 12.5mm/min, and vertical movement should continue to be applied to the sample until the load begins to decrease, indicating cracking. The peak load attained was used to calculate the material strength based on the Equation 2.5 below.

$$S_{t,n} = \frac{2 \times P_{f,n}}{\pi \times b_n \times D_n}$$

Where:
$S_{t,n}$ = tensile strength of specimens
$P_{f,n}$ = maximum load observed for specimens
$b_n$, $D_n$ = thickness and diameter of specimens

**Equation 2.5 Tensile Strength of Specimen**

#### 2.3.3.3 Cracking Temperature of Asphalt Mixture

Subsequently, the creep compliance data underwent processing via the LTSTRESS spreadsheet to generate a creep compliance master curve. This master curve was derived by shifting the $D(t)$

values as a function of time at each temperature. The Equation 2.6 below, was employed to formulate these master curves (Christensen, 1998).

$$D(t) = D_0 + D_1 \left[ \frac{t}{10^{C_2(T_r - T)}} \right]^m$$

Where:

*D(t)* = creep compliance over time
*t* = time
$D_0$, $D_1$, *m* = fitting parameters
$C_2$ = time-temperature shift constant
$T_r$ = reference temperature
*T* = temperature

**Equation 2.6 Creep Compliance Over Time**

Then the LTSTRESS spreadsheet was used to calculate the thermal stress of all SMA and HMA mixtures. The prediction of thermal cracking temperature involved comparing the thermal stress and strength at various temperatures, as illustrated in Figure 2.10 (Hills and Brien, 1966). As the temperature decreases, cracking occurs when the accumulated thermal stress surpasses the material' strength, indicated by the intersection of the tensile strength versus temperature and thermal stress versus temperature curves.

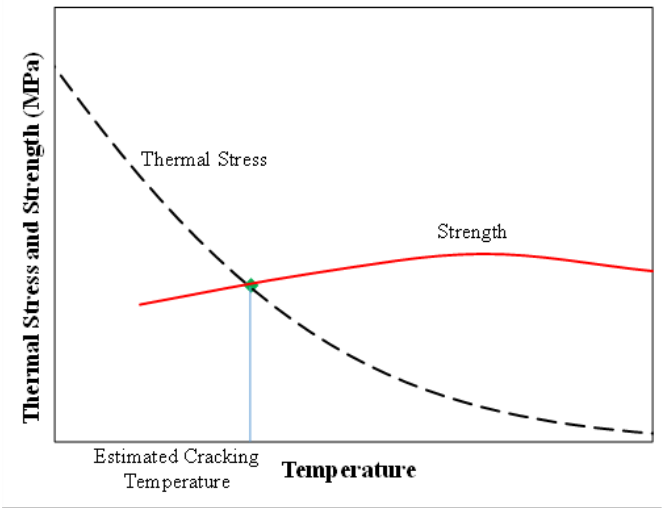


**Figure 2.10 Determination of cracking temperature for asphalt mixture.**

### 2.3.4 AMPT

MoDOT has been requiring contractors to provide AMPT samples for performance testing according to Standards NJSP2001 and NJSP2108. All samples for AMPT tests were cut and cored

from an original cylindrical specimen with a diameter of 150 mm and a height of 180 mm to provide a flat surface for setting up the LVDTs or attaching the loading platens, as shown in Figure 2.11. The AMPT device is depicted in Figure 2.12. These tests, including dynamic modulus, cyclic fatigue, and SSR tests, are advanced methods that access the fundamental material properties. In this study, after finishing the mix design for SMA and HMA mixtures with alternative aggregates, comprehensive data analysis was conducted on laboratory AMPT testing data at both material and structural levels to evaluate mixtures' performance in terms of cracking and rutting resistance, dynamic modulus, and fatigue damage.

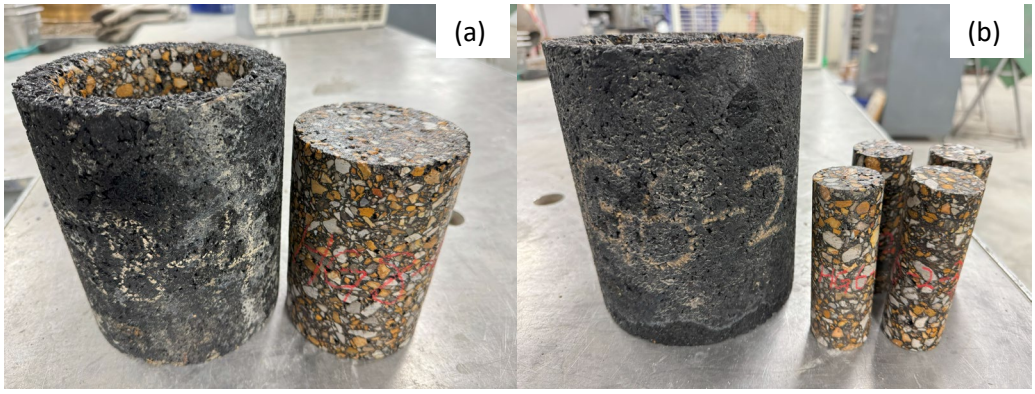


**Figure 2.11 AMPT test samples: (a) SSR Test samples, and (b) Cyclic Fatigue Test and Dynamic Modulus Test samples.**


**Figure 2.12 AMPT equipment.**

#### 2.3.4.1 AMPT Dynamic Modulus Test

Dynamic modulus is a fundamental material property for asphalt mixtures. The test characterizes material behavior under small loads in the linear viscoelastic range. The tests were conducted at 4°C, 20°C, and 40°C, and three loading frequencies, i.e., 10 Hz, 1 Hz, and 0.1 Hz were applied at each temperature as per AASHTO TP 132. The qualified test specimens had a

diameter of 38 mm and a height of 110 mm, with air voids of 5±0.5% for both SMA and HMA mixtures. The test provided a dynamic modulus master curve and the corresponding shift factors, which were used to process the cyclic fatigue testing data and calculate the strain/stress under traffic loads during pavement performance simulation.

The construction of dynamic modulus master curves of asphalt mixtures involved the application of two models in the FlexMAT™ program: the Sigmoidal model and the 2S2P1D model. Equations 2.7 and 2.8 detail the mathematical expressions for these models. Whereas the Sigmoidal model displays a simple symmetrical curve, the 2S2P1D model incorporates a blend of both linear and nonlinear mechanistic elements, as depicted in the schematic diagram presented in Figure 2.13 (Kim et al., 2015; Kim et al., 2022).

$$log|E^*| = a + \frac{b}{1 + \frac{1}{e^{d+g*logf_R}}}$$

Where:

$|E^*|$ = the dynamic modulus
*a, b, d*, and *g* = model coefficients
$f_R$ = the reduced frequency

**Equation 2.7 Sigmoidal Model**

$$E^*_{2S2P1D}(\omega) = E_{00} + \frac{E_0 - E_{00}}{1 + \delta(j\omega\tau)^{-k} + (j\omega\tau)^{-h} + (j\omega\beta\tau)^{-1}}$$

Where:

*E** = complex modulus
*j* = complex number defined by $j^2 = -1$
*ω* = the angular frequency
$\omega = 2\pi f$
*f* = the frequency
*k, h* = two constants such that $0 < k < h < 1$
*δ* = a constant
$E_{00}$ = the static modulus when ω tends towards 0
$E_0$ = the glassy modulus when ω tends towards+ ∞
*η* = the Newtonian viscosity of the dashpot, $\eta = (E_0 - E_{00})$ βτ
*τ* = the characteristic time, whose value varies only with temperature

**Equation 2.8 2S2P1D Model**

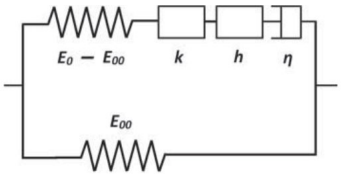


**Figure 2.13 Schematic of the 2S2P1D model.**

According to AASHTO T 378, to assess data quality, the repeatability coefficient of variation for dynamic modulus ($S_r$%) and the repeatability standard deviation of phase angle ($S_r$) were calculated using the following Equations 2.9 and 2.10.

$$S_r\% = \left[29.8e^{(0.014\times NMAS)}\right] \times |E^*|^{-\left[0.189e^{(0.012\times NMAS)}\right]}$$

Where:

$S_r$% = repeatability coefficient of variation for $|E^*|$
*NMAS* = mixture nominal maximum aggregate size
$|E^*|$ = average dynamic modulus

**Equation 2.9 Repeatability Coefficient of Variation for $|E^*|$**

$$S_r = \left[4.67e^{(0.022\times NMAS)}\right] \times |E^*|^{-0.23}$$

Where:

$S_r$ = repeatability standard deviation of phase angle
*NMAS* = mixture nominal maximum aggregate size
$|E^*|$ = average dynamic modulus

**Equation 2.10 Repeatability Standard Deviation of Phase Angle**

### 2.3.4.2 AMPT Cyclic Fatigue Test

The cyclic fatigue test characterized material damage evolution under cyclic loading. The tests were performed at 18°C according to the AASHTO TP 133 standard method on both SMA and HMA mixtures incorporating all candidate aggregates. The qualified test specimens had a diameter of 38 mm and a height of 110 mm, with air voids of 5±0.5% for both SMA and HMA mixtures. Employing the FlexMAT™ program, the fitting of testing data utilized the ViscoElastic

Continuum Damage (VECD) model (Wang and Kim, 2017). Subsequently, the energy-based damage characteristic curve, known as the C vs. S curve, was generated to illustrate the accumulation of damage as the stiffness of material changed under varying conditions of temperature, loading frequency, and amplitude. This curve depicted the response of tested material to fatigue traffic loading.

Additionally, the fatigue index $S_{app}$, considering all the parameters received from dynamic modulus and cyclic fatigue tests, was calculated. $S_{app}$ was developed by the research team from North Carolina State University, which is showed in the Equation 2.11 below (Wang et al. 2020). A higher value of the $S_{app}$ parameter means more resistance to fatigue cracking.

$$S_{app} = 1000^{\frac{\alpha}{2}-1} \frac{\alpha_T^{\frac{1}{\alpha+1}} \left(\frac{D^R}{C_{11}}\right)^{\frac{1}{C_{12}}}}{|E^*|^{\frac{\alpha}{4}}}$$

Where:

$D^R$ = the failure criterion
$\alpha$ = the damage evolution coefficient
$C_{11}$ and $C_{12}$ = the coefficients of the damage characteristic curve model
$a_T$ = the dynamic modulus shift factor adjusted to the critical climate temperature of the target region
$|E^*|$ = the dynamic modulus value of 10 Hz at the critical climate temperature

**Equation 2.11 Fatigue Index $S_{app}$**

#### 2.3.4.3 AMPT SSR Test

The SSR test measured the permanent deformation of the mixture under different loading amplitudes at different temperatures. The qualified test specimens had a diameter of 100 mm and a height of 150 mm, with air voids of 6±0.5% for SMA mixture and 7±0.5 % for HMA mixture. The testing temperatures were determined based on both the binder performance grade and the location of the project. In this case, two specimens were tested at 26°C and another two specimens were tested at 48.4°C, as per AASHTO TP 134. Three deviatoric stress levels including 70 psi, 100 psi, and 130 psi were applied to the sample under the confining pressure of 10 psi. The permanent strain during the tests was recorded at both high and low temperatures.

When evaluating rutting resistance for asphalt mixtures in field conditions, factors such as traffic volume, local climate, and permanent strain under various conditions over the long term were considered. After processing the data in the FlexMAT™ program, RSI parameters were calculated to predict the rutting resistance of asphalt mixtures over a 20-year period. A high RSI

value indicates significant permanent strain under identical loading conditions, signaling poorer rutting resistance (Kim et al. 2022, Wang et al. 2023).

### 2.3.5 M.i.S.T

The M.i.S.T test, a kind of conditioning procedure, simulates conditions wherein asphalt mixtures undergo dynamic vehicle loads in wet environments. The condition is achieved by submerging them in a water-filled chamber and applying dynamic pore pressure. The most rigorous M.i.S.T test is comprised of two parts: adhesion cycles followed by cohesion cycles. During adhesion cycles, specimens were immersed in hot water at 60°C for 20 hours. Subsequently, during cohesion cycles, the specimens underwent 3500 loading cycles at 40 psi in hot water at 60°C. The former simulates the adhesion failure of asphalt mixtures under wet conditions, while the latter replicates the combined effects of moisture and dynamic vehicle loads on pavement. To investigate the impact of moisture damage on asphalt mixture cohesion and adhesion, this study conducted both the M.i.S.T test with adhesion cycles and the M.i.S.T test without adhesion cycles, collectively referred to as the M.i.S.T series test. These tests followed the procedures outlined in AASHTO TP 140 and ASTM D 7870, respectively. Standard specimens for the M.i.S.T test are 100 mm in diameter and 63.5 ± 2.5 mm high with 7% ± 0.5% air voids for HMA and 6% ± 0.5% for SMA. The tensile strength ratio was calculated for all the mixtures after the M.i.S.T conditioning test.

# CHAPTER 3 MIX DESIGN AND PERFORMANCE WITH ALTERNATIVE AGGREGATES

## 3.1 Aggregate Tests

The candidate aggregates underwent revision following the aggregate screening and durability tests and mix design creations based on the initial roster.

### 3.1.1 Aggregate Screening Tests

All the screening tests' results for aggregates used in both SMA and HMA mixtures are shown in Tables 3.1 to 3.3, respectively. Certain aggregates, notably limestone and dolomite, demonstrated significant weight loss in LA Abrasion test. However, they also presented challenges in meeting mix design requirements when utilized alone in both SMA and HMA mixtures. Despite employing the Bailey method to determine a qualified gradation, none of the designs met the *VMA* requirement. To address this challenge, new candidate aggregates were created by blending limestone and dolomite with chat. Chat demonstrates excellent durability in screening tests but cannot be used alone in mixtures due to its smaller NMAS compared to other candidate aggregates. The resulting blends, namely limestone & chat (Blend S1 in SMA, Blend H1 in HMA) and dolomite & chat (Blend S2 in SMA, Blend H2 in HMA), exhibited acceptable volumetric properties and met all specified requirements for both SMA and HMA mixtures and aggregate screening tests.

**Table 3.1 Aggregate Screening Tests of Original Candidate Aggregates in SMA Mixtures**

| Aggregate Screening Tests | Limits | Traprock | Steel slag | Gravel | Limestone | Chat | Dolomite |
|---|---|---|---|---|---|---|---|
| **Deleterious Materials** | Deleterious Rock, <8% | 1.3 | 1.2 | 1.1 | 0.7 | 0.0 | 0.1 |
| | Shale, <1% | 0.1 | 0.0 | 0.0 | 0 | 0.0 | 0.1 |
| | Others, <0.5% | 0.1 | 0.1 | 0.1 | 0.1 | 0.0 | 0.1 |
| **LA Abrasion** | <40% | 21.0 | 19.5 | 17.1 | 25.1 | 20.9 | 28.5 |
| **Angularity** | One face, =100% | 100 | 100 | 98 | 100 | 100 | 100 |
| | Two faces, =100% | 100 | 100 | 95 | 100 | 100 | 100 |
| **Flat and Elongated Aggregates** | 3:1, <20% | 18 | 5 | 0 | 15 | 10 | 0 |
| | 5:1, <5% | 0 | 0 | 0 | 0 | 4 | 0 |
| **Sand Equivalent** | >50% | 56 | 55 | 59 | 53 | N/A | 51 |
| **Absorption** | <3.5% | 0.7 | 2.3 | 2.7 | 1.2 | 2 | 3 |

Except for gravel, all other candidate aggregates met the screening test criteria outlined in the Missouri standard specification. The angularity test results for gravel were determined as 98% for one face and 95% for two faces in SMA mixtures, and 98% for one face and 97% for two faces in HMA mixtures. These results were slightly below the required limit of 100% for both conditions. Given that this deviation is small, and the gravel met all other screening test criteria, it was included for further evaluation, including mix design and performance analysis. For candidate aggregates in HMA mixtures, both steel slag and gravel aligned with those used in SMA. Therefore, only a few additional tests were needed, such as the equivalent test, which involves mixing all aggregates listed in the mix design. However, for the two blended aggregates—limestone & chat and dolomite & chat—with varying blending ratios, all aggregate tests were reevaluated for all the screening tests.

**Table 3.2 Aggregate Screening Tests of New Candidate Aggregates in SMA Mixtures**

| Aggregate Screening Tests | Limits | Blend S1 | Blend S2 |
|---|---|---|---|
| **Deleterious Materials** | Deleterious Rock, <8% | 0.1 | 0.1 |
| | Shale, <1% | 0.1 | 0.1 |
| | Others, <0.5% | 0.1 | 0.1 |
| **LA Abrasion** | <40% | 23.0 | 24.8 |
| **Angularity** | One face, =100% | 100 | 100 |
| | Two faces, =100% | 100 | 100 |
| **Flat and Elongated Aggregates** | 3:1, <20% | 13 | 5 |
| | 5:1, <5% | 2 | 2 |
| **Sand Equivalent** | >50% | 65 | 57 |
| **Absorption** | <3.5% | 1.7 | 2.5 |

**Table 3.3 Aggregate Screening Tests of all Candidate Aggregates in HMA Mixtures**

| Aggregate Screening Tests | Limits | Steel slag | Gravel | Blend H1 | Blend H2 |
|---|---|---|---|---|---|
| **Deleterious Materials** | Deleterious Rock, <8% | 1.2 | 1.1 | 0.1 | 0.1 |
| | Shale, <1% | 0.0 | 0.0 | 0.1 | 0.1 |
| | Others, <0.5% | 0.1 | 0.1 | 0.1 | 0.1 |
| **LA Abrasion** | <40% | 19.5 | 17.1 | 24 | 25.2 |
| **Angularity** | One face, =100% | 100 | 98 | 100 | 100 |
| | Two faces, =100% | 100 | 97 | 100 | 100 |
| **Flat and Elongated Aggregates** | 3:1, <20% | 5 | 0 | 6 | 9 |
| | 5:1, <5% | 0 | 0 | 1 | 1 |
| **Sand Equivalent** | >50% | 80.2 | 89.1 | 79.2 | 85.4 |
| **Absorption** | <3.5% | 2.3 | 2.7 | 1.7 | 2.3 |

### 3.1.2 Aggregates Durability Tests

The results of durability tests for aggregates utilized in both SMA and HMA mixtures are outlined in Tables 3.4 to 3.6, respectively. Typically, a weight loss threshold of 18%, as employed in prior studies (Liu et al. 2012) for the Micro-Deval Abrasion test, was considered in this study. Furthermore, the soundness test for aggregates used in asphalt mixtures typically necessitates a maximum loss of 12% in mass after being subjected to five cycles of freezing and thawing. All candidate aggregates met these two criteria.

The degradation of SMA and HMA mixtures with each candidate aggregate was assessed by manufacturing samples under design gyrations (100 gyrations for SMA and 125 gyrations for HMA), followed by sieve analysis after subjecting the samples to an ignition oven at 538°C. The change in the percentage of aggregates remaining on each sieve with potential aggregate breakdown after compaction was evaluated and the results are presented in Figure 3.1. Notably, the majority of aggregates breakdown occurred on #4 sieve, leading to more aggregate particles on #8 sieve. Except for SS, which showed a slightly higher value of 5.7% than the limit, the mixtures containing all other candidate aggregates adhered to the limit proposed in Kansas DOT's report (Cross 1999), which limit the increase on the #8 sieve to 4%.

**Table 3.4 Aggregate Durability Tests of Original Candidate Aggregates in SMA Mixtures**

| Durability of Aggregates | Limits | Traprock | Steel slag | Gravel | Limestone | Chat | Dolomite |
|---|---|---|---|---|---|---|---|
| **Micro-Deval Abrasion** | <18% | 2.4 | 7.1 | 2.5 | 14.9 | 4.4 | 21 |
| **Soundness** | <12% | 0.2 | 0.2 | 0.1 | 0.6 | 0.9 | 0.5 |
| **Degradation** | Increases on Sieve #8, <4% | 2.1 | 5.7 | 2.9 | N/A | N/A | N/A |

N/A: The degradation test was not conducted for aggregates that did not complete the mix designs.

**Table 3.5 Aggregate Durability Tests of New Candidate Aggregates in SMA Mixtures**

| Durability of Aggregates | Limits | Blend S1 | Blend S2 |
|---|---|---|---|
| **Micro-Deval Abrasion** | <18% | 8.6 | 13.1 |
| **Soundness** | <12% | 1.0 | 0.7 |
| **Degradation** | Increases on Sieve #8, <4% | 2.7 | 3.7 |

**Table 3.6 Aggregate Durability Tests of All Candidate Aggregates in HMA Mixtures**

| Durability of Aggregates | Limits | Steel slag | Gravel | Blend H1 | Blend H2 |
|---|---|---|---|---|---|
| **Micro-Deval Abrasion** | <18% | 7.1 | 2.5 | 14.1 | 13.2 |
| **Soundness** | <12% | 0.2 | 0.1 | 0.5 | 0.7 |
| **Degradation** | Increases on Sieve #8, <4% | 0.3 | 1 | 0.1 | 1.7 |

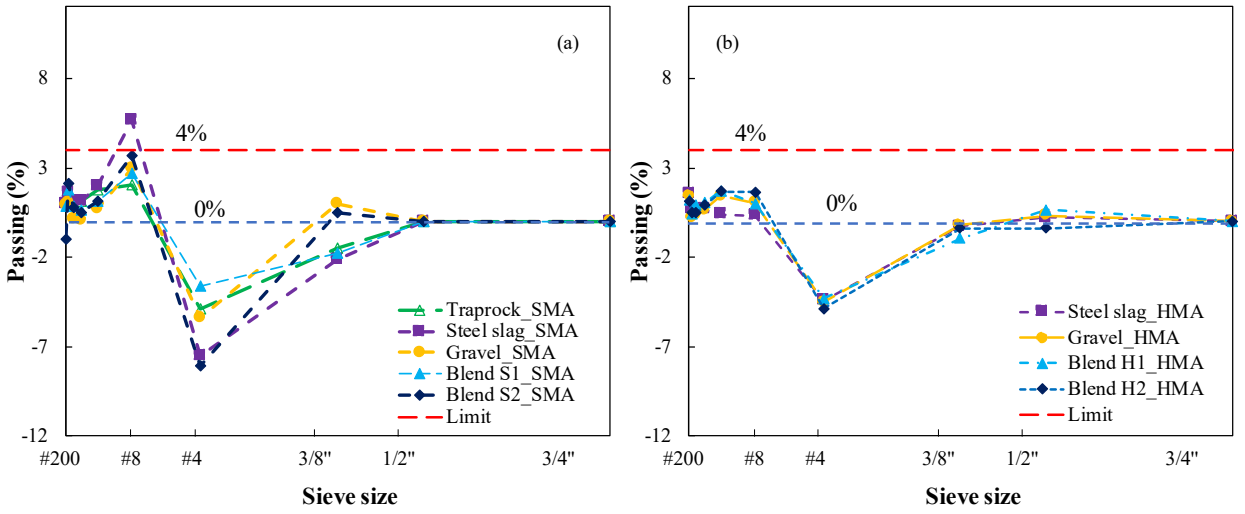


**Figure 3.1 Changes on each sieve for all candidate aggregates in mixtures after degradation tests: (a) in SMA mixtures, and (b) in HMA mixtures.**

### 3.1.3 Correlation between the LA and Micro-Deval Abrasion Test Results

Figure 3.2 (a) illustrates the weight loss results from both LA Abrasion and Micro-Deval Abrasion tests for all candidate aggregates. Traprock, gravel, chat, and steel slag exhibited notable resistance to abrasion in both tests. The original candidate aggregates of dolomite and limestone exhibit significant weight loss in two abrasion tests, but this value decreased notably when they are blended with chat, which demonstrated a lower weight loss. Additionally, consistent trends were observed in the results for the same aggregates across both abrasion tests, and a strong linear relationship between the two tests is evident, as depicted in Figure 3.2 (b). However, Figure 3.3 illustrates the disparity between the same samples following two different abrasion tests. The aggregates subjected to the Micro-Deval Abrasion test exhibited smooth surfaces resulting from abrasion by small steel spheres. In contrast, those exposed to the LA Abrasion test displayed numerous crushed fine particles, indicating the damage caused by the big steel spheres.

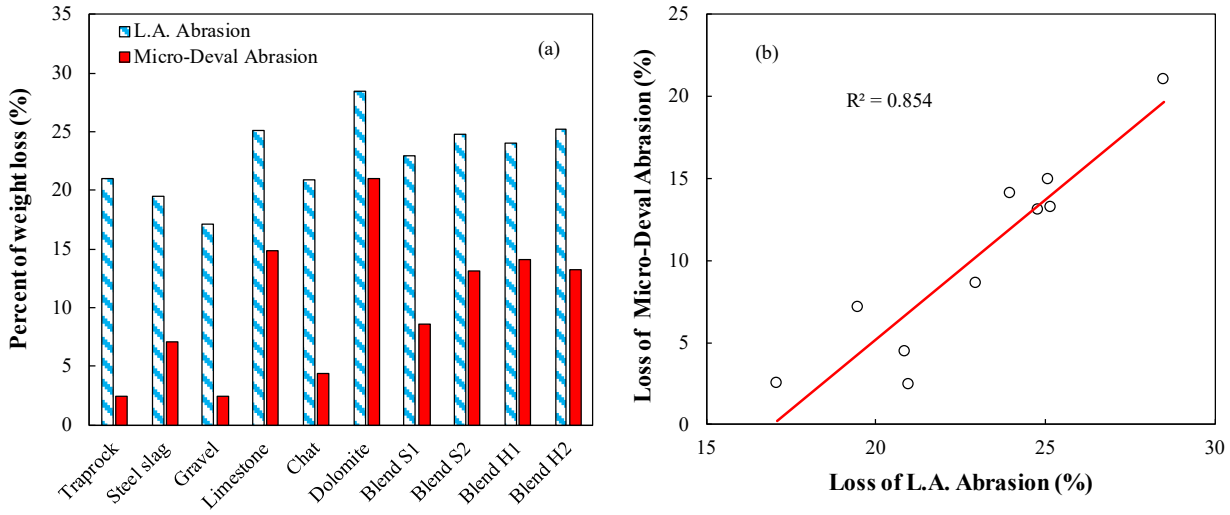


**Figure 3.2 (a) The loss of the two abrasion tests for each candidate aggregates, and (b) the relationship between the results of the two abrasion tests.**

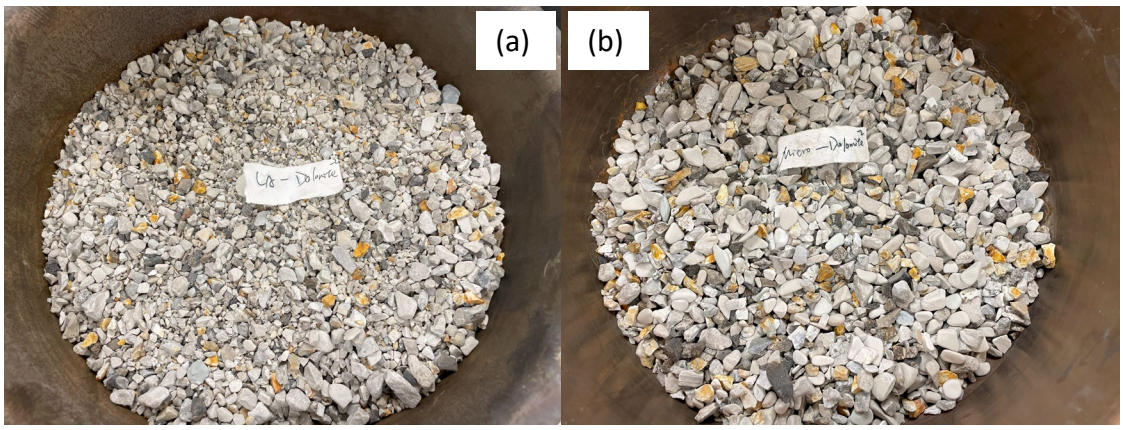


**Figure 3.3 Aggregate samples after abrasion tests: (a) LA abrasion test, and (b) Micro-Deval abrasion test.**

## 3.2 Volumetric Mix Design

Superpave volumetric mix designs for both SMA and HMA mixtures with candidate aggregates referenced the designs for control mixtures, followed by several trials to align with volumetric requirements in AASHTO M 325 and M 323 respectively. All the details of trailed gradation, design process, final volumetric designs and verification results of durability and workability are presented in APPENDIX C. The composition of the final volumetric mix design for each SMA and HMA mixture is presented in Tables 3.7 and 3.8.

**Table 3.7 Composition of Final Volumetric Designs for All SMA Mixtures**

| Mixtures | Candidate Aggregates | | Remaining Parts in JMF | | | | |
|---|---|---|---|---|---|---|---|
| | | | Other Aggregates Stockpiles | | Binder Content | Fly Ash | Fiber |
| | Stockpiles | Ratio | Dolomite _1/2"C | Dolomite_ 3/8"M | PG 64-22V | Class C | Cellulose Fibers |
| **ST (Control)** | Traprock_ 1/2"M | 10% | 22% | 6% | 7.50% | 7% | 0.30% |
| | Traprock_ 1/2" | 37% | | | | | |
| | Traprock_ 3/8"#4 | 18% | | | | | |
| **SS** | Steel slag_0*1" Slag | 65% | 22% | 6% | 6.50% | | |
| **SG** | Gravel_1/ 2"C | 58% | 19% | 16% | 7.40% | | |
| **SLC** | Limestone _CM14 | 30% | 11% | 10% | 7.40% | | |
| | Chat_3/8" | 42% | | | | | |
| **SDC** | Dolomite_ 1/2" | 35% | 7% | 11% | 6.90% | | |
| | Chat_3/8" | 40% | | | | | |

**Table 3.8 Composition of Final Volumetric Designs for All SMA Mixtures**

| Mixtures | Candidate Aggregates | | Remaining Parts in JMF | | | | | |
|---|---|---|---|---|---|---|---|---|
| | | | Other Aggregates Stockpiles | | | Binder Content | | Filler |
| | **Stockpiles** | **Ratio** | **Limestone _1/2"** | **Limestone _MAN SAND** | **RAP (5.5% AC )** | **PG 64-22 (Virgin)** | **Total** | **Bag House Fines** |
| **HLC (Control)** | Limestone _3/8" | 13% | 12% | 14% | 40% | 3.61% | 5.80% | 1% |
| | Chat_1/2" | 20% | | | | | | |
| **HS** | Steel slag_0*1" Slag | 34% | 13% | 13% | 39% | 3.15% | 5.30% | |
| **HG** | Gravel_ 1/2"C | 38% | 11% | 12% | 38% | 4.33% | 6.40% | |
| **HDC** | Dolomite_ 3/8"C | 10% | 12% | 17% | 38% | 3.72% | 5.80% | |

## 3.3 BMD in SMA

### 3.3.1 BMD Performance Verification for SMA

Following the successful compliance with all volumetric parameters, draindown, and moisture resistance limits stipulated in the Superpave volumetric design, the mixture performance verification including IDEAL-CT and HWTT was conducted to evaluate the resistance of SMA mixtures to cracking and rutting.

#### 3.3.1.1 IDEAL-CT

Figure 3.4 (a) illustrates the variations in load during the IDEAL-CT tests for all SMA mixtures with candidate aggregates. A higher $CT_{Index}$ indicates superior cracking resistance for an asphalt mixture. However, having a higher tensile strength in a mixture doesn't necessarily equate to better cracking resistance. For instance, while the SS exhibited the highest peak load, it also demonstrated the highest rate of loading decrease after cracking, resulting in the lowest $CT_{Index}$. Figure 3.4 (b) demonstrates the $CT_{Index}$ results for SMA mixtures with all candidate aggregates. Except for the SS, all SMA mixtures with other candidate aggregates met the $CT_{Index}$ limit of 135, which means that the resistance of cracking for SS is not qualified even though the mixture passes all the requirements in the Superpave volumetric design.

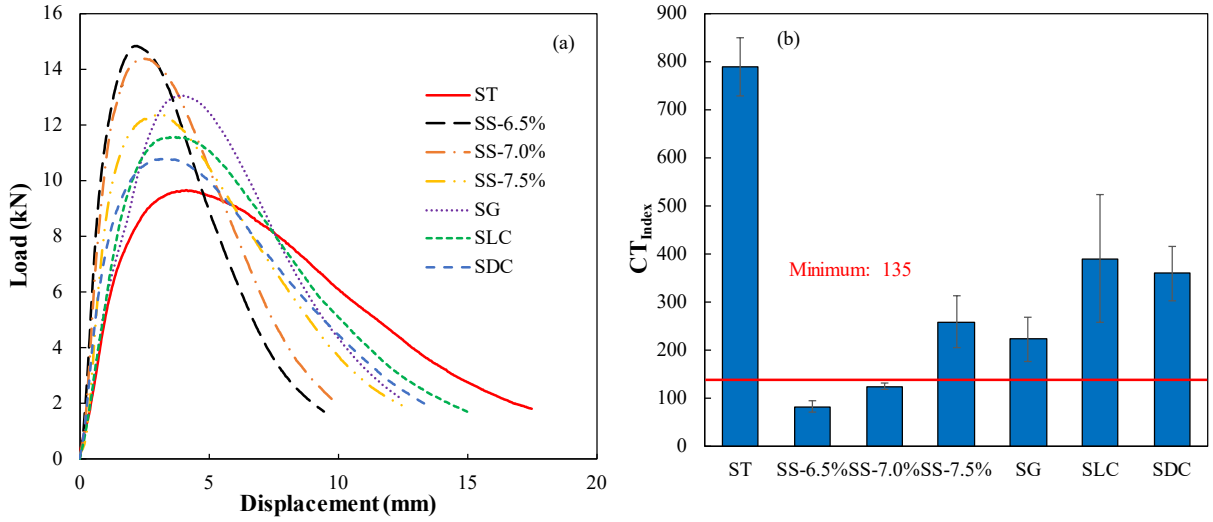


**Figure 3.4 IDEAL-CT tests results of SMA mixtures: (a) the load vs. displacement, and (b) $CT_{Index}$.**

According to the methodology in this study, the binder content was revised for SS by conducting the two performance tests at different binder contents. Considering the optimum binder content determined as 6.5% by the Superpave volumetric design, additional higher binder contents were used to conduct the performance tests to ensure comprehensive coverage of the $CT_{Index}$ and RRI results across trialed binder contents. With the escalation of binder content, the $CT_{Index}$ for the SS experienced an upward trajectory, achieving a notable value of 390.2 at a binder content of 7.5%. Then the $CT_{Index}$ of SS surpassed the prescribed limit

of 135, indicating enhanced resistance to cracking. The load-versus-displacement curves and $CT_{Index}$ for SS at the binder contents of 7.0% and 7.5% were calculated, as shown in Figure 3.4.

Figure 3.5 illustrates the IDEAL-CT results of SMA mixtures with candidate aggregates on the interaction diagram. Notably, SLC and SDC manifest closely aligned $CT_{Index}$ values. However, the SLC exhibited a higher $G_f$, denoting superior toughness compared to SDC. Besides, the results of SS using varying binder contents are also depicted in Figure 3.5. As the binder content increases, both $G_f$ and $l_{75}/m_{75}$ experienced an elevation, resulting in a heightened $CT_{Index}$.

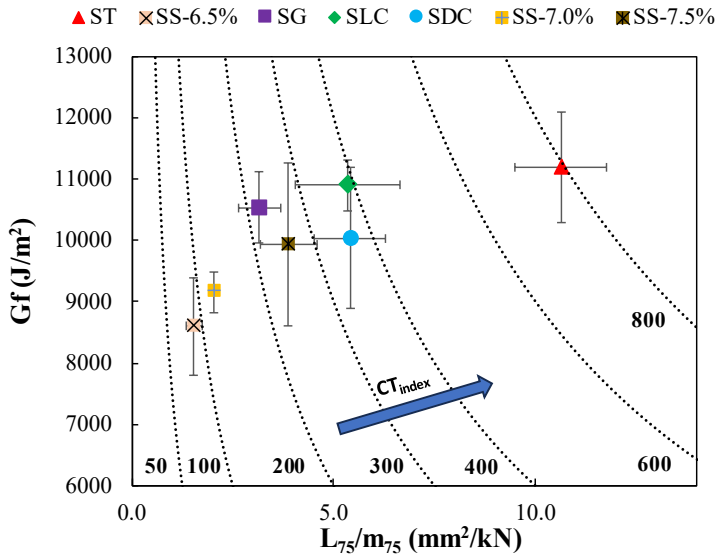


**Figure 3.5 $G_f$ versus $l_{75}/m_{75}$ interaction diagrams of SMA mixtures.**

### 3.3.1.2 HWTT

Figure 3.6 (a) illustrates the rut depth for all SMA mixtures across various loading cycles. All mixtures successfully adhered to the maximum requirement of a 12.5mm rut depth at 20,000 loading cycles. Figure 3.6 (b) summarizes the RRI results for SMA mixtures with candidate aggregates. Importantly, all these results met the minimum RRI requirement of 9.9, as calculated for a 12.5mm rut depth at 20,000 loading cycles. The rut depth increased along with the increase of binder content of the SS, but it still satisfied the requirement for SS at a binder content of 7.5%. The SLC and SDC demonstrated comparable RRI values with the control mixture ST, all significantly lower than that of the SG.

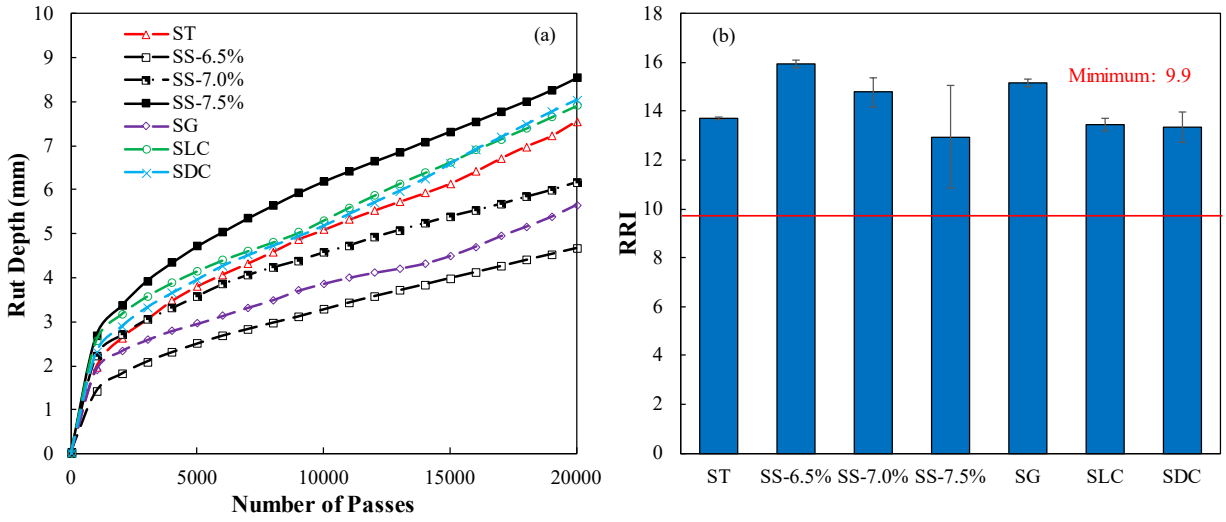


**Figure 3.6 HTWW results of SMA mixtures: (a) rut depth vs. the number of passes, and (b) RRI.**

### 3.3.2 Determine Optimum Performance Binder Content for SS

The trends of the cracking and rutting resistance changes as a function of binder content are presented in Figure 3.7. The range of the design binder content was determined based on the acceptable performance limits. As shown in Figure 3.7, the cracking resistance requirement restrained the lower limit of binder content, and the upper limit was estimated through the projection of the rutting resistance testing result. The highlighted area in the figure represents the range of binder content that allows the mix to meet performance requirements. The suitable binder content was approximately 7.1% to 7.9%; whereas the optimum volumetric binder content was 6.5%. Considering the variability, uncertainty, and cost in construction, based on the testing results, the performance optimum binder content was determined as 7.3% in this design. There is a certain possibility that, in some design cases, the lower limit determined by the cracking test is higher than the upper limit restricted by the rutting test. In this scenario, as indicated in Figure 2.4, the design iteration may return further to the gradation adjustment. While ensuring a well-structured gap gradation, the proportions in the aggregate combination can be revised.

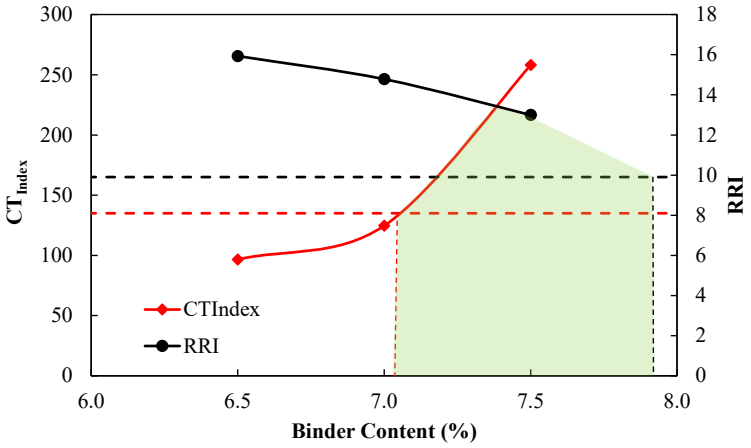


**Figure 3.7 Range of binder content for performance requirements.**

### 3.3.3 Moisture Susceptibility and Draindown Verification for SS

After the performance optimum binder content for SMA was determined, the durability and the constructability of the newly designed mix were verified since a different binder content was used. The moisture susceptibility and the draindown tests were performed again under the new design. Compared to the results tested at the original binder content of 6.5%, increasing the binder content led to a slight increase in draindown percentages from 0.17% to 0.21%, and a decrease in TSR value from 0.96 to 0.85. However, both TSR values and draindown percentages still met the requirements of 0.8 and 0.3%, respectively. According to the design flowchart in Figure 2.4, the design formula can be finalized with the volumetric optimum gradation and the performance optimum binder content.

### 3.3.4 Finial Design for SS

The composition of the final volumetric mix design for SS is presented in Table 3.9. The optimum performance binder content was 7.3%, compared to 6.5% as determined by the volumetric mix design.

**Table 3.9 Composition of Final Design for SS**

| Mixture | Candidate Aggregate | | Remaining Parts in JMF | | | | |
|---|---|---|---|---|---|---|---|
| | | | Other Aggregates Stockpile | | Binder Content | Fly Ash | Fiber |
| | Stockpiles | Ratio | Dolomite _1/2"C | Dolomite _3/8"M | PG 64-22V | Class C | Cellulose Fibers |
| **SS** | Steel slag_0*1" Slag | 65% | 22% | 6% | 6.50% | 7.3% | 0.3% |

## 3.4 BMD in HMA

### 3.4.1 BMD Performance Verification for HMA

Following the successful compliance with all volumetric parameters and moisture resistance limits stipulated in the Superpave volumetric design, the mixture performance verification including IDEAL-CT and HWTT was conducted to evaluate the resistance of HMA mixtures to cracking and rutting.

#### 3.4.1.1 IDEAL-CT

Figure 3.8 (a) depicts the load vs. the vertical displacement during the IDEAL-CT tests for all HMA mixtures, while Figure 3.8 (b) illustrates the $CT_{Index}$ results for HMA mixtures with all candidate aggregates. Except HS, all HMA mixtures with other candidate aggregates met the $CT_{Index}$ limit of 45. The resistance to cracking for the HS did not meet the qualification criteria, despite passing all requirements in the Superpave volumetric design.

To address this issue, the binder content for the HS was revised using the methodology outlined in this study. Two BMD performance tests were conducted at different binder contents, considering the optimum binder content determined as 5.3% by the Superpave volumetric design. Additional higher binder contents were utilized to ensure comprehensive coverage of the $CT_{Index}$ and RRI results across various binder contents trialed. As the binder content increased, the $CT_{Index}$ for the HS exhibited an upward trend, reaching a significant value of 137.8 at a binder content of 6.3%. Then the $CT_{Index}$ of HS exceeded the prescribed limit of 45, indicating improved resistance to cracking. The load vs. displacement curve and $CT_{Index}$ for HS at the binder contents of 5.8% and 6.3% were calculated, as presented in Figure 3.8.

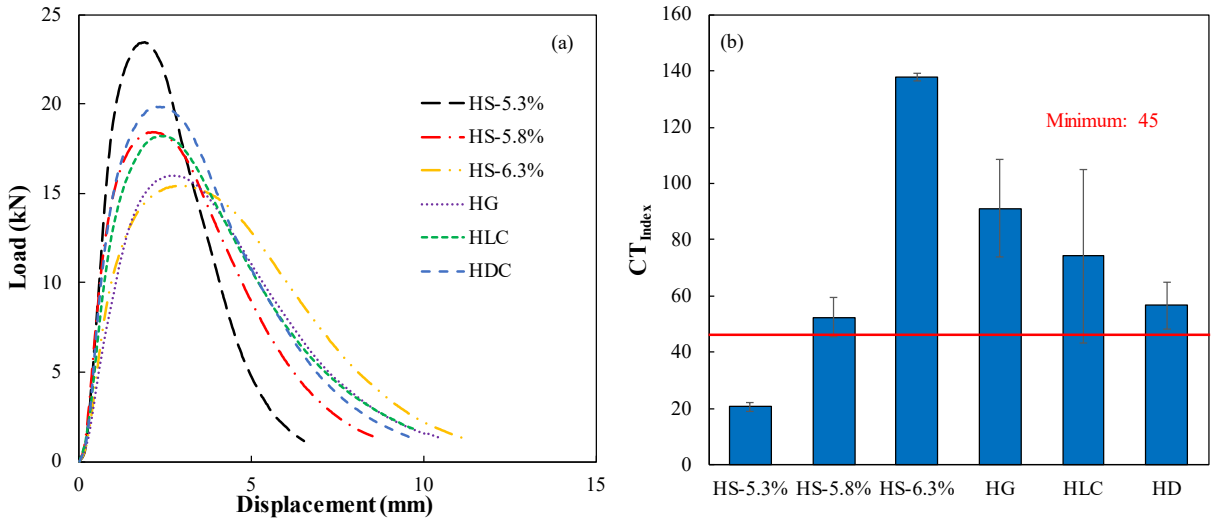


**Figure 3.8 IDEAL-CT tests results of HMA mixtures: (a) the load vs. displacement, and (b) $CT_{Index}$.**

Figure 3.9 presents the IDEAL-CT results of HMA mixtures on the interaction diagram. The results of HS using varying binder contents are also displayed in Figure 3.9. Notably, HMA

mixture with HS with a binder content of 5.3% exhibited the lowest *Gf* and $l_{75}/m_{75}$, resulting in the lowest $CT_{Index}$. With increasing binder content, HS demonstrated enhanced toughness and a transition towards better ductile behavior. Among the other three HMA mixtures featuring candidate aggregates, HG exhibited superior ductile-brittle behavior, resulting in higher $CT_{Index}$ values, despite having the lowest toughness.

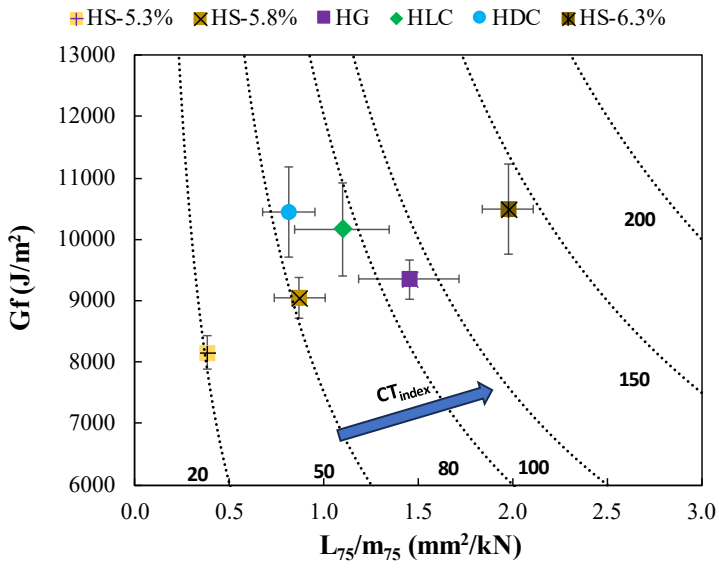


**Figure 3.9 $G_f$ versus $l_{75}/m_{75}$ interaction diagrams of HMA mixtures.**

### 3.4.1.2 HWTT

Figure 3.10 (a) depicts the rut depth for all HMA mixtures across various loading cycles. All mixtures met the maximum requirement of a 12.5mm rut depth at 20,000 loading cycles. The RRI results for HMA mixtures with candidate aggregates are summarized in Figure 4.28 (b). All these results satisfied the minimum RRI requirement of 9.9. While the rut depth increased with the binder content of the HS, it still fulfilled the requirement for the HS at a binder content of 6.3%. HMA mixtures with HG and HDC demonstrated comparable RRI values with HLC, which served as the control HMA mixtures.

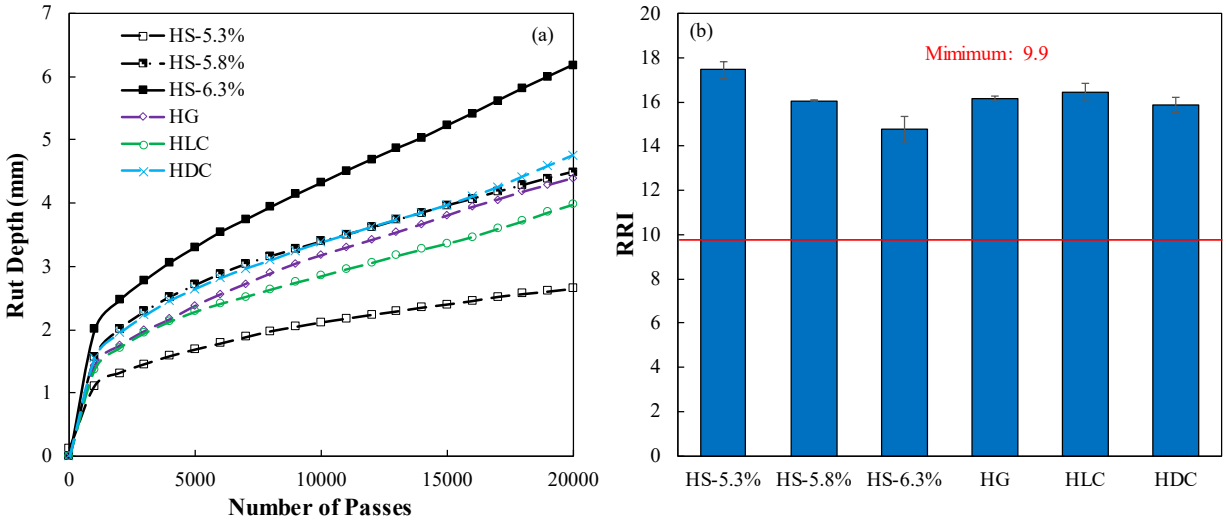


**Figure 3.10 HWTT results of HMA mixtures: (a) rut depth versus the number of passes, and (b) RRI.**

### 3.4.2 Determine Optimum Performance Binder Content for HS

Figure 3.11 illustrates the trends in cracking and rutting resistance changes relative to binder content. The limits of cracking and rutting resistance delineate an area representing the range of binder content allowing the mixture to meet performance requirements. The suitable binder content fell approximately within the range of 5.8% to 7.5%, with the optimum volumetric binder content identified as 5.3%. Considering variability, uncertainty, and construction costs, the performance optimum binder content was determined as 6.0% in this design based on the testing results. In certain design scenarios, there is a possibility that the lower limit determined by the cracking test exceeds the upper limit restricted by the rutting test. In these cases, the design iteration may necessitate further adjustments to the gradation.

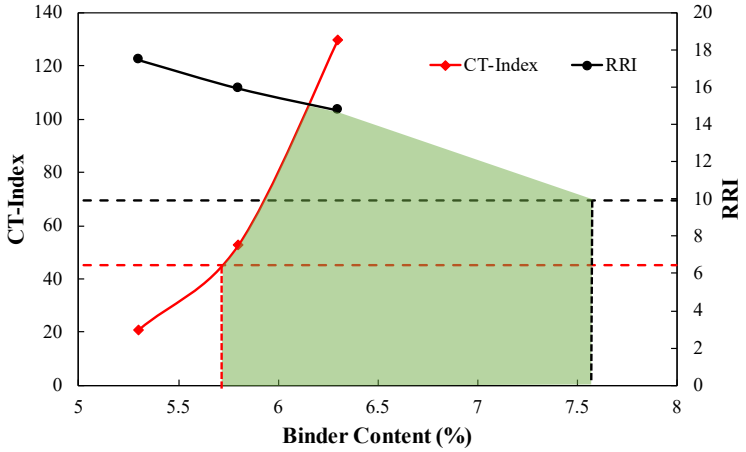


**Figure 3.11 Range of binder content for performance requirements.**

### 3.4.3 Moisture Susceptibility Verification for HS

After the performance optimum binder content for HMA was determined, the durability of the newly designed mix was verified, as a different binder content was utilized. The moisture susceptibility test was conducted again under the new design conditions. It indicated that the TSR value decreased from 0.85 to 0.80 when the binder content changed from 5.3% to 6.0%, yet it remained within the acceptable limit. As per the design flowchart outlined in Figure 2.4, the design formulation was finalized incorporating both the volumetric optimum gradation and the performance optimum binder content.

### 3.4.4 Finial Design for HS

The composition of the final volumetric mix design for HS is presented in Table 3.10. The optimum performance binder content was 6.0%, compared to 5.3% as determined by the volumetric mix design. The other components were kept consistent with the results obtained from the volumetric design.

**Table 3.10 Composition of Final Volumetric Design for HS**

| Mixture | Candidate Aggregate | | Remaining Parts in JMF | | | | | |
|---|---|---|---|---|---|---|---|---|
| | | | Other Aggregates Stockpiles | | | Binder Content | | Filler |
| | Stockpile | Ratio | Limestone _1/2" | Limestone_ MAN SAND | RAP (5.5% AC) | PG 64-22 (Virgin) | Total | Bag House Fines |
| **HS** | Steel slag_ 0*1" Slag | 34% | 13% | 13% | 39% | 3.87% | 6.00 % | 1% |

## 3.5 Summary

This chapter presents the outcomes of a comprehensive study involving materials characterization, mix design, and performance assessments of potential aggregate used as potential substitutes for traprock in SMA mixture and limestone & chat in HMA mixture. The following conclusions are drawn based on the results and discussions presented in this study.

- Gravel aggregate could be utilized to replace traprock in SMA mixtures and limestone & chat in HMA mixtures, respectively, while passing the aggregate durability tests and forming mixtures with adequate performance.
- In terms of limestone and dolomite, the testing results showed that using limestone or dolomite alone as the coarse aggregate in both SMA and HMA mixtures would create challenges to meet the requirement in *VMA*. To resolve the issue, the researchers created new stockpiles by blending them with chat, which exhibited relatively fine gradation and excellent durability in the screening tests. The SMA mixtures with dolomite & chat and limestone & chat, and HMA mixture with dolomite & chat, achieved acceptable volumetric properties and promising cracking and rutting resistance.

- During the design of both SMA and HMA mixtures with steel slag, while the mixture passed the volumetric and moisture susceptibility tests, they failed to meet the IDEAL-CT cracking threshold, and thus, the binder content was revised by conducting the performance tests at different binder contents. The performance optimum binder content was then identified, and the revised SMA and HMA mixtures with steel slag satisfied all the requirements in volumetric properties, moisture susceptibility, workability, and resistance to cracking and rutting.

# CHAPTER 4 MULTISCALE PERFORMANCE ANALYSIS

## 4.1 Performance Analysis on Materials Level

### 4.1.1 AMPT Performance Tests

At the material level, data from AMPT dynamic modulus, cyclic fatigue, and SSR tests were processed using the Excel-based FlexMAT™ program. The fundamental properties obtained from the program include dynamic modulus master curves with shift factors, fatigue damage accumulation curves, and permanent deformation under various loading conditions such as temperature, loading frequency, and amplitudes. Subsequently, these properties were further analyzed by considering local climate conditions, enabling the calculation of indices such as $S_{app}$ and the RSI to evaluate the fatigue and rutting resistance of the asphalt mixtures, respectively.

#### 4.1.1.1 AMPT Dynamic Modulus Test

Dynamic modulus tests were conducted on both SMA and HMA mixtures using all candidate aggregates. Figures 4.1 and 4.2 display the dynamic modulus master curve along with the results fitted by Sigmoidal and 2S2P1D models for SMA and HMA mixtures, respectively. The findings reveal that both the two models effectively fit the dynamic modulus data measured at three frequencies and three temperatures.

Following AASHTO T 378, two statistical indexes, $S_r\%$ and $S_r$, were calculated to assess the data quality of the dynamic modulus and phase angle. The results are presented in Appendix D. All $S_r\%$ and $S_r$ values were below the limits suggested in the standard for mixtures with NMAS 12.5mm. Furthermore, all dynamic modulus and phase angle values fell within the required range, indicating that all data were valid for performance analysis.

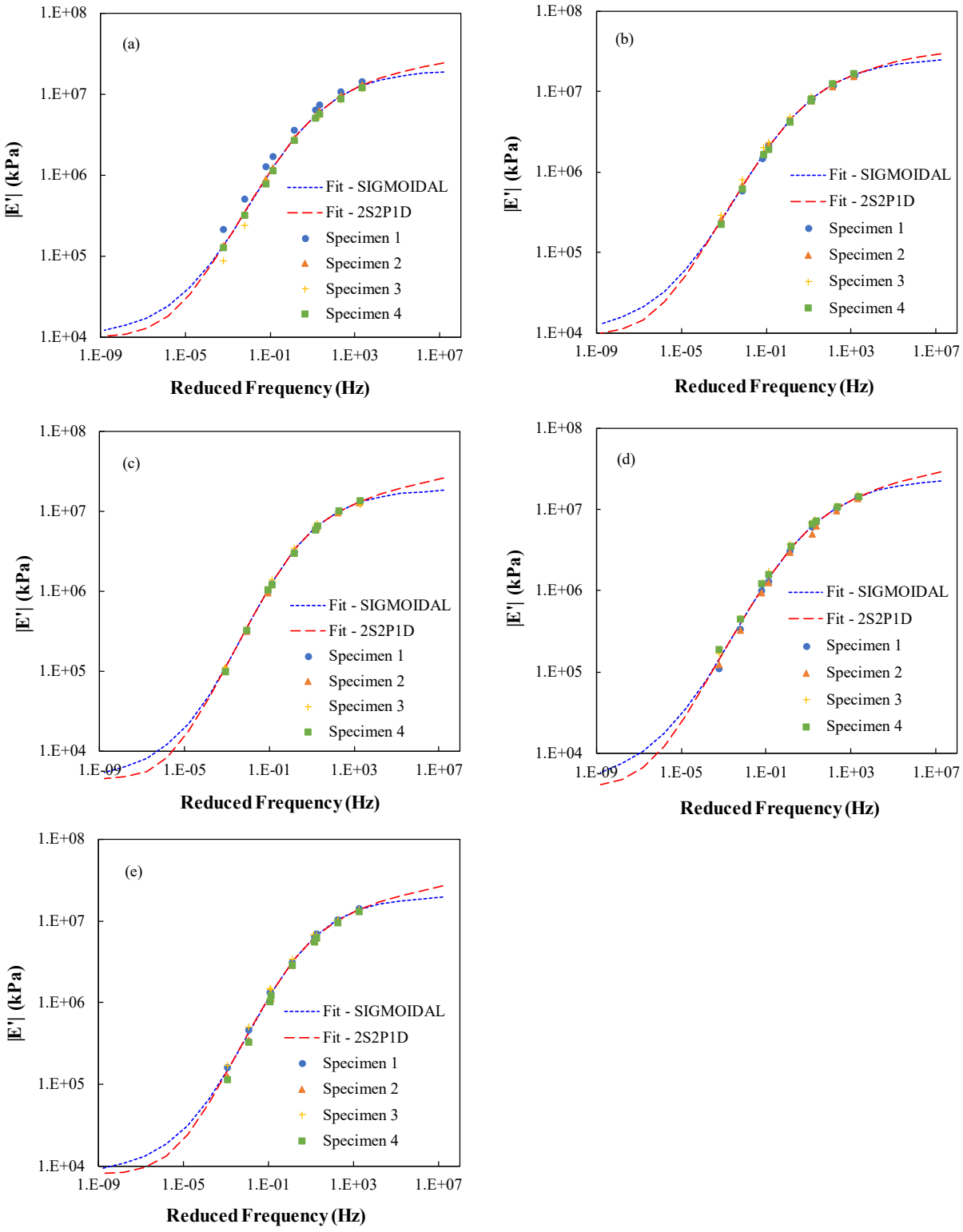


**Figure 4.1 Dynamic modulus data for all SMA mixtures: (a) ST, (b) SS, (c) SG, (d) SLC, and (e) SDC.**

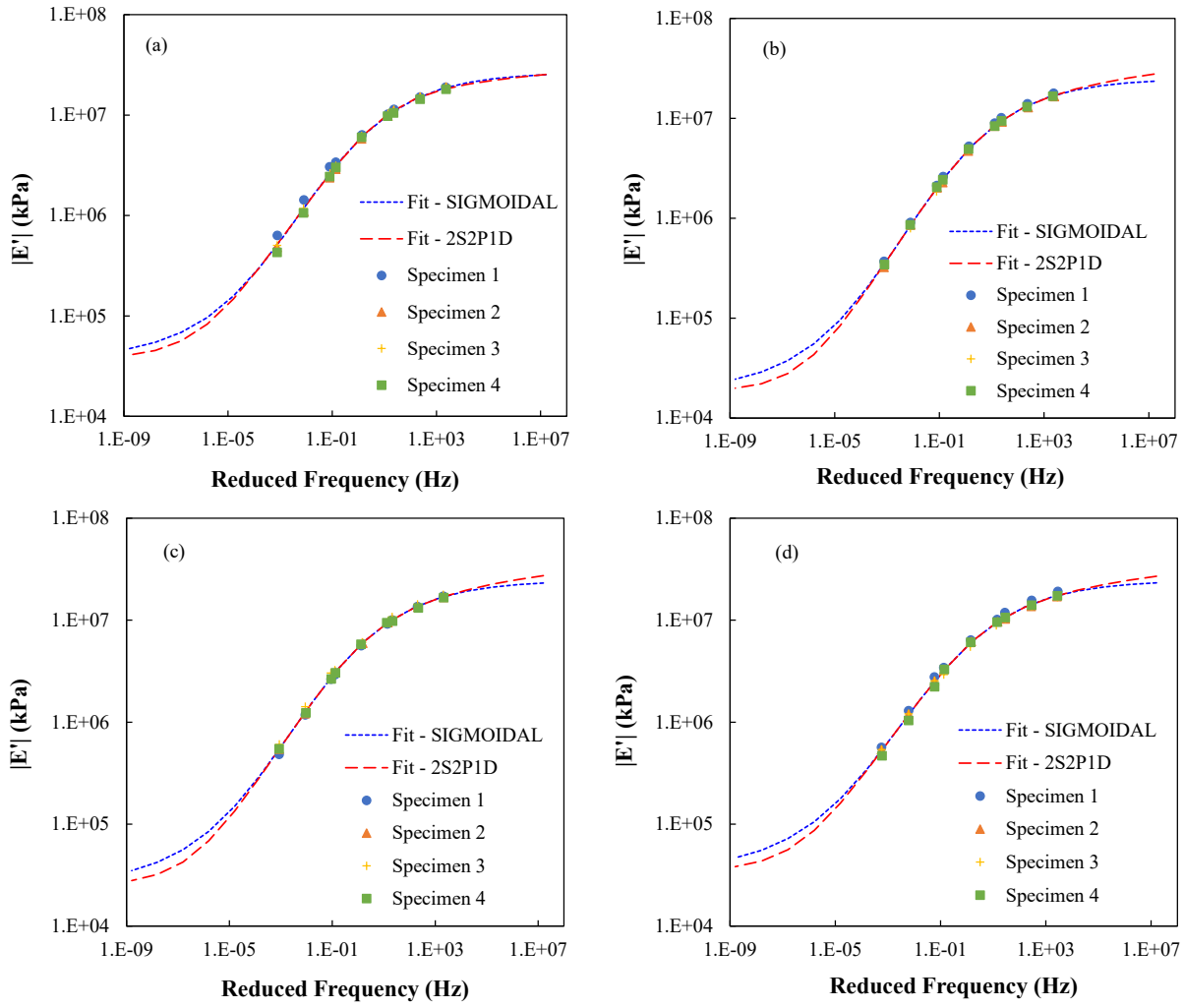


**Figure 4.2 Dynamic modulus data for all HMA mixtures: (a) HS, (b) HG, (c) HLC, and (d) HDC.**

Figures 4.3 and 4.4 provide an overall comparison of the dynamic modulus master curves for all SMA and HMA samples, employing the 2S2P1D model in this analysis. Notably, in the high-frequency, low-temperature region, the modulus of different SMA mixtures showed slight differences, as illustrated in Figure 4.3(b). All the SMA mixtures with candidate aggregates exhibited a higher dynamic modulus than the control mixture ST, with SS demonstrating the highest modulus. The moduli of SG and SDC closely aligned and were slightly lower than that of SLC. Additionally, except HMA mixture with HS, the fitted curves for HMA mixtures with various aggregates closely overlapped. The modulus values of different HMA mixtures were similar, particularly in the high-frequency, low-temperature region, highlighted in the semi-log plot shown in Figure 4.4(b). The fitted curve for HS tended to increase more slowly than the others, resulting in the lowest modulus at high frequency and low temperature among all HMA mixtures.

Table 4.1 presents the results of dynamic modulus values at the end of fitted curves for all SMA and HMA Mixtures. All the candidate aggregates demonstrated comparable dynamic modulus to the control in both SMA and HMA mixtures, respectively, suggesting a similar response for all candidate aggregates compared to the control under small loading amplitudes.

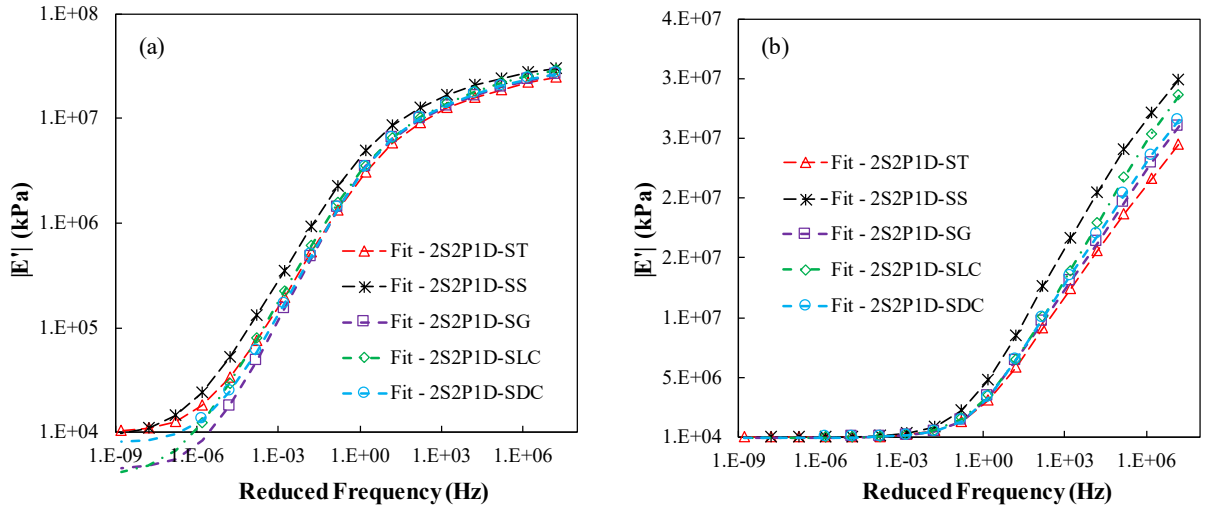


**Figure 4.3 Dynamic modulus data of SMA mixtures _2S2P1D: (a) in log-log scale, and (b) in semi-log scale.**

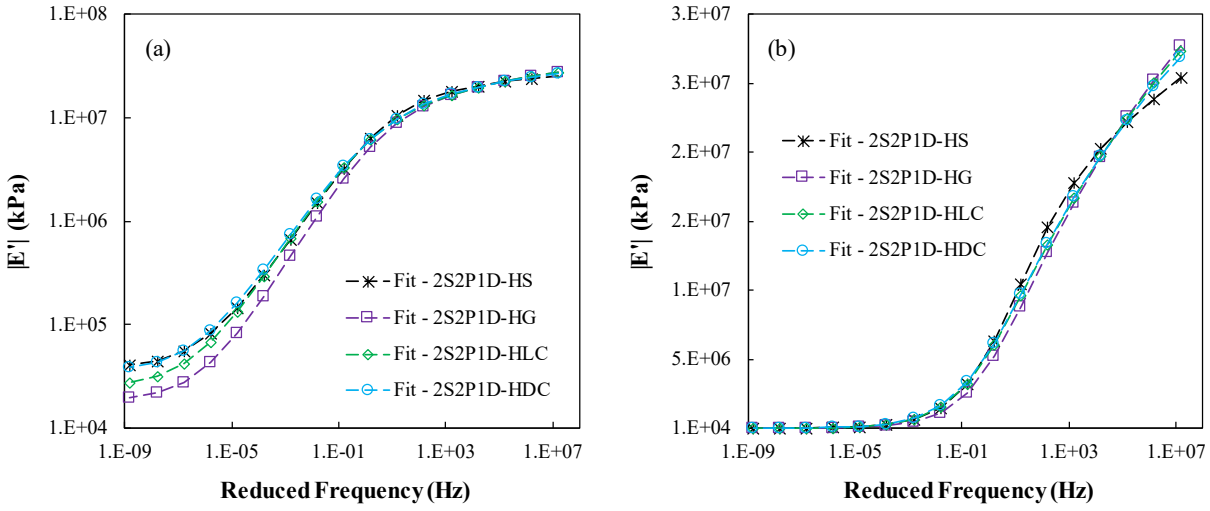


**Figure 4.4 Dynamic modulus data of HMA mixtures _2S2P1D: (a) in log-log scale, and (b) in semi-log scale**

**Table 4.1 Results of Dynamic Modulus Values at the End of Fitted Curve for All SMA and HMA Mixtures**

| Mixture Type | \|E'\|, kPa | % Increase vs. Control |
|---|---|---|
| **ST** | 2.446E+07 | 0.00 |
| **SS** | 2.991E+07 | 22.30 |
| **SG** | 2.600E+07 | 6.31 |
| **SLC** | 2.859E+07 | 16.90 |
| **SDC** | 2.654E+07 | 8.53 |
| **HLC** | 2.730E+07 | 0.00 |
| **HS** | 2.540E+07 | -6.96 |
| **HG** | 2.770E+07 | 1.47 |
| **HDC** | 2.690E+07 | -1.47 |

#### 4.1.1.2 AMPT Cyclic Fatigue Test

Cyclic fatigue tests were conducted on both SMA and HMA mixtures with all candidate aggregates. The damage characteristic curves of all SMA and HMA samples are presented in Figures 4.5 and 4.6. All the results for each sample showed the acceptable variability between the replicates.

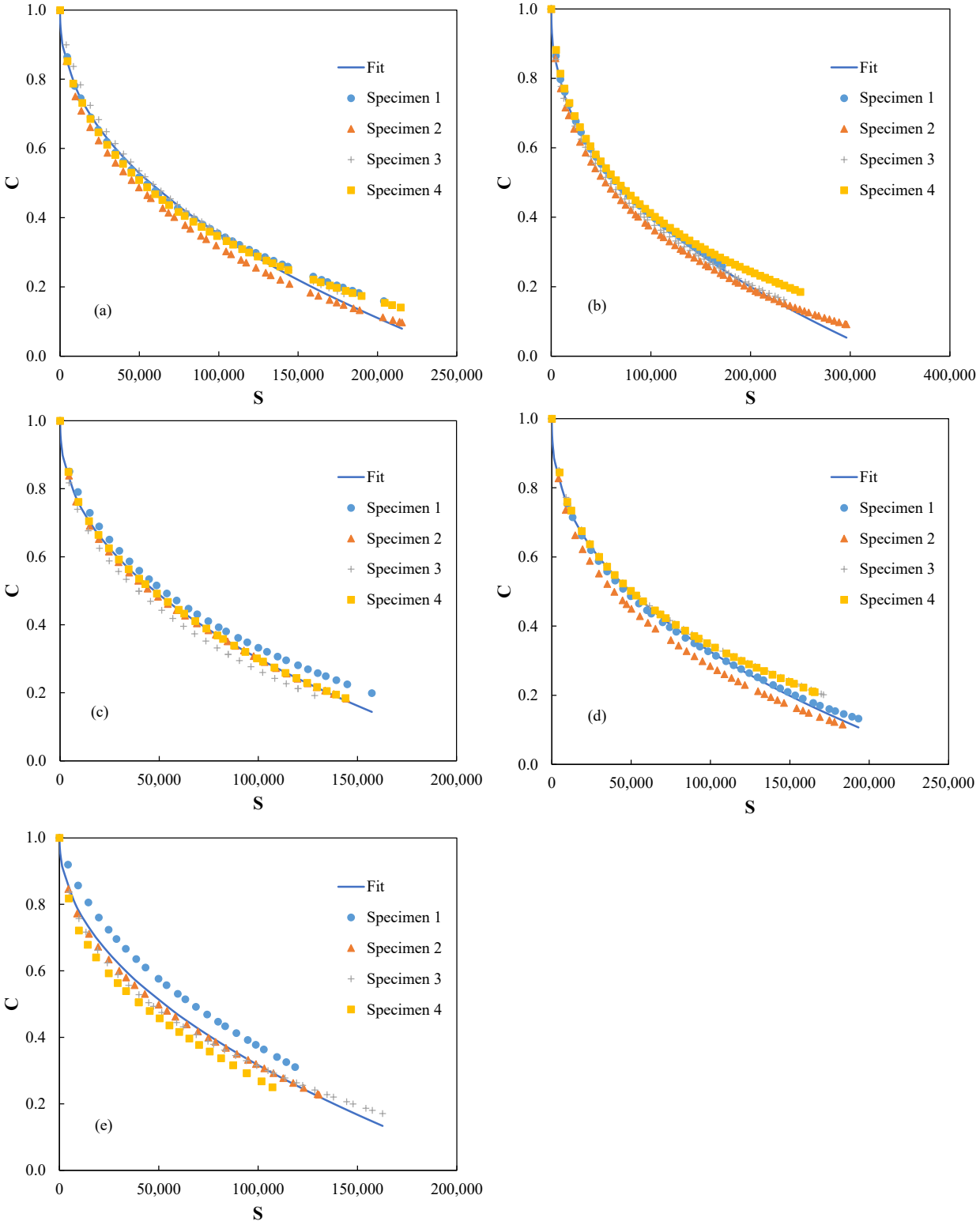


**Figure 4.5 Damage characteristic curves of all SMA mixtures: (a) ST, (b) SS, (c) SG, (d) SLC, and (e) SDC.**

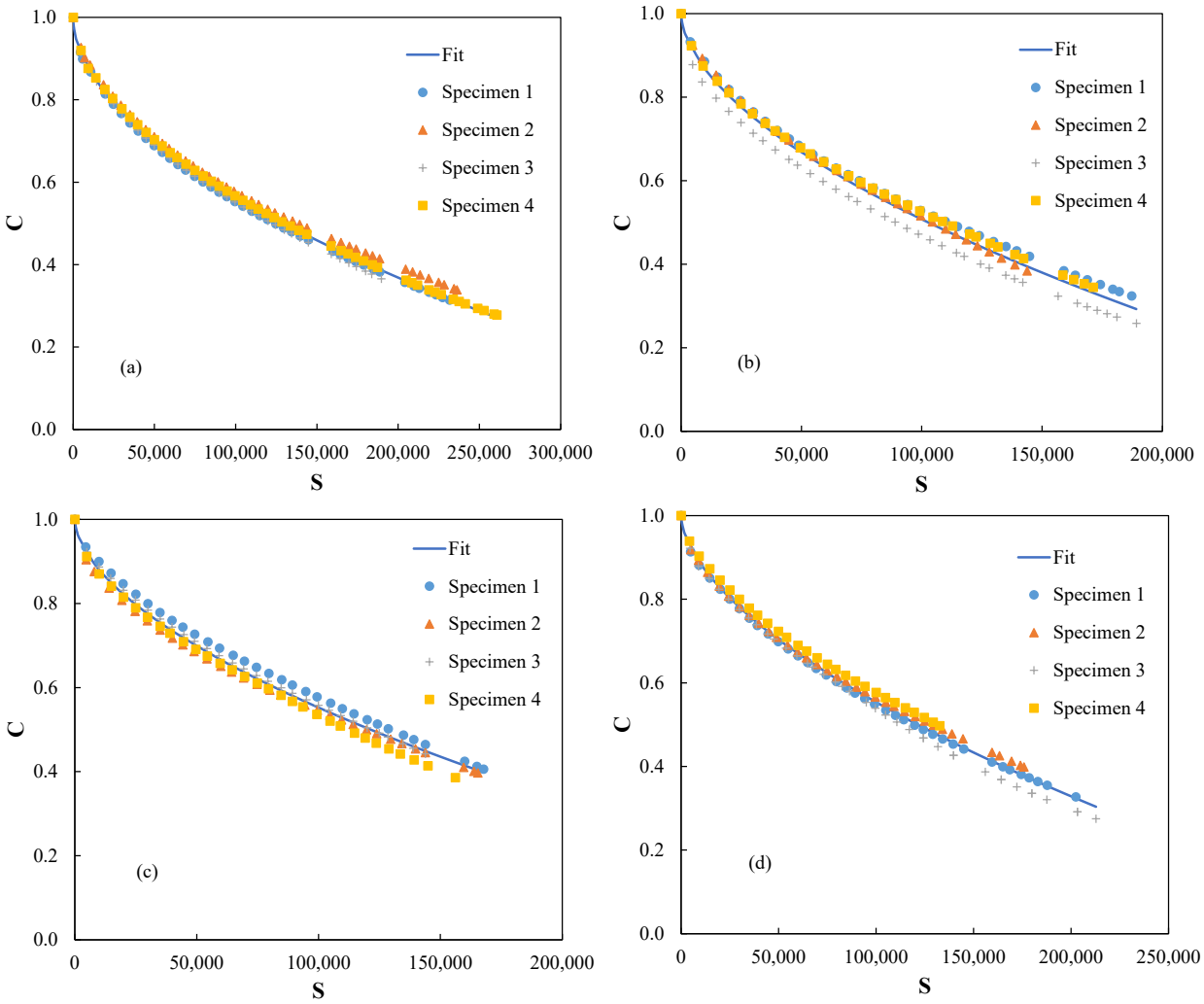


**Figure 4.6 Damage characteristic curves of the HMA mixtures with candidate aggregates: (a) HS, (b) HG, (c) HLC, and (d) HDC.**

Figure 4.7 illustrates the comparison of C vs. S curves among various SMA and HMA mixtures. Within SMA mixtures, SS occupied the highest position on the C vs. S curve. SG and SDC closely aligned and slightly fell below SDC and the control mixture ST. A similar trend was observed in HMA mixtures among different candidate aggregates. HS occupied the highest position while HG occupied the lowest. The results from HLC and HDC overlapped each other and fell in the middle position between the two extremes. This pattern was consistent with the dynamic modulus test results and supported previous research findings that stiffer mixtures tended to have higher positions on the C vs. S curve (Wang et al. 2020, Kim et al. 2022).

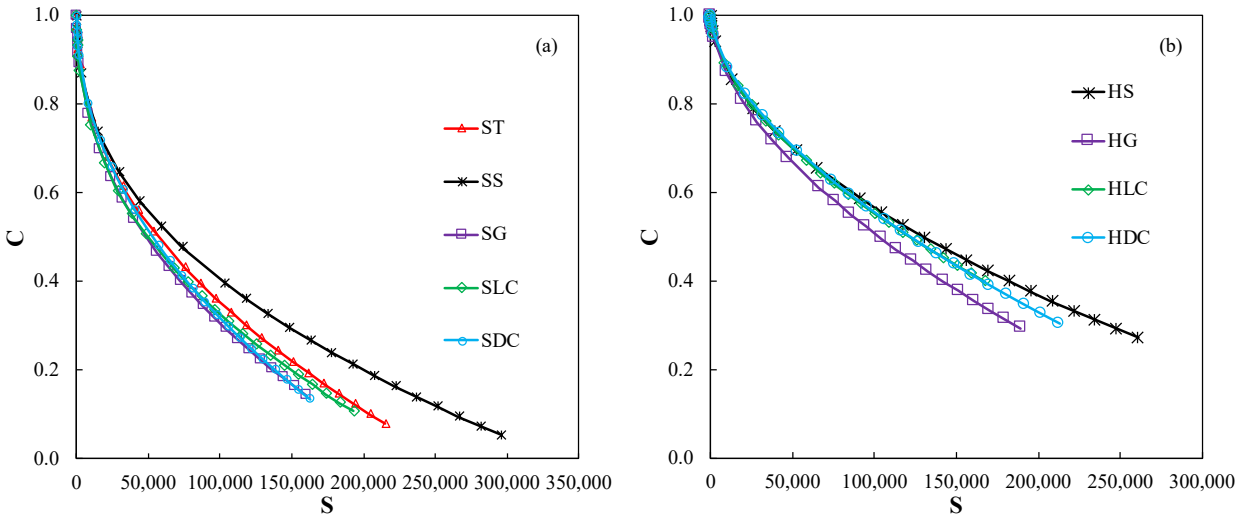


**Figure 4.7 Comparison of the damage characteristic curves of all mixtures: (a)SMA mixtures, and (b) HMA mixtures.**

However, the trend in the C vs. S curves did not necessarily translate to fatigue performance. Fatigue damage was also influenced by the material's tolerance capacity. In this context, another parameter, $D^R$, was proposed by other researchers as a failure criterion, representing material ductility on a scale from 0 to 1. Materials with a higher $D^R$ value were considered more ductile (Wang and Kim 2017; Wang et al. 2021).

Figure 4.8 presents the $D^R$ values of all SMA and HMA mixtures. Within SMA mixtures, SDC exhibited the lowest $D^R$ value, indicating the lowest ductility while SG slightly trails behind ST, SS, and SLC in $D^R$ value. Overall, the SMA mixtures with candidate aggregates demonstrated $D^R$ values comparable to the control mixture, ST. Among HMA mixtures, HS boasted the highest $D^R$ value, whereas the control mixture HLC demonstrated the lowest. Notably, HMA mixtures with all candidate aggregates exhibited superior ductility compared to the control mixtures represented by HLC.

Figure 4.9 and Table 4.2 present the $S_{app}$ values of all SMA and HMA samples. Among SMA mixtures, the control mixture ST exhibited the highest $S_{app}$, indicating superior resistance to fatigue cracking. The SMA mixtures with other candidate aggregates showed $S_{app}$ values close to each other, slightly lower than ST. Overall, the SMA mixtures with candidate aggregates had $S_{app}$ values comparable to the control mixture, ST. In HMA mixtures, all mixtures with candidate aggregates demonstrated higher $S_{app}$ values compared to the control mixture HLC, indicating enhanced resistance to fatigue cracking. Notably, SDC and HDC exhibited the lowest $S_{app}$ value among the SMA and HMA mixtures with candidate aggregates, respectively.

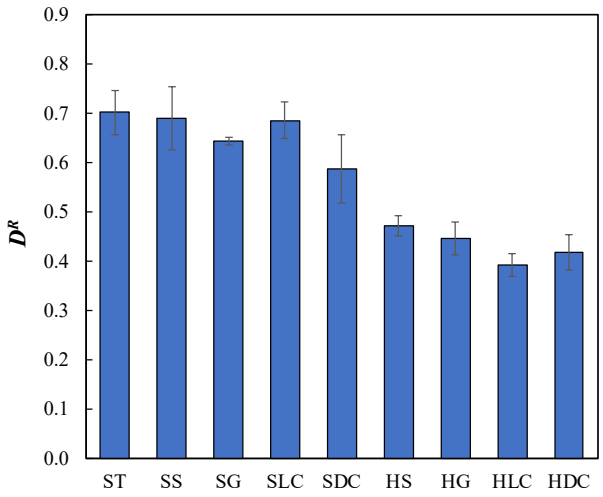


**Figure 4.8 $D^R$ value of all SMA and HMA mixtures.**

**Table 4.2 Results of $S_{app}$ Values for All SMA and HMA Mixtures**

| Mixture Type | $S_{app}$ | % Increase vs. Control |
|---|---|---|
| **ST** | 32.4 | 0.00 |
| **SS** | 29.1 | -10.12 |
| **SG** | 26.2 | -18.97 |
| **SLC** | 28.2 | -12.83 |
| **SDC** | 20.9 | -35.41 |
| **HLC** | 11.5 | 0.00 |
| **HS** | 14.5 | 25.95 |
| **HG** | 14.6 | 26.71 |
| **HDC** | 11.8 | 2.51 |

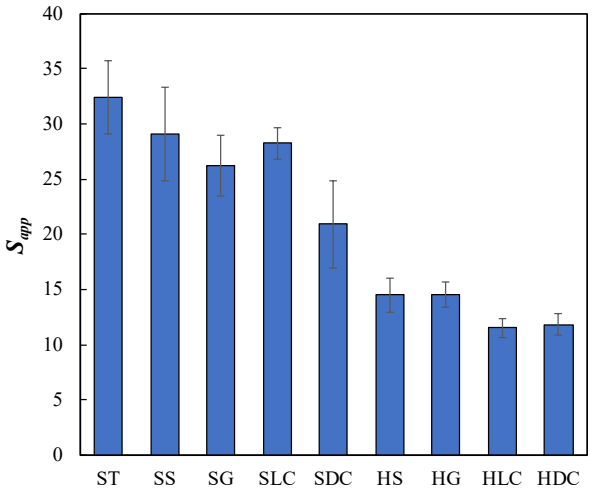


**Figure 4.9 $S_{app}$ for all SMA and HMA mixtures.**

#### 4.1.1.3 AMPT SSR Test

The SSR test was performed on all SMA and HMA mixtures. Figures 4.10 and 4.11 display the permanent strain resulting from applying three different deviatoric stress levels at both intermediate and high temperatures for all samples. The results of permanent strain at high and low temperatures for all SMA and HMA mixtures are consolidated in Figures 4.12 and 4.13, respectively.

Figure 4.12 reveals consistent rankings of permanent strain among SMA mixtures, except for the control mixture ST, at both high and low temperatures. Among the SMA mixtures with candidate aggregates, SS exhibited the lowest permanent strain while SG and SDC showed similar results, both higher than SLC.

Figure 4.13 illustrates consistent trends in permanent strain among HMA mixtures at different temperatures, except for HDC. HG exhibited the highest permanent strain at both high and low temperatures, potentially due to its binder content of 6.4%, which exceeded that of other HMA mixtures—5.8% for HLC, HDC, and 6.0% for HS, respectively. Similarly, the majority of HMA mixtures in this study demonstrated lower permanent strain than that of SMA mixtures overall, which could be attributed to the higher binder content of SMA mixtures.

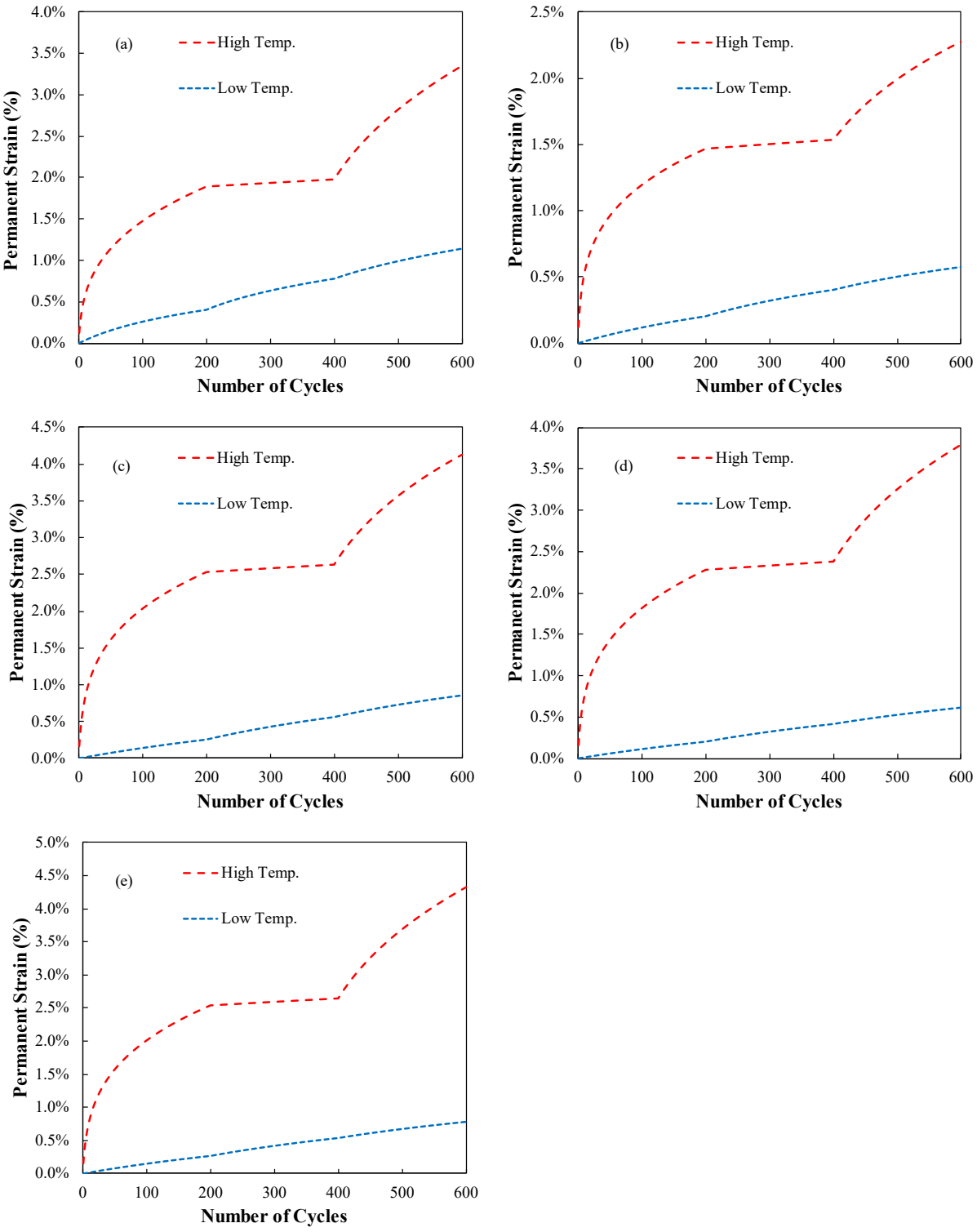


**Figure 4.10 Permanent strain at both high and low temperatures for all SMA mixtures: (a) ST, (b) SS, (c) SG, (d) SLC, and (e) SDC.**

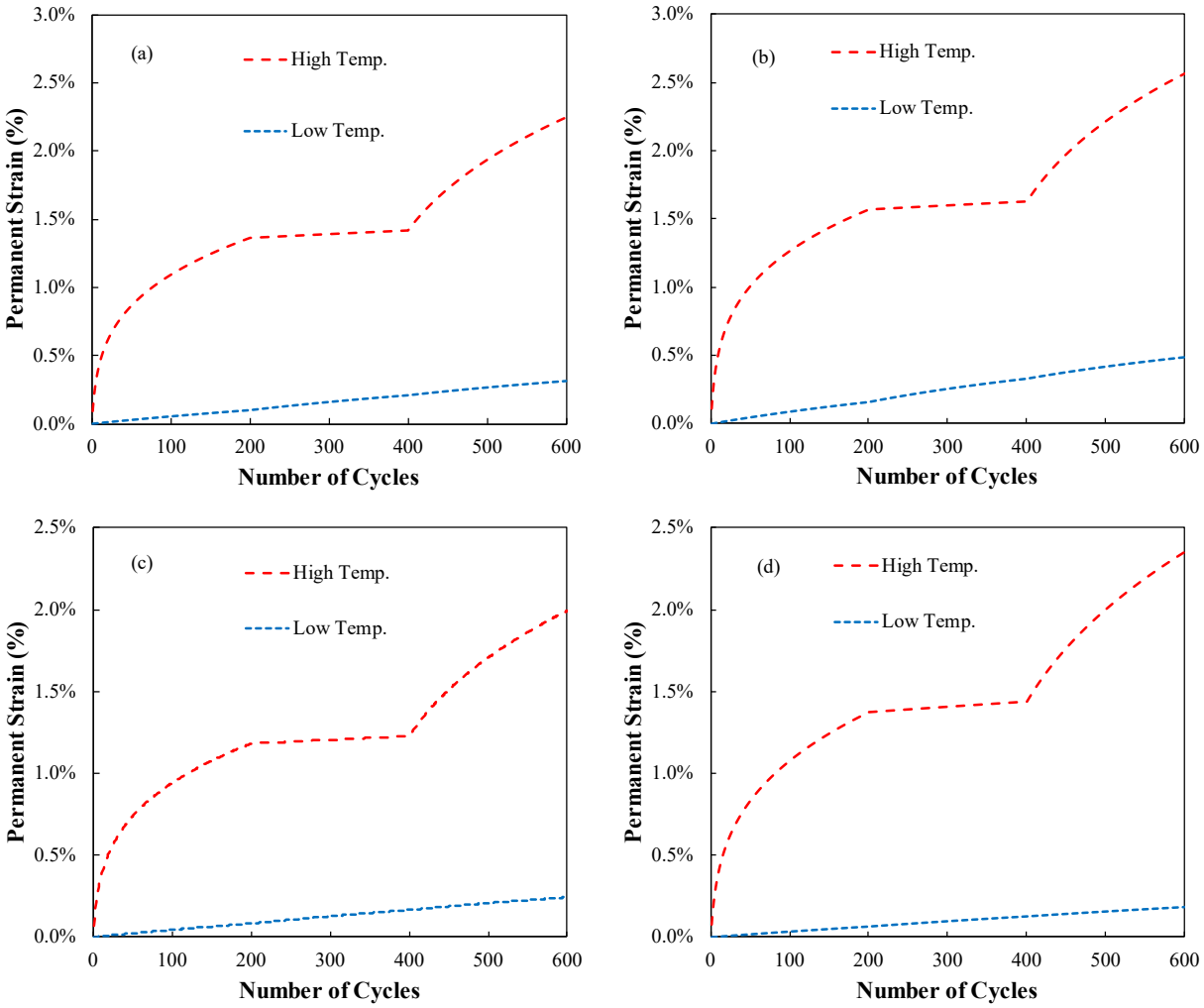


**Figure 4.11 Permanent strain at both high and low temperatures for all HMA mixtures: (a) HS, (b) HG, (c) HLC, and (d) HDC.**

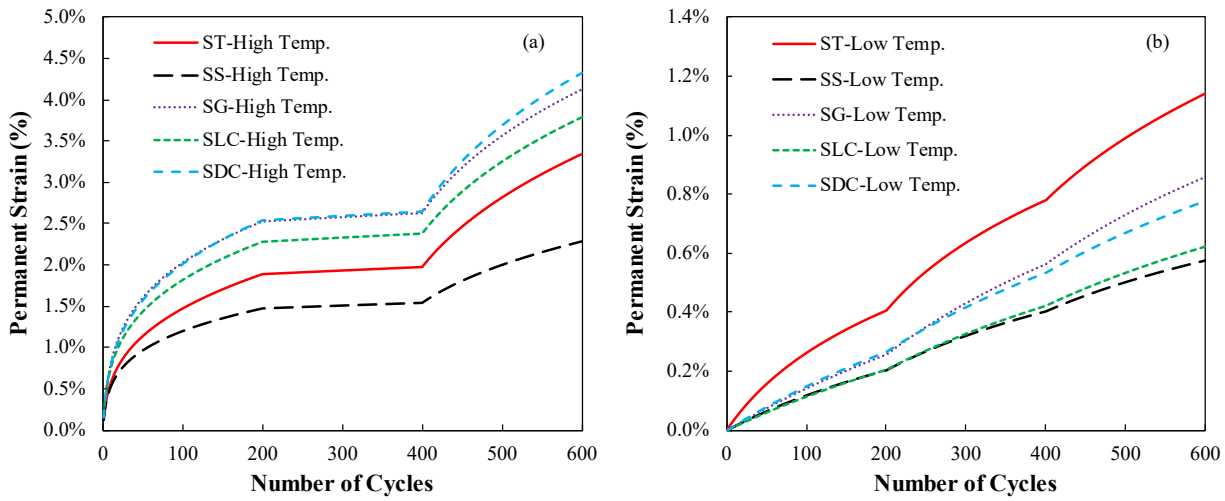


**Figure 4.12 Comparison of the permanent strain of all SMA mixtures: (a) at high temperature, and (b) at low temperature.**

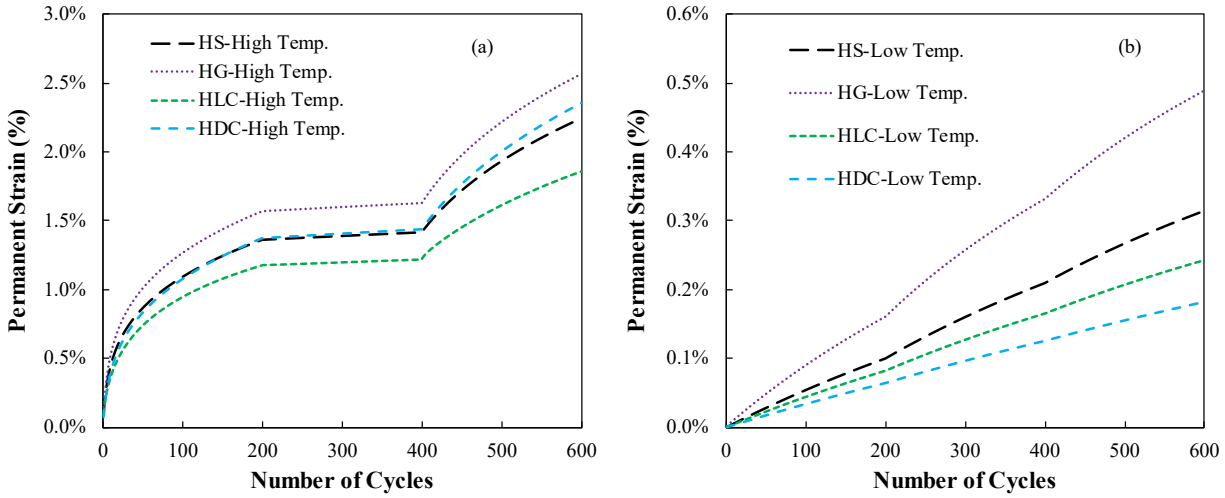


**Figure 4.13 Comparison of the permanent strain of all HMA mixtures: (a) at high temperature, and (b) at low temperature.**

Figure 4.14 and Table 4.3 present the RSI for all SMA and HMA samples. All SMA mixtures with candidate aggregates showed lower RSI values than the control mixture ST, suggesting better rutting resistance. Among the mixtures with candidate aggregates, SS exhibited the lowest RSI, while SDC showed the highest. The RSI values of HMA mixtures ranged from 7.8 to 10.1. There were no notable differences among all HMA mixtures, indicating that the HMA mixtures with candidate aggregates had rutting resistance comparable to the control mixture, HLC.

**Table 4.3 Results of RSI for All SMA and HMA Mixtures**

| Mixture Type | RSI | % Increase vs. Control |
|---|---|---|
| **ST** | 24.6 | 0.00 |
| **SS** | 9.6 | -61.06 |
| **SG** | 17.2 | -30.09 |
| **SLC** | 16.5 | -32.93 |
| **SDC** | 20.3 | -17.66 |
| **HLC** | 7.8 | 0.00 |
| **HS** | 8.7 | 10.59 |
| **HG** | 10.1 | 28.44 |
| **HDC** | 10.0 | 28.06 |

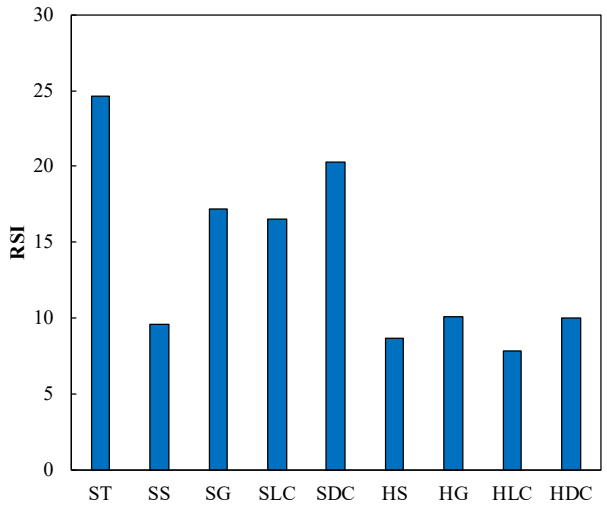


**Figure 4.14 RSI value for all SMA and HMA samples.**

## 4.1.2 IDT at Low Temperature

### 4.1.2.1 Creep Compliance

The creep compliance *D(t)* for all SMA and HMA mixtures, using various candidate aggregates at different temperatures, was calculated. Subsequently, the creep compliance data underwent processing via the LTSTRESS spreadsheet to generate a creep compliance master curve (Bonaquist 2011). Table 4.4 presents a summary of the fitting parameters for the master curves of all SMA and HMA mixtures. The standard error in fitting the master curves varied from 1.1 to 3.1%, indicating an excellent alignment of the master curve equation to the compliance data for all samples. Figures 4.15 and 4.16 display the creep compliance master curves for SMA and HMA mixtures with all candidate aggregates. All samples exhibited consistent trends in the evolution of *D(t)* over the loading time across varying temperatures. Across the same materials, as temperature decreased, the *D(t)* also decreased, signifying increased stiffness of the asphalt mixture at lower temperatures and heightened susceptibility to thermal cracking. Hence, a

higher *D(t)* suggested enhanced resistance of the asphalt mixture against cracking at low temperatures.

**Table 4.4 Creep Compliance Master Curve Shifting Parameters**

| Mixtures | log D0 | Log D1 | M | C2 | Standard Error, % |
|---|---|---|---|---|---|
| **ST** | -6.486 | -7.44 | 0.362 | -0.086 | 3.1 |
| **SS** | -6.423 | -7.862 | 0.448 | -0.077 | 1.9 |
| **SG** | -6.411 | -7.674 | 0.397 | -0.067 | 1.8 |
| **SLC** | -6.485 | -7.837 | 0.352 | -0.108 | 2.1 |
| **SDC** | -6.386 | -7.905 | 0.445 | -0.078 | 1.7 |
| **HS** | -6.514 | -7.93 | 0.334 | -0.114 | 2.1 |
| **HG** | -6.646 | -7.082 | 0.256 | -0.079 | 2.8 |
| **HLC** | -6.624 | -7.35 | 0.245 | -0.106 | 1.1 |
| **HDC** | -6.641 | -7.41 | 0.269 | -0.089 | 1.4 |

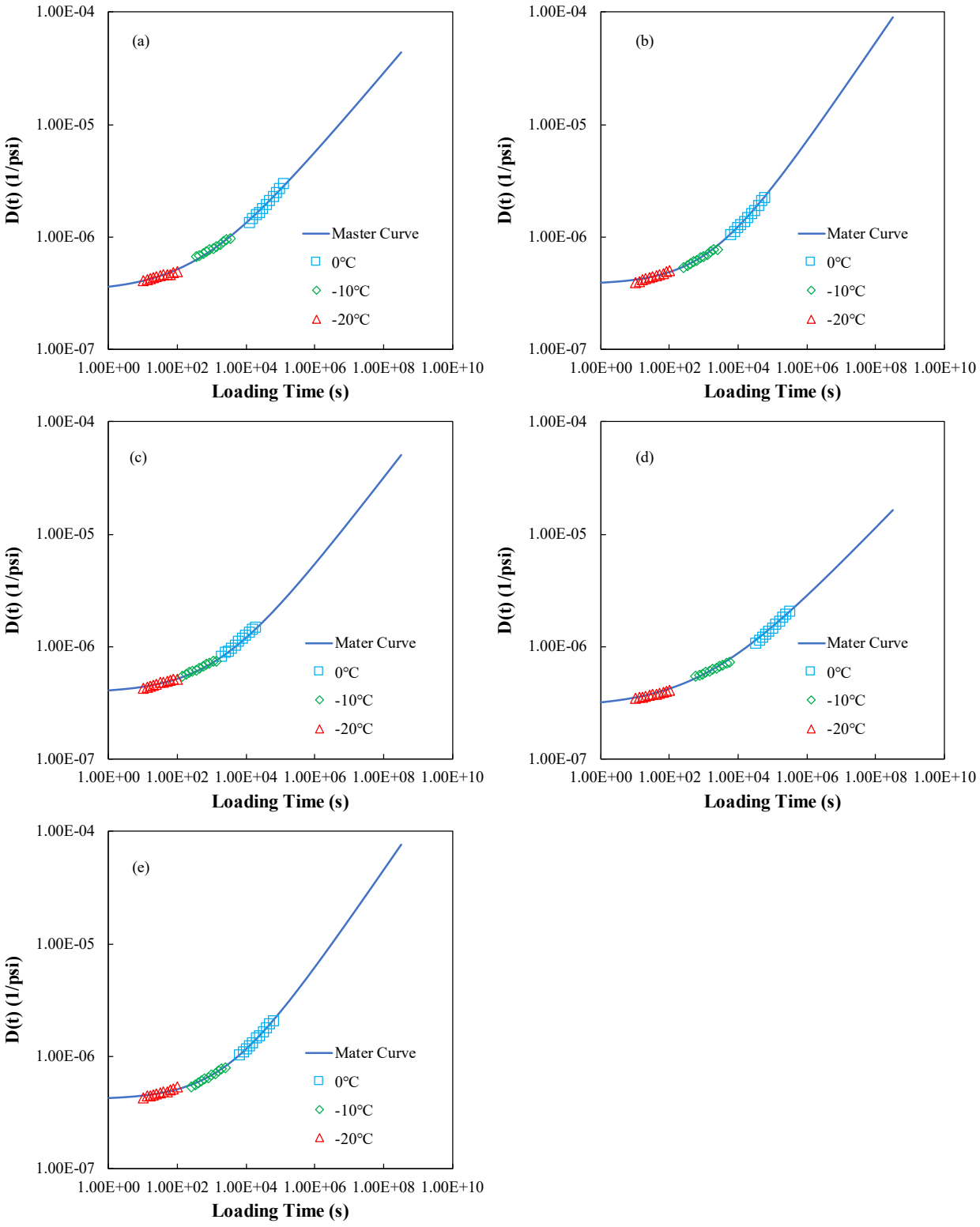


**Figure 4.15 Creep compliance master curves for all SMA mixtures: (a) ST, (b) SS, (c) SG, (d) SLC, and (e) SDC.**

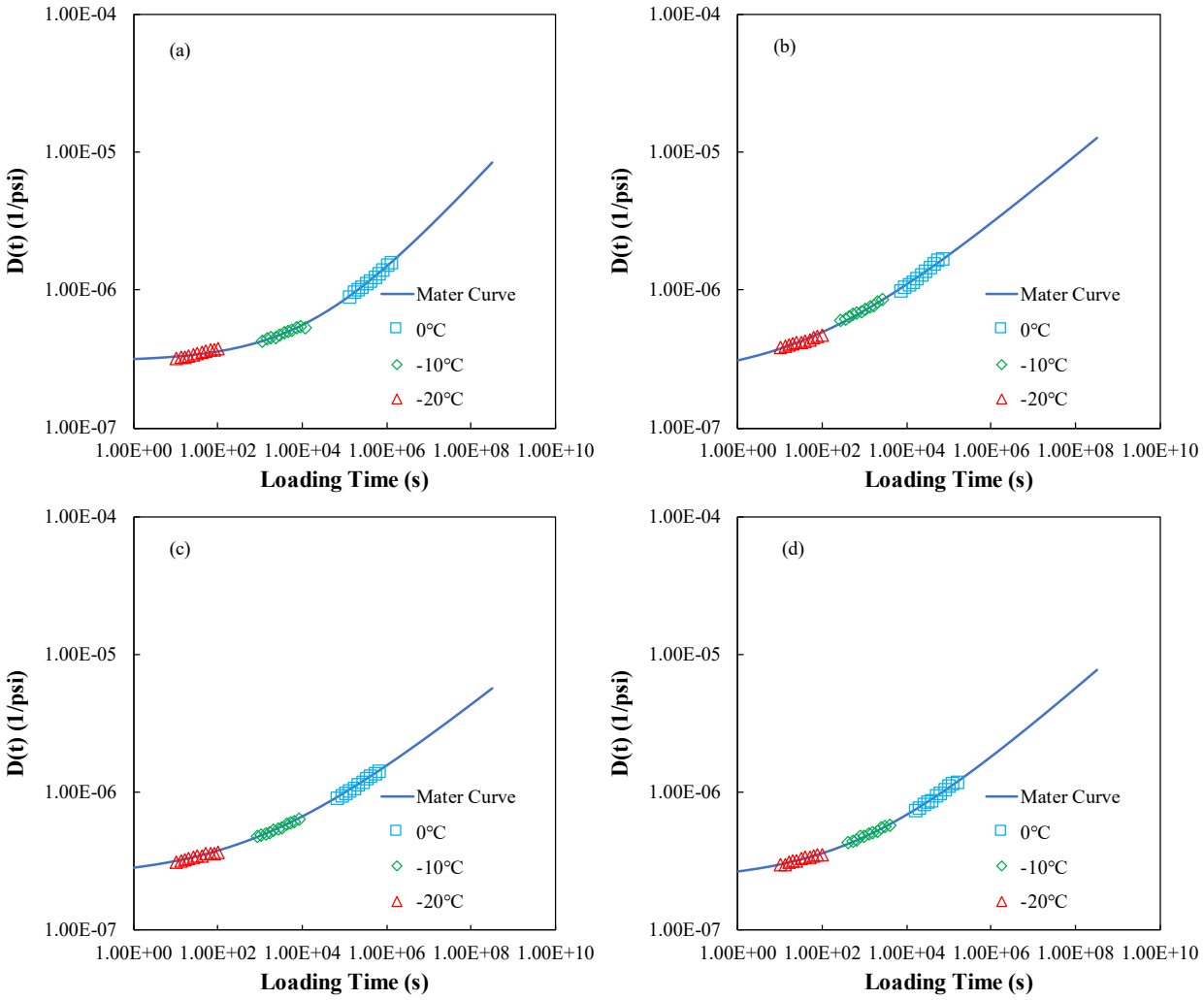


**Figure 4.16 Creep compliance master curves for all HMA mixtures: (a) HS, (b) HG, (c) HLC, and (d) HDC.**

Figures 4.17 (a) and (b) provide overviews of the creep compliance master curves for all SMA and HMA mixtures, respectively. In SMA mixtures, the SLC exhibited the lowest *D(t)*, signifying the lowest resistance to low temperature cracking. The *D(t)* of SMA mixtures with all other candidate aggregates was slightly higher than that of the control mixtures ST, suggesting that SS, SG, and SDC exhibit better resistance to low temperature cracking than ST. HLC mixture served as the control mixture and displayed the lowest *D(t)*. HG mixture exhibited the highest *D(t)* while HDC and HS demonstrated *D(t)* values close to each other and slightly higher than that of HLC.

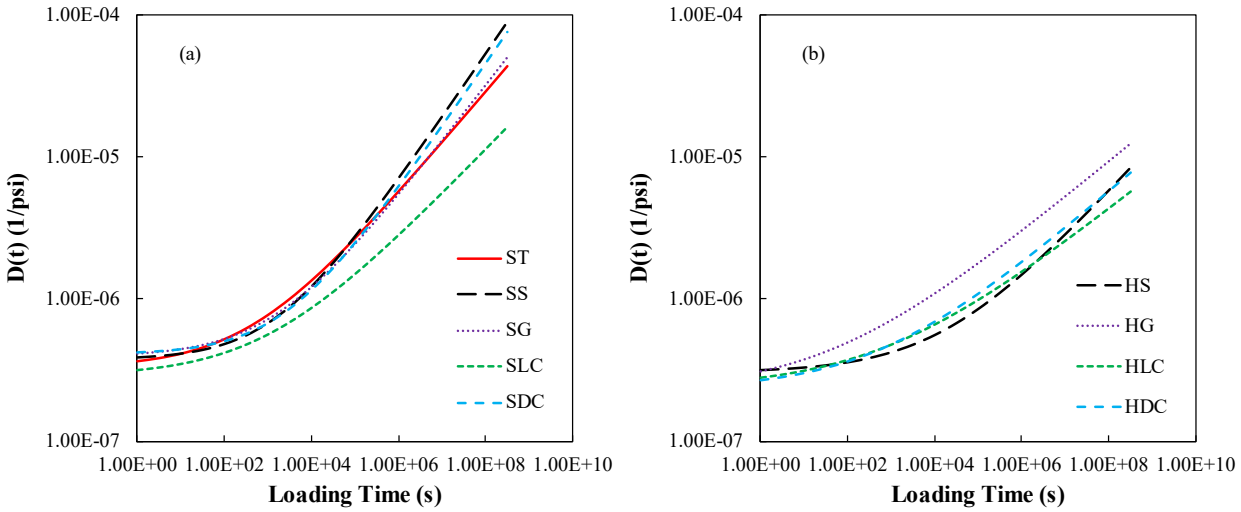


**Figure 4.17 Comparison of creep compliance master curve for all mixtures: (a)SMA mixtures, and (b) HMA mixtures.**

### 4.1.2.2 Thermal Stress of the Mixtures

The LTSTRESS spreadsheet was used to calculate thermal stresses of all SMA and HMA mixtures. The cooling rate was set at 5.6℃/hr, and the linear coefficient of thermal contraction was determined to be $1.25*10^{-5}$/℃ for SMA mixtures and $1.05*10^{-5}$/℃ for HMA mixtures based on their *VMA* and *VFA*. The development of thermal stresses for all SMA and HMA mixtures is summarized in Figure 4.18.

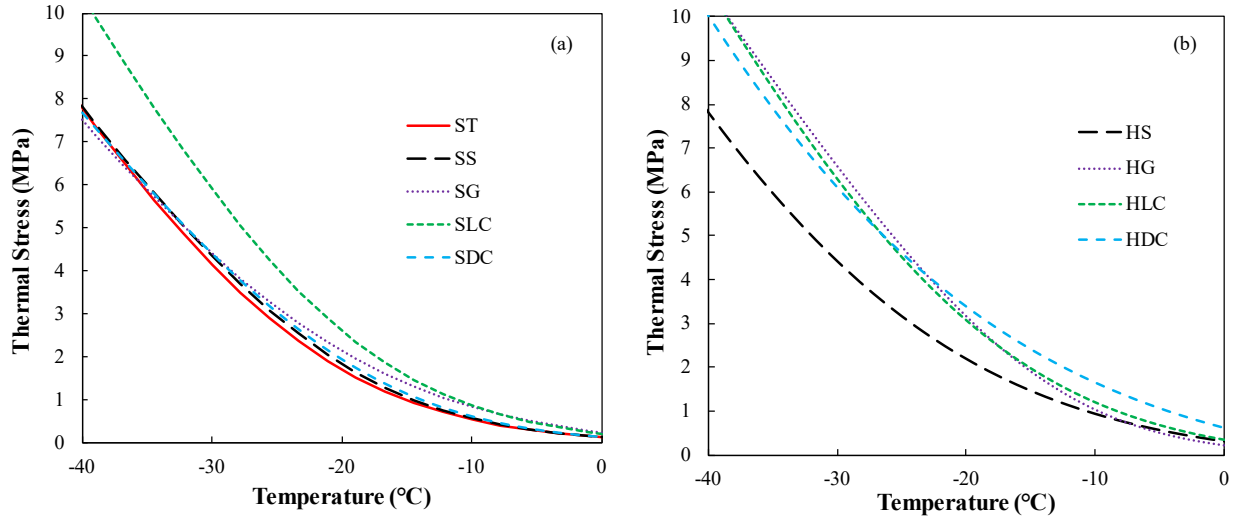


**Figure 4.18 Comparison of thermal stress for all mixtures: (a) SMA mixtures, and (b) HMA mixtures.**

### 4.1.2.3 Strength

The IDT strength tests were conducted at three different temperatures, consistent with the creep compliance tests. Tensile strength values were calculated, and all results are summarized in Table 4.5.

Relying solely on this parameter for evaluating the thermal cracking resistance of the mixture was insufficient. A higher tensile strength at low temperatures did not guarantee better resistance to thermal cracking. Additionally, it depended on how thermal stress in the asphalt mixtures evolved with temperature decreased. In this study, cracking temperature of the asphalt mixtures was predicted by comparing thermal stress and strength.

**Table 4.5 IDT Strength of All SMA and HMA Mixtures at Three Different Temperatures**

| Mixtures | Tensile strength, MPa | | |
|---|---|---|---|
| | -20℃ | -10℃ | 0℃ |
| **ST** | 2.71 | 3.03 | 2.75 |
| **SS** | 2.91 | 3.13 | 2.35 |
| **SG** | 2.91 | 2.95 | 2.75 |
| **SLC** | 3.26 | 3.13 | 2.82 |
| **SDC** | 3.09 | 2.88 | 2.61 |
| **HS** | 3.73 | 3.63 | 3.06 |
| **HG** | 2.95 | 3.39 | 2.88 |
| **HLC** | 3.51 | 3.97 | 3.48 |
| **HDC** | 3.93 | 3.89 | 3.39 |

#### 4.1.2.4 Cracking Temperatures of Mixtures

By comparing thermal stresses of all SMA and HMA mixtures generated from LTSTRESS with strengths at different temperatures, the critical temperature was determined for each mixture, as demonstrated in Figures 4.19 and 4.20.

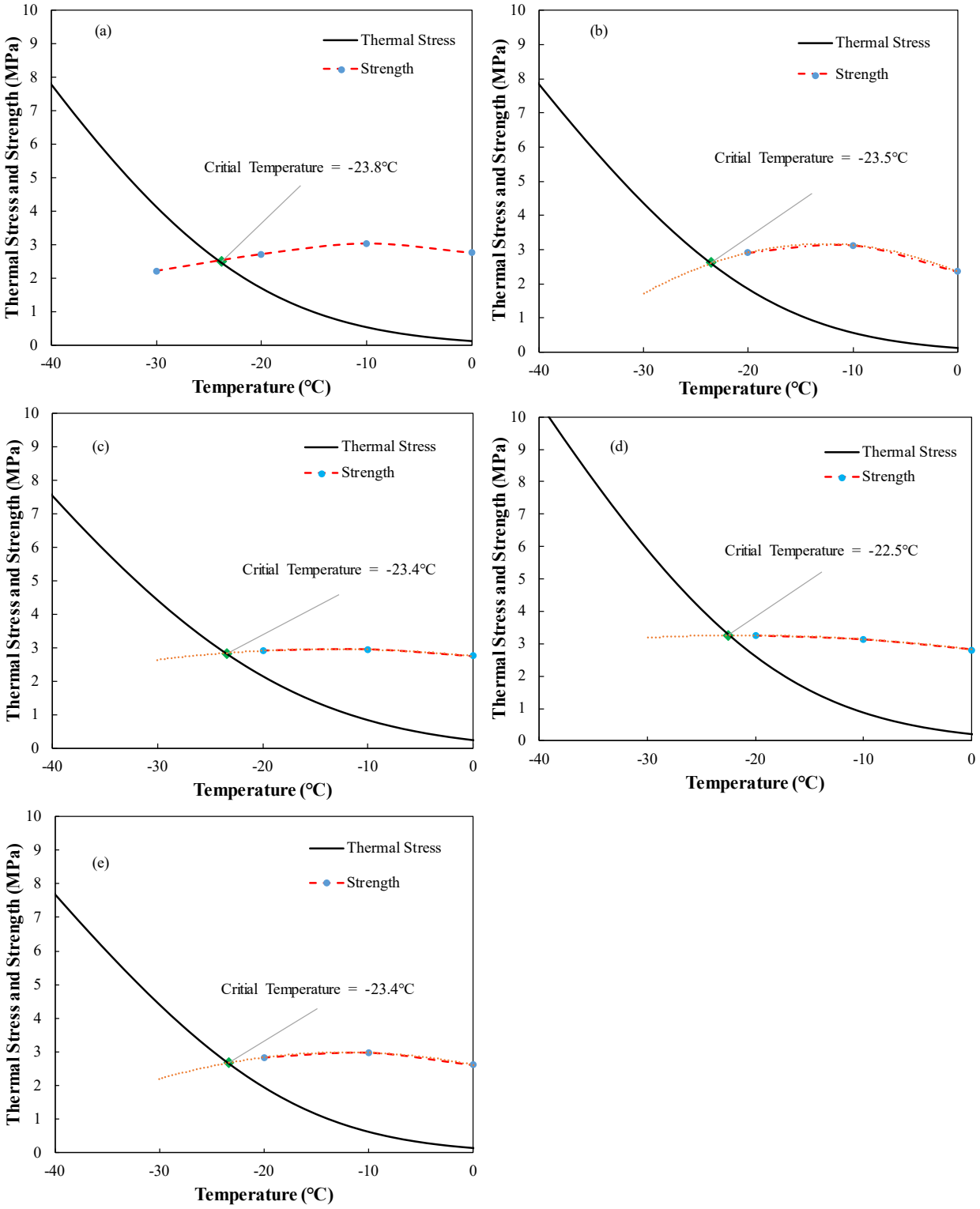


**Figure 4.19 Determination of cracking temperature for all SMA mixtures: (a) ST, (b) SS, (c) SG, (d) SLC, and (e) SDC.**

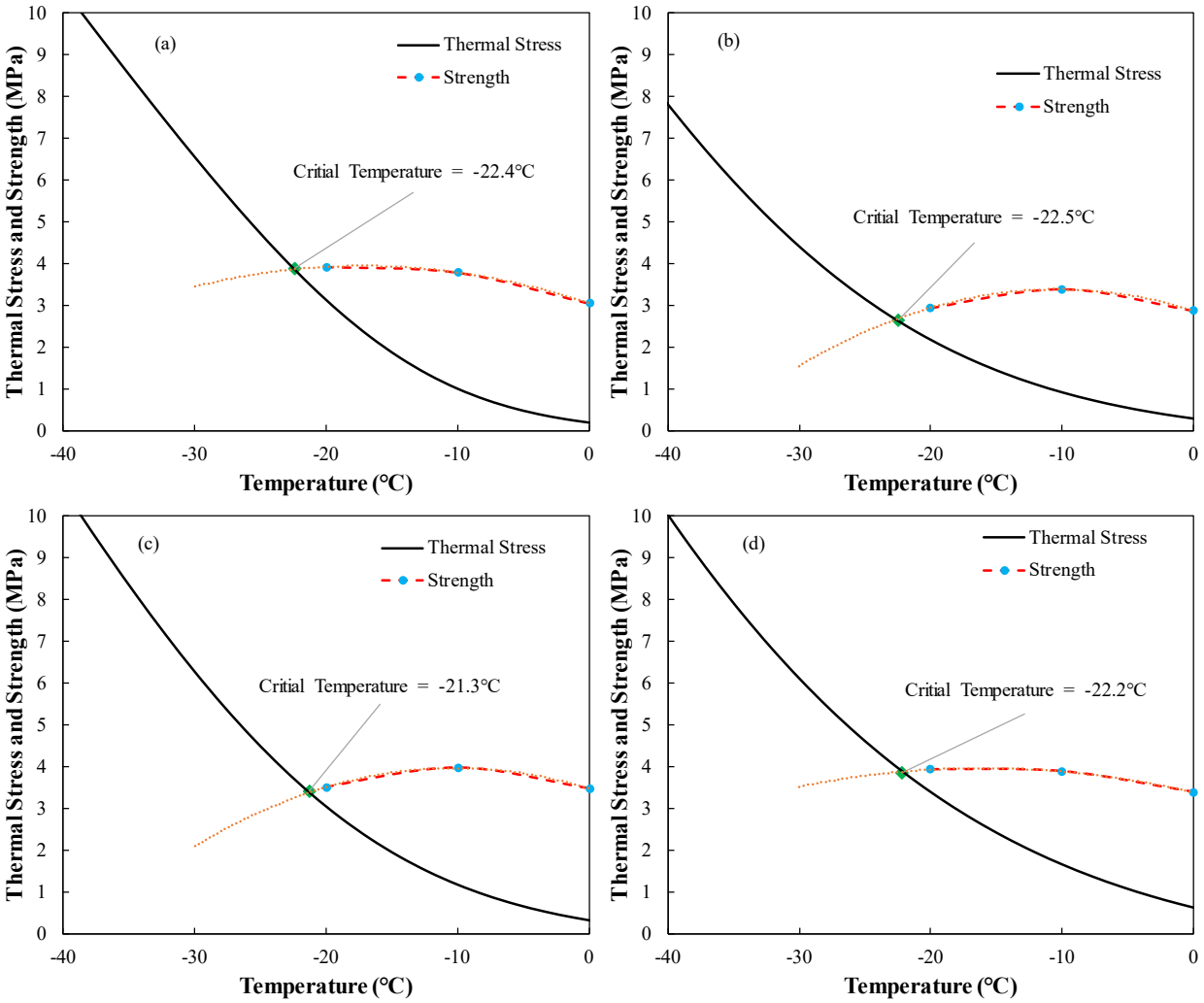


**Figure 4.20 Determination of cracking temperature for all HMA mixtures: (a) HS, (b) HG, (c) HLC, and (d) HDC.**

Figure 4.21 (a) and Table 4.6 provide a summary of all critical temperatures for both SMA and HMA mixtures with all candidate aggregates. Among SMA mixtures, the control mixture ST exhibited the lowest critical temperature, suggesting the best resistance to thermal cracking. The SS, SG, and SDC yielded close results to the control mixture ST, indicating that the candidate aggregates demonstrated comparable performance in resisting thermal cracking to traprock when used in SMA mixtures.

Among HMA mixtures, the control mixture HLC displayed the highest critical temperature, implying that all HMA mixtures featuring other candidate aggregates performed better in resisting thermal cracking than the control mixture HLC. In essence, substituting limestone & chat with the candidate aggregates in HMA enhanced resistance to cracking at low

temperatures. Generally, the SMA mixtures showed better thermal cracking resistance than HMA mixtures, reflecting on the lower thermal stress and lower critical temperature.

Additionally, Figure 4.21 (b) illustrates the correlation between the critical temperatures of SMA and HMA mixtures utilizing the same candidate aggregates: gravel, steel slag, limestone & chat, and dolomite & chat. The SMA and HMA mixtures featuring identical candidate aggregates consistently exhibited similar responses regarding the critical temperature.

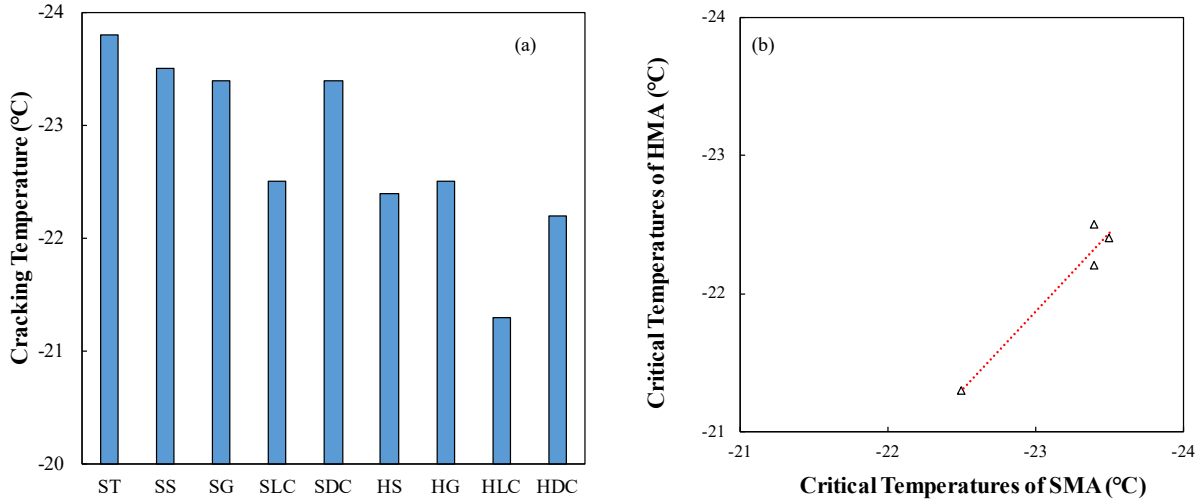


**Figure 4.21 (a)Comparison of critical temperature for all SMA and HMA mixtures,and (b) the relationship between same candidate aggregates used in SMA and HMA mixtures.**

**Table 4.6 Results of Cracking Temperatures for all SMA and HMA Mixtures**

| Mixture Type | Cracking Temperatures, ℃ | % Increase vs. Control |
|---|---|---|
| **ST** | -23.8 | 0.00 |
| **SS** | -23.5 | -1.26 |
| **SG** | -23.4 | -1.68 |
| **SLC** | -22.5 | -5.46 |
| **SDC** | -23.4 | -1.68 |
| **HLC** | -21.3 | 0.00 |
| **HS** | -22.4 | 5.16 |
| **HG** | -22.5 | 5.63 |
| **HDC** | -22.2 | 4.23 |

### 4.1.3 Moisture Susceptibility Testing Results and Analysis

Higher TSR values indicated a lower percentage loss of IDT strength in specimens under moisture conditions, signifying better resistance to moisture damage. Figures 4.22 (a) and (b) show TSR values obtained from SMA and HMA after three humidity treatments: TSR test, M.i.S.T without adhesion cycle test, and M.i.S.T with adhesion cycle test, respectively.

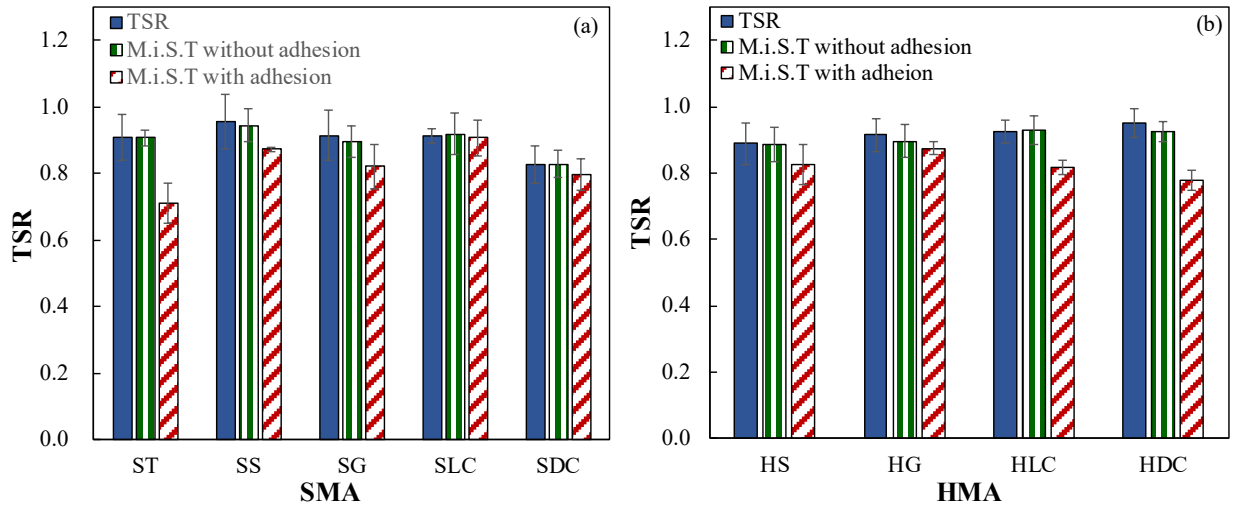


**Figure 4.22 TSR Results: (a) SMA; (b)HMA.**

In both TSR (T 283) test and M.i.S.T without adhesion cycle test, all mixtures met the Missouri TSR value standard of 0.8, with no noticeable differences observed among the various mixtures. However, in M.i.S.T with adhesion cycle test, the TSR index values of ST, SDC, and HDC asphalt mixtures were less than 0.8. The TSR values of almost all mixtures decreased with the addition of adhesion cycles. Some mixtures experienced only slight declines, such as HG and SCL, while others, such as ST, experienced significant declines. This indicated that the loss of adhesion in the mixture due to moisture exposure was influenced by aggregate type.

A paired t-test with a confidence level of 95% was conducted on TSR series test results. The obtained p-value (two-tailed) for the paired samples of the TSR (T 283) test results and M.i.S.T test without adhesion cycles results was 0.0898. Therefore, there was no significant difference between the results of TSR (T 283) test and M.i.S.T test without adhesion cycles.

In contrast, for the paired samples of TSR (T 283) test results and M.i.S.T test with adhesion cycles results, as well as for the paired samples of M.i.S.T test without adhesion cycles results and M.i.S.T test with adhesion cycles results, the obtained p-values (two-tailed) were 0.0033 and 0.0042, respectively, indicating a statistically significant difference between the two pairs of samples. Therefore, the adhesion cycles of M.i.S.T test significantly impacted on the moisture damage of the specimen.

## 4.2 Performance Analysis on Pavement Level

### 4.2.1 Structural Performance Prediction Using FlexPAVE™

The merit of the AMPT tests was that they not only provided performance thresholds to pass/fail the products, but also calibrated the fundamental mechanistic models that could be used in a full structural simulation that considered the in-situ pavement structure, traffic level, and realistic climate conditions. On a structural level, the FlexPAVE™ software was utilized to forecast pavement structure performance, encompassing fatigue damage and rutting. For

fatigue damage in the pavement, FlexPAVE™ utilized parameters obtained from FlexMAT™, including $S_{app}$, $D^R$ failure criterion, and factors comprising the C VS. S curve. It employed three-dimensional finite element analysis and the VECD model to predict fatigue damage over 20 years under selected traffic volume, climate conditions, and pavement structure specific to the project location. The analysis provided insights into asphalt layer damage over time and its spatial distribution. Similarly, the factors used to calculate RSI were inputted into FlexPAVE™ to predict pavement rut depth over service time. The analysis generated damage contours of cross-sections of the asphalt layers, which were plotted to show the location of damage (e.g., top-down versus bottom-up cracking) as well as the level of damage.

This study focused on a typical Missouri asphalt pavement structure with a 4" asphalt mixture layer to highlight differences between mixtures with various candidate aggregates. The pavement structure presented in Figure 4.23 was used. Key parameters such as structure, thickness, and Poisson ratio are summarized in the Table 4.7 below. The climate condition for the study area was set to Rolla, MO, with a traffic volume of 13 million ESALs over 20 years.

**Table 4.7 Parameters of Pavement Structure for Predicting Pavement Temperature**

| Layer | Thickness, inch | Specific Gravity | Expansion Coefficient, 1/℃ | Poisson Ratio | Elastic Modulus, psi |
|---|---|---|---|---|---|
| **Asphalt Mixture** | 4 | 2.5 | 5E-05 | 0.3 | - |
| **Aggregate Base** | 8 | 2.5 | 1E-05 | 0.35 | 3.0E+04 |
| **Subgrade** | 106 | - | - | - | 1.0E+04 |

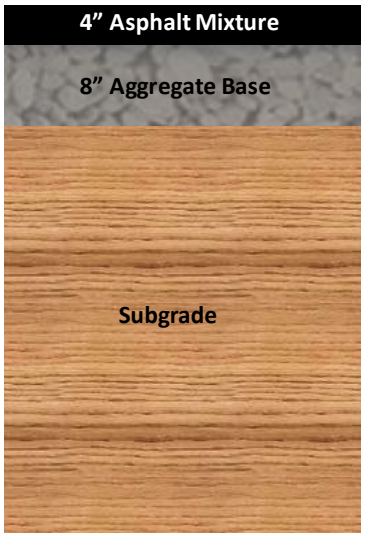


**Figure 4.23 Schematic of pavement structure used in FlexPAVE™ performance simulation.**

The summary of predicted fatigue damage for all SMA and HMA mixtures in pavement is depicted in Figure 4.24 and Table 4.8. A similar trend was also evident in the fatigue damage

contours. Figures 4.25 and 4.26 depict the damage distributions of the most and least damaged sections within the asphalt layer cross-sections after 20 years of service life. The fatigue damage tended to increase gradually under the traffic loading and climate condition over the 20-year design life, with the rate of increase becoming progressively slower.

Among SMA mixtures, the control mixture ST demonstrated the lowest fatigue damage value, at 15.6% after 20 years, indicating superior resistance to fatigue damage. However, the fatigue damage values for SMA mixtures with candidate aggregates ranged from 18.2% for SS to 22.1% for SG, indicating limited differences between these SMA mixtures and the control. In HMA mixtures, the mixtures with candidate aggregates exhibited predicted fatigue damage values similar to the control mixture HLC. Specifically, values ranged from 15.2% for HS to 16.9% for HG.

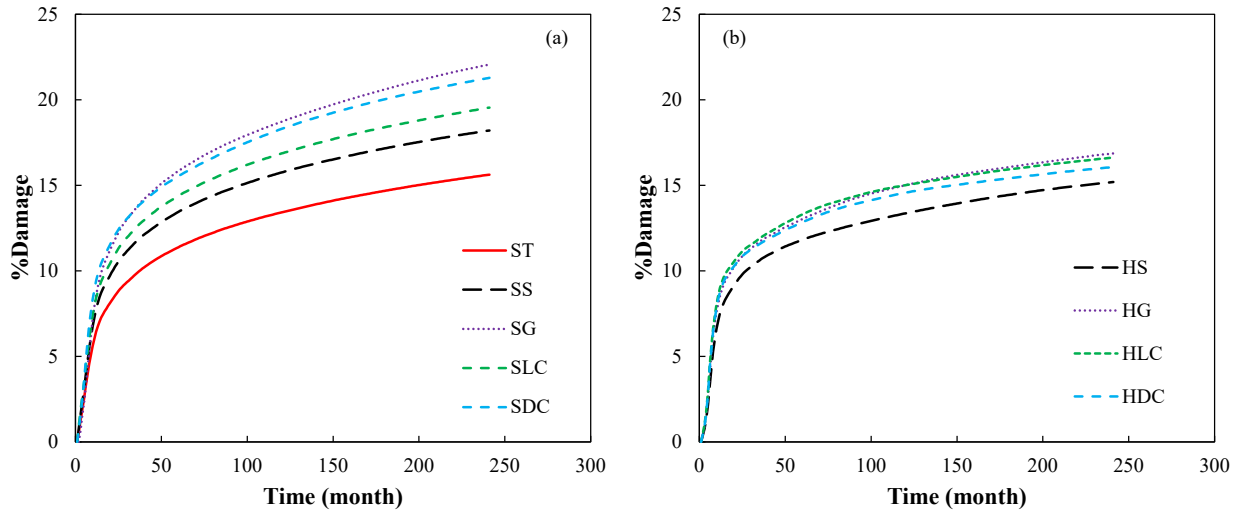


**Figure 4.24 Predicted fatigue damage growth for all mixtures: (a) SMA mixtures, and (b) HMA mixtures.**

**Table 4.8 Results of %Damage for All SMA and HMA Mixtures**

| Mixture Type | %Damage, % | % Increase vs. Control |
|---|---|---|
| **ST** | 15.6 | 0.00 |
| **SS** | 18.2 | 16.51 |
| **SG** | 22.1 | 41.34 |
| **SLC** | 19.5 | 25.08 |
| **SDC** | 21.3 | 36.21 |
| **HLC** | 16.6 | 0.00 |
| **HS** | 15.2 | -8.61 |
| **HG** | 16.9 | 1.47 |
| **HDC** | 16.1 | -3.34 |

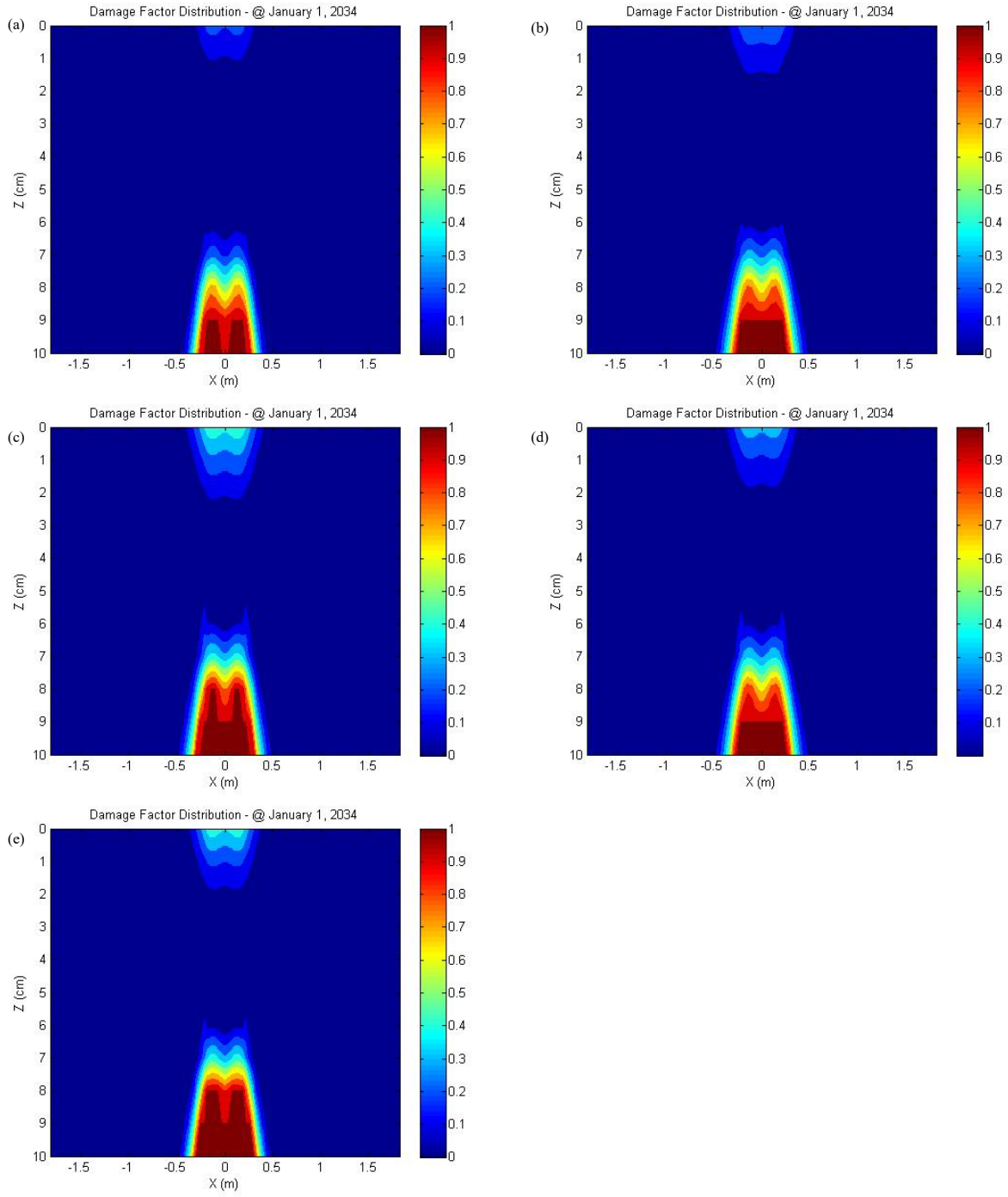


**Figure 4.25 Damage contours in asphalt layer cross sections with all SMA mixtures: (a) ST, (b) SS, (c) SG, (d) SLC, and (e) SDC.**

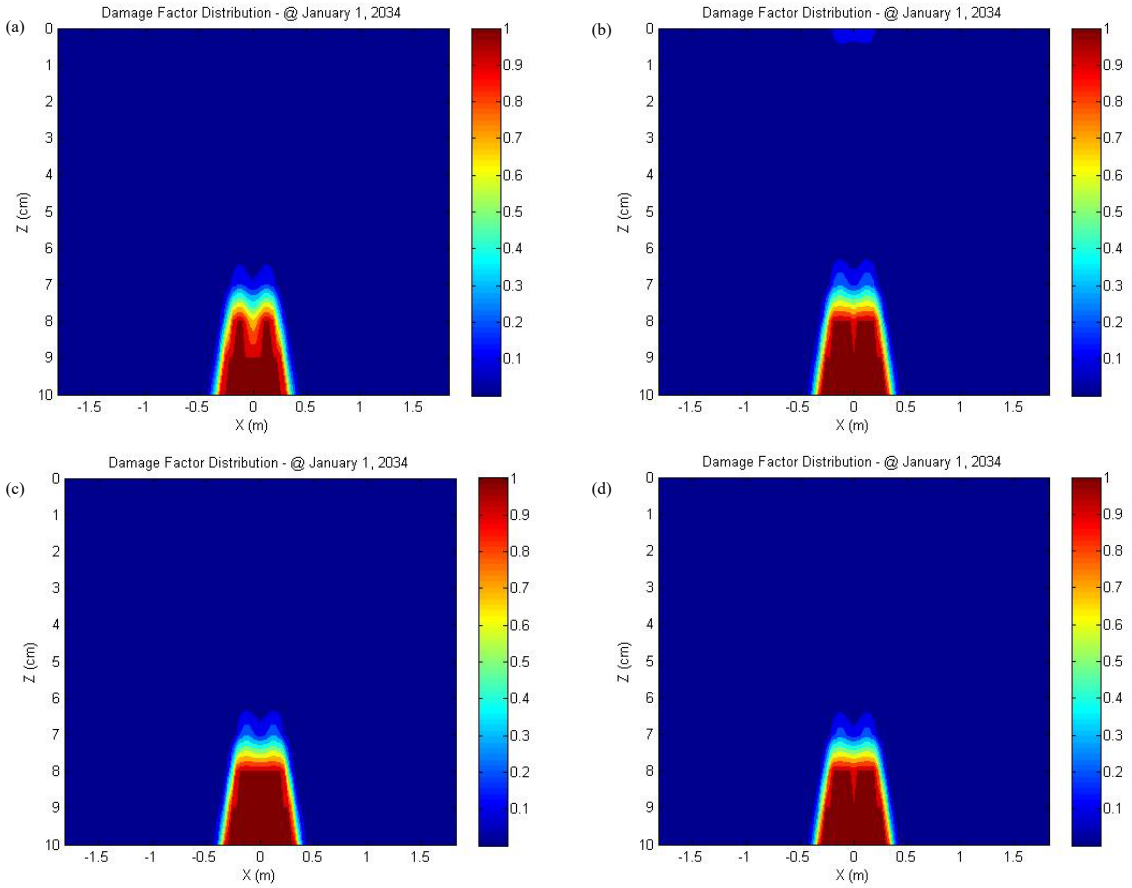


**Figure 4.26 Damage contours in asphalt layer cross sections with all HMA mixtures: (a) HS, (b) HG, (c) HLC, and (d) HDC.**

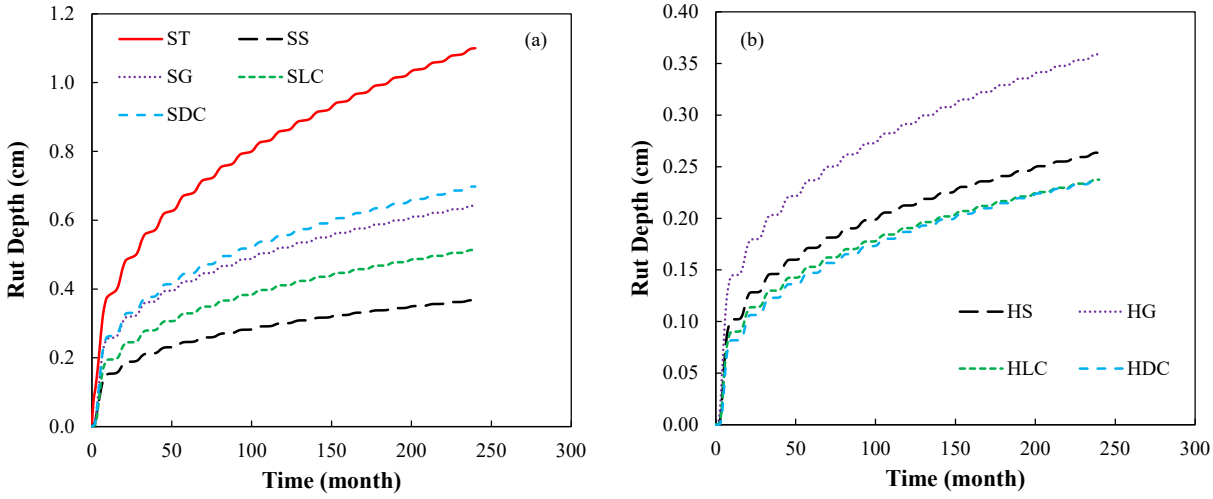


**Figure 4.27 Comparison of the rut depth of the asphalt mixture layer in the pavement for all mixtures: (a) SMA mixtures, and (b) HMA mixtures.**

**Table 4.9 Results of Rut Depth in Pavement after 20 years for All SMA and HMA Mixtures**

| Mixture Type | Rut Depth in Pavement, mm |
|---|---|
| **ST** | 11.0 |
| **SS** | 3.7 |
| **SG** | 6.4 |
| **SLC** | 5.1 |
| **SDC** | 7.0 |
| **HS** | 2.6 |
| **HG** | 3.6 |
| **HLC** | 2.4 |
| **HDC** | 2.4 |

Figure 4.27 and Table 4.9 display the predicted rut depth of the asphalt layer within the pavement structure under the specified climate and traffic conditions. Among SMA mixtures, all mixtures with candidate aggregates exhibited significantly lower rut depths compared to the control mixture, ST. In HMA mixtures, HG displayed the highest rut depth, while HS and HDC demonstrated results similar to the control mixture, HLC.

### 4.2.2 Thermal Cracking Prediction on Pavement

The prediction of low-temperature cracking in pavement involved comparing the critical cracking temperatures of SMA and HMA mixtures to the pavement temperatures (Liu et al. 2017). The software Temperature Estimate Model for Pavement Structures (TEMPS) was utilized to estimate hourly temperatures at specific depths in asphalt pavement. TEMPS employed the Finite Control Volume Method (FCVM) with a fully implicit scheme to address known limitations in current pavement temperature profile models (ARC-UNR 2016).

Various factors, including pavement structure, materials, surface characteristics, and climate data, were considered in TEMPS to predict pavement temperatures. A typical asphalt pavement structure was adopted, with all relevant parameters summarized in Table 4.10. Surface characteristics were assigned typical values of 0.7, 0.2, and 0.85 for absorption, albedo, and emissivity, respectively. Climate data, sourced from the Long-Term Pavement Performance (LTPP) database, encompassed hourly temperature, solar radiation, and wind speed.

**Table 4.10 Parameters of Pavement Structure for Predicting Pavement Temperature**

| Layer | Thickness, inch | Specific Heat, J*kg/K | Conductivity, W/m*K | Density, lb/ft$^3$ |
|---|---|---|---|---|
| **Asphalt Mixture** | 4 | 2.40 | 1.0 | 57.4 |
| **Aggregate Base** | 8 | 2.40 | 1.0 | 57.4 |
| **Subgrade** | 106 | 2.65 | 0.5 | 57.4 |

Given the analysis focused on predicting pavement cracking at low temperatures, only the winter period was analyzed. Based on climatic data collected from LTPP database, the coldest

air temperature in in Jefferson City occurred in January 2021. Thus, hourly climate data from October 2020 to March 2021 was utilized for calculating pavement temperature profiles.

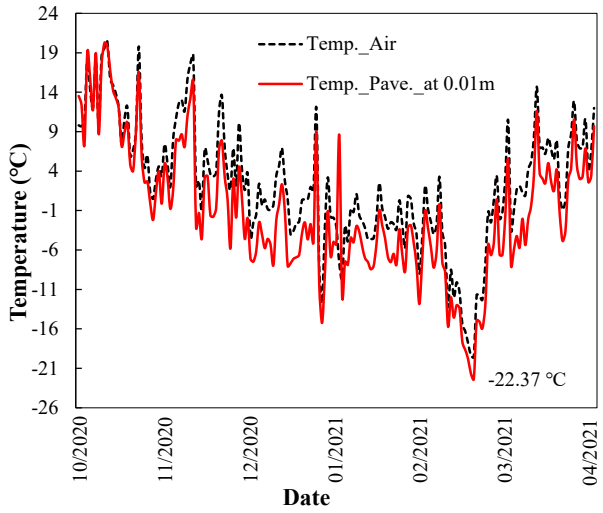


**Figure 4.28 Lowest pavement temperature and air temperature in JC over the past 20 years.**

The anticipated daily lowest temperatures at a depth of 0.01m in the asphalt mixture layer, along with the relative air temperatures from October 2020 to March 2021, are depicted in Figure 4.28. The coldest air temperature, -19.6 ℃, occurred in February 2021, coinciding with a pavement temperature of -22.37 ℃. The cracking temperature of SMA and HMA mixtures with all the candidate aggregates were then compared to the coldest pavement temperature, as shown in Figures 4.29 and 4.30.

In SMA mixtures, the cracking temperature of mixtures with all candidate aggregates fell below the lowest predicted pavement temperature over the past 20 years. The SMA mixtures featuring all candidate aggregates, were expected to offer robust resistance to thermal cracking in the project's field. In HMA mixtures, the cracking temperature of HS and HG mixtures slightly dipped below the lowest recorded pavement temperature, indicating satisfactory resistance to thermal cracking. However, there were only one and two days during the entire coldest winter period, respectively, where the coldest pavement temperature fell below the cracking temperature of HDC mixture and the control mixture HLC. Thus, HLC and HDC also demonstrated relatively good resistance to thermal cracking.

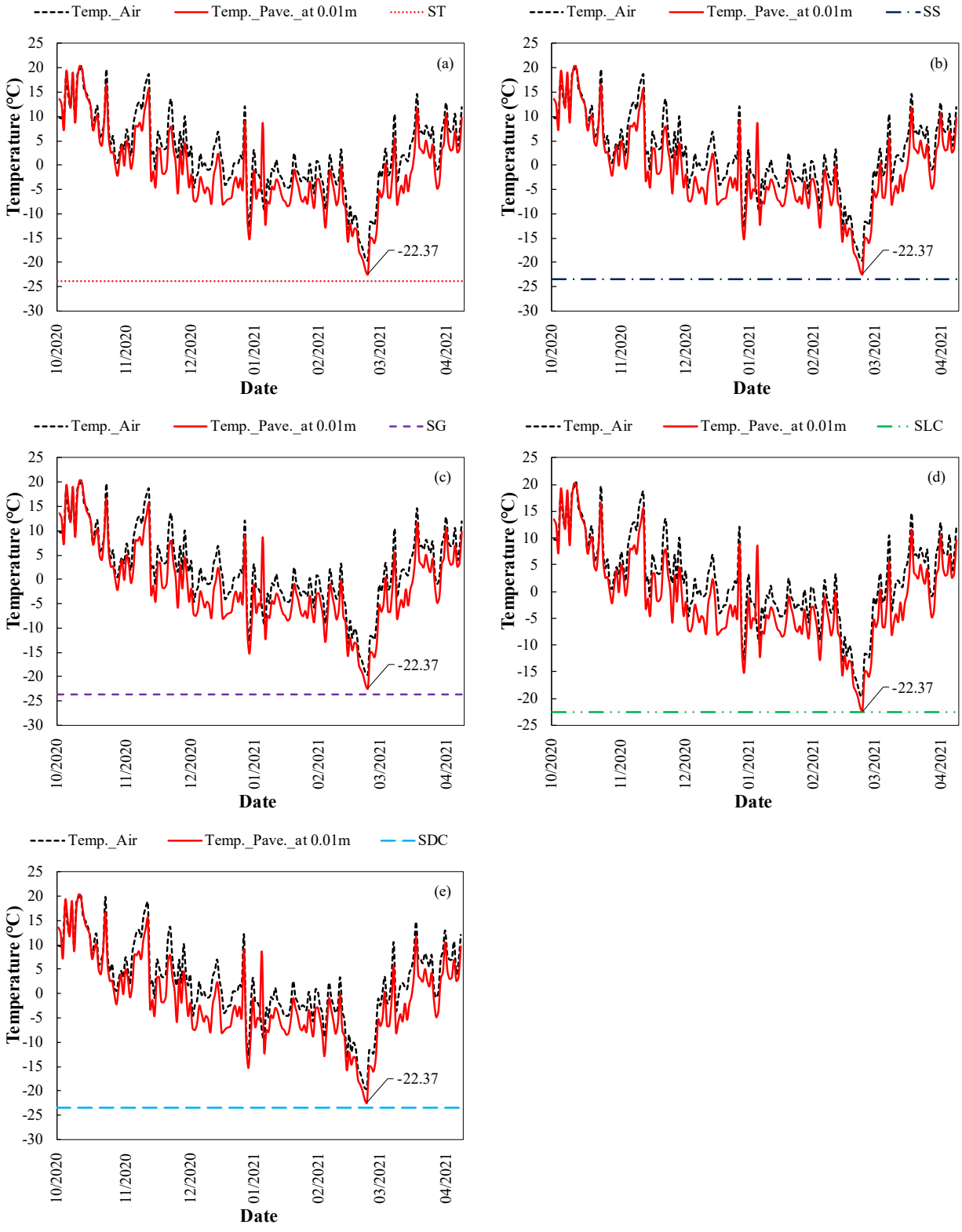


**Figure 4.29 Comparison of lowest pavement temperature with critical temperature of all SMA mixtures: (a) ST, (b) SS, (c) SG, (d) SLC, and (e) SDC.**

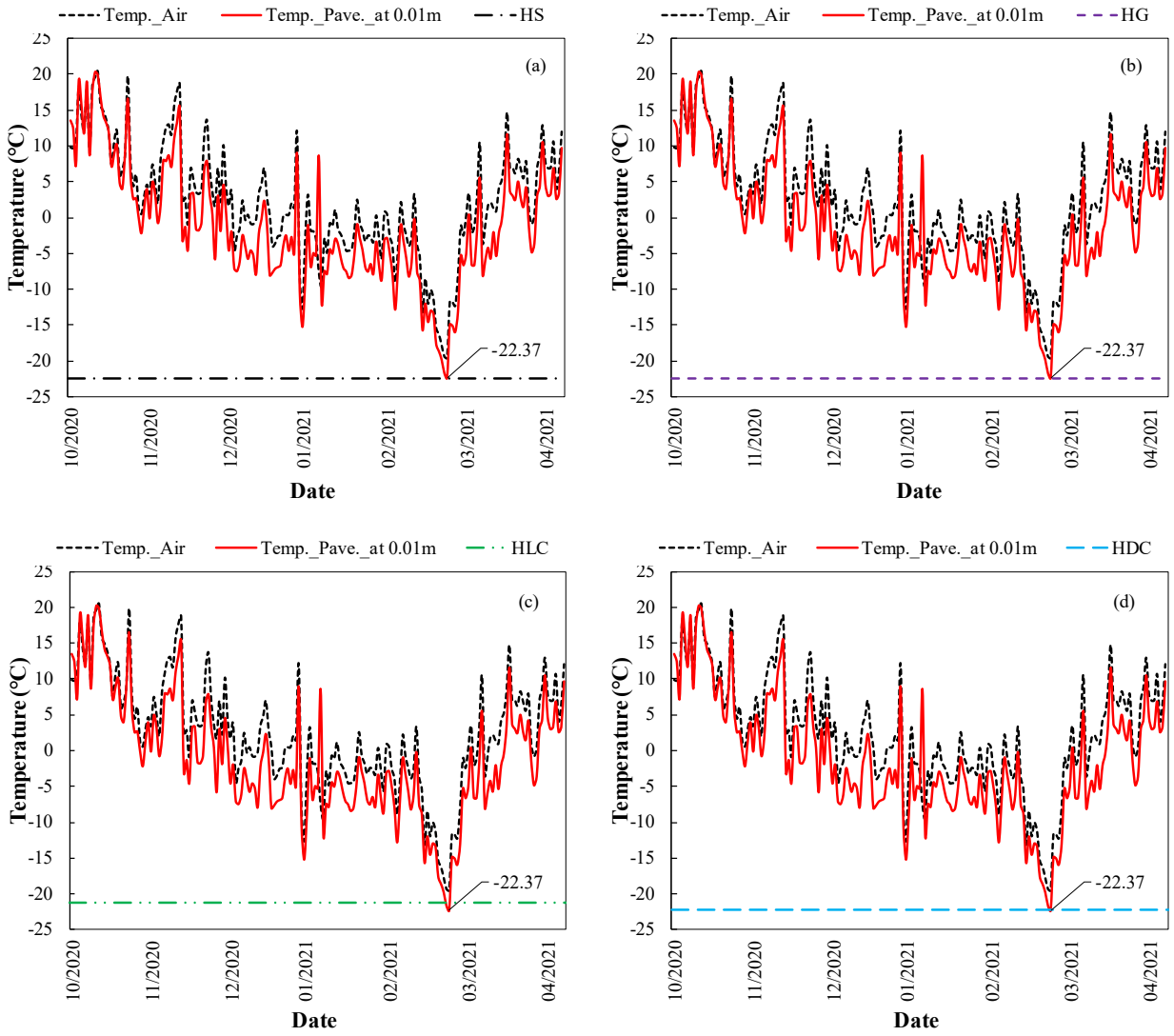


**Figure 4.30 Comparison of lowest pavement temperature with critical temperature of all HMA mixtures: (a) HS, (b) HG, (c) HLC, and (d) HDC.**

## 4.3 Life-cycle Cost Analysis

The cost analysis including initial construction and maintenance cost was conducted to evaluate the cost effectiveness of use of alternative aggregates in SMA and higher level Superpave mixtures.

### 4.3.1 Initial Construction Cost Analysis

The initial cost varied depending on the type of aggregate used. An initial construction cost analysis was conducted for a hypothetical four-lane highway in a rural area to compare proposed asphalt mixtures with various candidate aggregates. Unit costs for initial construction

were determined based on information from MoDOT, local quarries, and relevant literature, as detailed in Table 4.11. These costs were influenced by factors such as availability and market conditions. It was anticipated that for large-scale pavement projects, these costs would likely decrease due to bulk material purchases. Subsequently, the initial construction costs for five SMA mixtures and four HMA mixtures in this study were calculated using the recommended unit costs and the material quantities specified in their respective mix designs.

**Table 4.11 Surveyed Unit Costs of Materials in Missouri**

| Materials | Unit cost |
|---|---|
| **Asphalt binder** | $56.08 / ton |
| **Fly ash** | $37.50 / ton |
| **Fiber** | $8.57 / ton |
| **Fines** | $34.95 / ton |
| **Traprock** | $72.08 / ton |
| **Steel slag** | $31.42 / ton |
| **Gravel** | $41.38 / ton |
| **Limestone** | $38.52 / ton |
| **Dolomite** | $19.15 / ton |
| **Chat** | $43.10 / ton |
| **Aggregate used for base** | $8.00/ ton |

Table 4.12 displays the initial construction costs for all asphalt pavement structures. The sole variance in construction costs among alternatives stemmed from materials. Hence, only material costs within the pavement structure were considered for comparison. While shipping costs fluctuate based on location, additional hauling fees were not factored in. However, all alternative aggregates were expected to yield significant hauling savings compared to traprock, predominantly situated in the southeast of Missouri. In SMA mixtures, the initial construction costs of SS, SG, SLC, and SDC were approximately 24%, 23%, 23%, and 27% lower than that of the control mixture ST, respectively. Within HMA mixtures, the initial construction costs of HS, HG, and HDC were approximately 2%, 5%, and 0.1% higher than that of the control mixture HLC, respectively. The initial cost analysis suggested that the proposed local candidate aggregates exhibited considerable potential as alternatives for both SMA and HMA mixtures without inflating construction costs.

**Table 4.12 Assumed Initial Construction Costs for the Pavement Structures**

| Scenario | Item | Asphalt mix layer ($/mile) | Base layer ($/mile) | Subbase layer ($/mile) | Total initial construction cost ($/mile) |
|---|---|---|---|---|---|
| **Case1: ST** | Asphalt mix layer_ST | 333,778 | 90,409 | 111,546 | 535,734 |
| **Case2: SS** | Asphalt mix layer_SS | 206,771 | 90,409 | 111,546 | 408,727 |
| **Case3: SG** | Asphalt mix layer_SG | 211,905 | 90,409 | 111,546 | 413,861 |
| **Case4: SLC** | Asphalt mix layer_SLC | 211,787 | 90,409 | 111,546 | 413,743 |
| **Case5: SDC** | Asphalt mix layer_SDC | 191,408 | 90,409 | 111,546 | 393,363 |
| **Case6: HS** | Asphalt mix layer_HS | 132,134 | 90,409 | 111,546 | 334,089 |
| **Case7: HG** | Asphalt mix layer_HG | 141,311 | 90,409 | 111,546 | 343,266 |
| **Case8: HLC** | Asphalt mix layer_HLC | 124,980 | 90,409 | 111,546 | 326,936 |
| **Case9: HDC** | Asphalt mix layer_HDC | 125,234 | 90,409 | 111,546 | 327,190 |

### 4.3.2 LCCA

In this study, LCCA was performed using the LCCA module within the RealCost 3.0 software, developed by the Federal Highway Administration (FHWA), to assess the overall long-term economic efficiency of alternative options (Kim et al. 2018, Smith et al. 2023). It incorporated initial construction and discounted future agency, user, and other relevant costs over the life of the pavement structures. The analysis was conducted under the assumption of rural settings and daytime construction. An analysis period of 20 years and a discount rate of 4% were selected, as outlined in the *Missouri Department of Transportation Pavement Design and Type Selection Process*. The two-way Average Annual Daily Traffic (AADT) was estimated to be 30,866 vehicles per day, with an annual growth rate of 1.9%. The number and timing of pavement rehabilitations during the design period significantly impacted life cycle costs. Routine maintenance depended on the predicted fatigue cracking index %Damage of the asphalt mixture obtained from AMPT data analysis in Chapter 5. This study assumed annual maintenance at a cost of $26,420 per year in Missouri (Feigenbaum et al. 2023). Additionally, rehabilitation was assumed to occur when the predicted %Damage of the asphalt mixture reaches 20%. The cost of rehabilitation was assumed to be 40% of the original construction cost. According to the %Damage results, only SG and SDC reached 20% at 13 and 14 years, respectively, during the 20-year service life. The details of activities during the service life for each scenario are listed in Table 4.13 below.

**Table 4.13 Schedule for Maintenance and Rehabilitation Activities During Service Life**

| Scenario | Activity and estimated design life (years) |
|---|---|
| **Case1: ST** | Initial construction and annual maintenance, 20 years |
| **Case2: SS** | Initial construction and annual maintenance, 20 years |
| **Case3: SG** | Initial construction and annual maintenance, 13 years; Rehabilitation, 7 years |
| **Case4: SLC** | Initial construction and annual maintenance, 20 years |
| **Case5: SDC** | Initial construction and annual maintenance, 14 years; Rehabilitation, 6 years |
| **Case6: HS** | Initial construction and annual maintenance, 20 years |
| **Case7: HG** | Initial construction and annual maintenance, 20 years |
| **Case8: HLC** | Initial construction and annual maintenance, 20 years |
| **Case9: HDC** | Initial construction and annual maintenance, 20 years |

Figure 4.40 and Table 4.14 illustrates the estimated life-cycle costs for the pavement structures, juxtaposed with the initial construction costs listed in Table 4.12. In SMA mixtures, the total NPV of SS, SG, SLC, and SDC was approximately 14%, 4%, 14%, and 8% lower, respectively than that of the control mixture ST. The disparity between SG and SDC with ST decreased due to rehabilitation during the service life. The LCCA revealed considerable cost savings when utilizing candidate aggregates to substitute traprock in SMA mixtures, despite the need for occasional rehabilitations due to acceptable performance differences. For HMA mixtures, the total NPV of HS, HG, and HDC was approximately 1%, 2%, and 0.04% higher than that of the control mixture HLC, respectively, indicating no significant cost difference when using candidate aggregates as alternatives in HMA mixtures.

Upon comparing the initial construction cost and life cycle cost, incorporating predicted fatigue performance for each mixture with candidate aggregates, it was evident that utilizing all candidate aggregates as alternatives in SMA and high-quality HMA would be more cost-effective, with comparable performance.

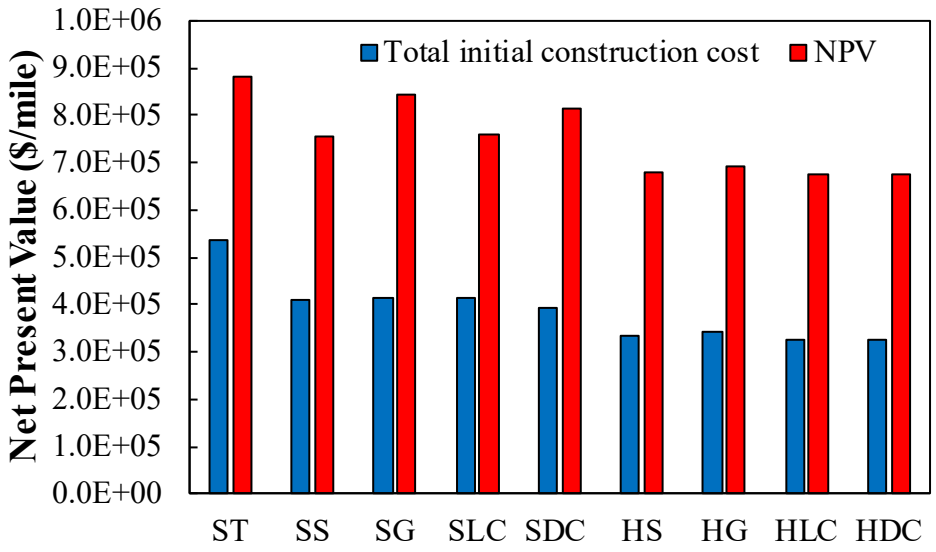


**Figure 4.31 Comparison of the initial costs and life-cycle costs of the pavement structures.**

**Table 4.14 Results of NPV After 20 years for All SMA and HMA Mixtures**

| Mixture Type | NPV, $/mile | % Increase vs. Control |
|---|---|---|
| **ST** | 882732.6 | 0.00 |
| **SS** | 755725.5 | -14.39 |
| **SG** | 844413.8 | -4.34 |
| **SLC** | 760741.6 | -13.82 |
| **SDC** | 815967.5 | -7.56 |
| **HLC** | 673934.6 | 0.00 |
| **HS** | 681087.5 | 1.06 |
| **HG** | 690264.5 | 2.42 |
| **HDC** | 674188.5 | 0.04 |

# CHAPTER 5 FRICTION EVALUATION OF MIXTURES WITH ALTERNATIVE AGGREGATES

## 5.1 Introduction

SMA is a gap-graded bituminous mixture which is designed to be tough, stable, and rut-resistant. SMA has good resistance to both cracking and rutting due to higher binder content and aggregate-to-aggregate contact, respectively. SMA mixtures use high quality rock and therefore it is more expensive compared to conventional Superpave mixes. In this study, the friction characteristics of SMA mixes prepared with alternatives aggregates including traprock, gravel, chat, steel slag, and dolomite were evaluated and compared to conventional dense graded Superpave mixes prepared using two different aggregates including gravel and chat.

The skid resistance of roads depends on microtexture and macrotexture of the pavement (Dahir 1979). The macrotexture of a pavement surface is affected mostly by mixture design, aggregate size distribution, and compaction level. Microtexture is related primarily to aggregate texture, angularity, and shape (Kandhal and Parker 1998, Crouch et al. 1995). Hogervorst (1974) has shown that skid resistance changes with vehicle speed and it depends on both microtexture and macrotexture (Figure 5.1). The results showed that the skid resistance decreased with vehicle speed, and pavements with coarse and rough surface provided better skid resistance compared to the ones with fine and polished surface. Other studies showed that the surface of asphalt pavements must maintain a minimum acceptable safe limit of texture (Bloem 1971).

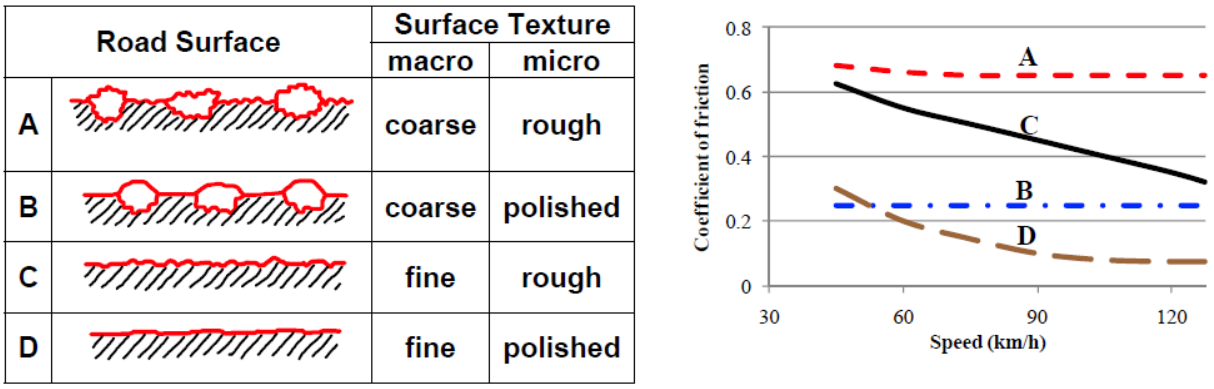


**Figure 5.1 The relationships of surface friction to surface texture and vehicle speed (after Hogervorst 1974).**

The main objective of the work conducted at the University of Idaho is to evaluate the frictional characteristics of SMA and conventional Superpave mixes prepared using different types of aggregates. The researchers evaluated seven different mixes: five SMA and two conventional dense graded Superpave mixes. SMA mixtures were prepared with traprock, gravel, blend S1, steel slag, and blend S2 aggregates, while dense graded HMA mixtures were prepared with gravel and blend H1 aggregates. The three-wheel polisher was used to simulate surface

polishing due to abrasion under traffic. The DFT was used to measure the coefficient of friction at different polishing stages.

## 5.2 Asphalt Mixture Test Slabs

The test asphalt mixtures were prepared at Missouri S&T and delivered to the researchers at the University of Idaho in 40-lb boxes. The loose mixtures were heated to the compaction temperature, and test slabs were prepared from various mixtures following procedure below:

- A steel mold (20 in × 20 in × 2 in) (Figure 5.2a) was heated to the compaction temperature.
- A non-stick thermal paper was placed in the steel mold (Figure 5.2a).
- The loose mixture was heated to the compaction temperature and placed and spread in the steel mold (Figure 5.2b and c).
- Another layer of non-stick thermal paper was placed at the top of the loose mixture (Figure 5.2d).
- Place the top steel plate of the compaction mold on the top of the non-stick paper (Figure 5.2e).
- Use a plate compactor to compact the mixtures (Figure 5.2f).
- Disassemble the compaction mold to extract the compacted slab (Figure 5.2g).
- The prepared test slab after compaction (20 in × 20 in × 2 in) is shown in Figure 5.2h.

## 5.3 Mearing the Frictional Characteristics of Test Slabs

The asphalt mixture test slabs (20 in × 20 in × 2 in) were subjected to accelerated polishing using a three-wheel polisher (Figure 5.3) and the friction characteristics are evaluated at different polishing cycles (0, 5000, 25000, 50000, 100000, and 150000 cycles). The three-wheel polisher has a set of three rubber tires that are attached to a turntable that rotates on the test slabs. The three-wheel polisher has a water spray system to reduce the wear of the rubber tires and wash away the fines at the surface due to polishing and expose the surface for further polishing. The total weight applied on the tires is about 120 lb.

The DFT was used in accordance with ASTM E1911 to measure the coefficient of friction at different speeds. The DFT provides continuous friction measurements over a range of speeds (from 20 km/h to 80 km/h). This device consists of a circular disk with three rubber pads (Figure 5.4). The circular disk rotates up to 100 km/h. Once the disk reaches the specified speed, the disk is lowered to the pavement surface, and the coefficient of friction is measured as the speed of the rotating disk gradually decreases.

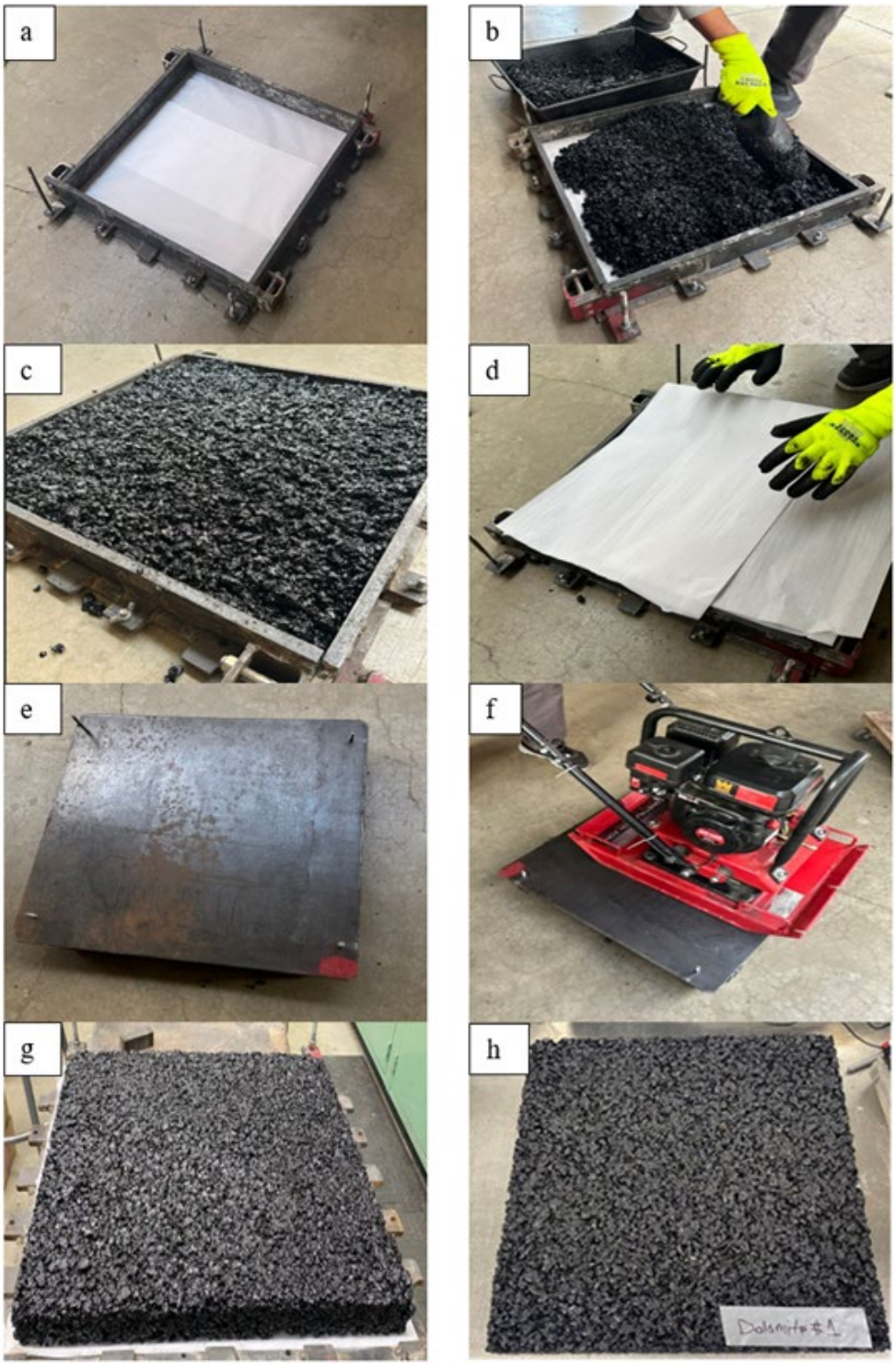


**Figure 5.2 Preparing and compaction of asphalt mixture test slabs.**

**Figure 5.3 Accelerated polishing testing using three-wheel polisher.**

**Figure 5.4 Dynamic friction tester and the bottom of the DFT with three rubber sliders attached.**

The sand patch test was conducted on the test slabs to measure the mean texture depth (MTD) of the surface. The test is conducted in accordance with ASTM E965. Equation 6.1 was used to calculate the MTD according to the following steps (Figure 5.5).

- Clean the surface of the slab with a brush as needed.
- Fill a standard cylinder with a known volume (80ml) of clean silica Ottawa sand.
- Pour the Ottawa sand on the surface of the slab at the desired location.
- Using the provided spreader tool, distribute the sand on the surface in a circular motion.
- Measure the diameter of the circle to calculate the MTD using Equation 5.1.

$$MTD = 4V/(\pi D^2)$$

where:

MTD = mean texture depth, mm
V = sand volume, $mm^3$
D = average diameter of sand patch circle, mm

**Equation 5.1 MTD Calculation**

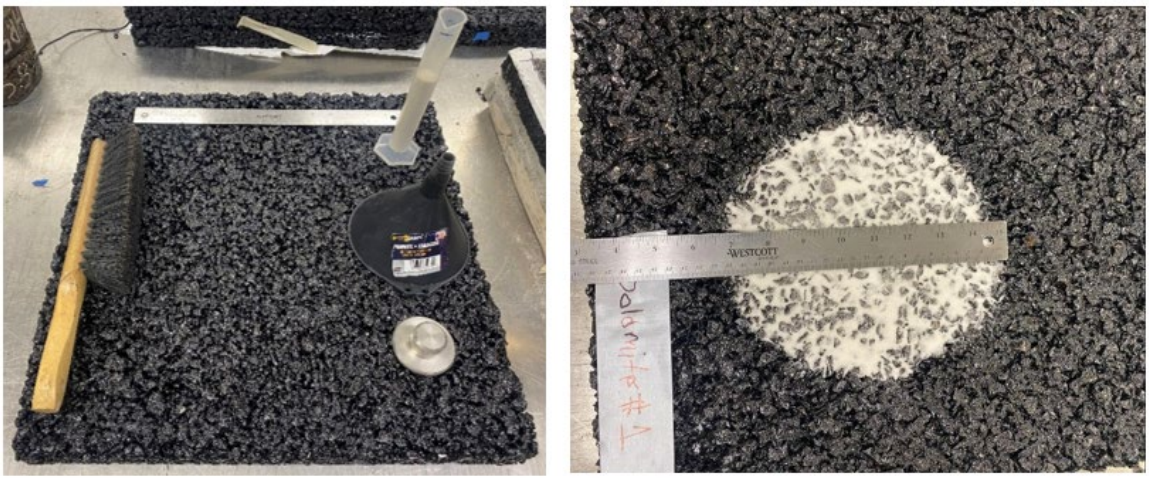

**Figure 5.5 Sand patch test.**

## 5.4 Texture and Coefficient of Friction Results

Table 5.1 summarizes the MTD results of the test surfaces. The MTD in Table 5.1 was the average for two slabs, and three MTD measurements were taken on each slab. It should be noted that two slabs were tested from each mixture. The MTD of SMA mixtures ranged from 2.21 mm to 1.47 mm with an average MTD of 1.85 mm. On the other hand, the MTD of HMA mixtures ranged from 1.05 to 0.92 mm with an average MTD of 0.99 mm. SMA mixtures have higher MTD compared to HMA since they have coarser aggregate gradations. In addition, for the same aggregate gradation, the aggregate surface properties such as aggregate angularity and morphology may also affect the surface MTD.

**Table 5.1 MTD Measured Using the Sand Patch Test**

| Mixture ID | MTD, mm |
|---|---|
| **ST** | 2.10 |
| **SG** | 1.89 |
| **SLC** | 1.57 |
| **SS** | 2.21 |
| **SDC** | 1.47 |
| **HLC** | 1.05 |
| **HG** | 0.92 |

Table 5.2 summarizes the coefficient of friction measurements for the SMA and HMA mixtures at different speeds (i.e., 20, 40, 60, and 80 km/h) and after different polishing cycles (i.e., 0 cycles [initial friction], 5k, 25k, 50k, 100k, and 150k cycles [terminal friction]). The coefficient of friction values in Table 5.2 are the average for two slabs and at least two DFT measurements were taken on each slab at each speed. Figures 5.6 to 5.9 show the DFT measurements at 20, 40, 60, and 80 km/h, respectively.

The results demonstrated that there was an initial increase in friction, until 5000 cycles, for most of the test mixtures. The early increase in friction was related to removing the asphalt binder film covering the aggregates. The friction increased as the aggregates got exposed and then the friction decreased due to aggregate polishing until a terminal value. These observations were supported by visual inspection of the surface in the laboratory and reported in previous studies (Al-Assi et al. 2018). More importantly, the results demonstrated that at higher speeds (i.e., 60 and 80 km/h), the SS had the highest friction compared to all remaining SMA and HMA mixtures. The control mixture ST had higher friction compared to other SMA and HMA mixtures. Furthermore, all SMA mixtures had higher friction compared to HMA mixtures.

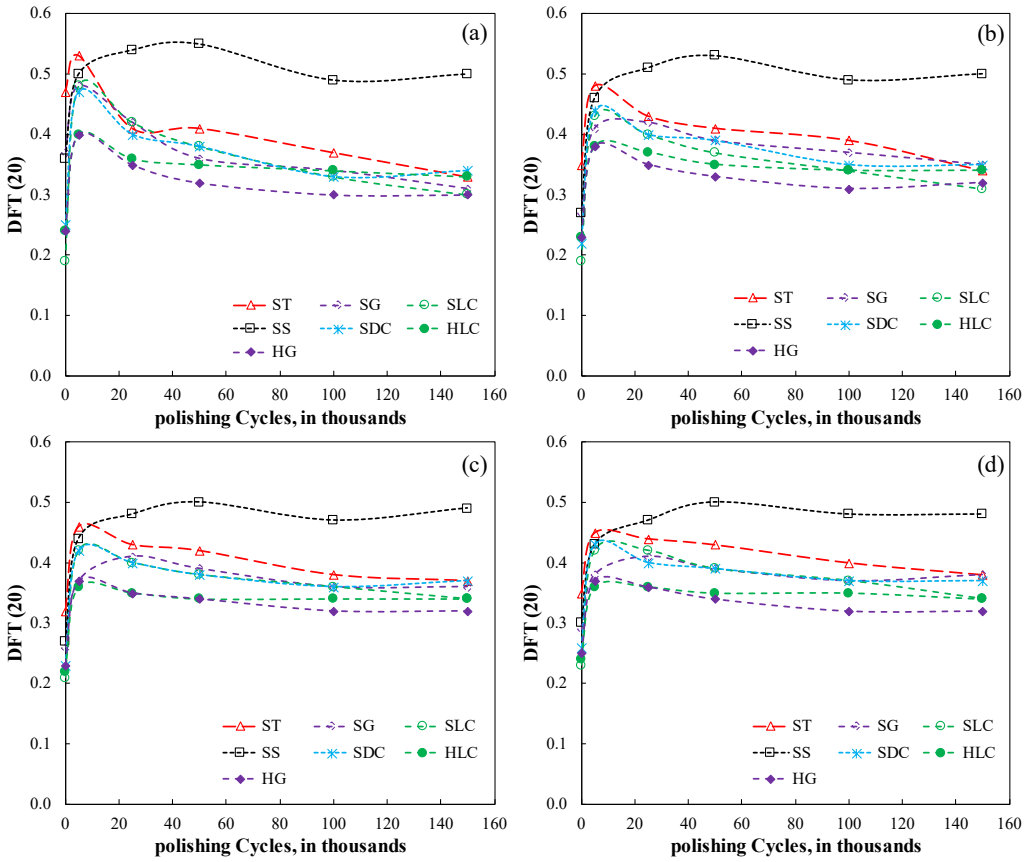


**Figure 5.6 DFT measured after different polishing cycles: (a) at 20 km/h, (b) at 40 km/h, (c) at 60 km/h, and (d) at 80 km/h.**

**Table 5.2 Summary of the Coefficient of Friction Measurements Using DFT at Different Polishing Cycles and Speeds**

| Mixture ID | Speed | Polishing Cycles, in thousands | | | | | |
|---|---|---|---|---|---|---|---|
| | | 0 | 5 | 25 | 50 | 100 | 150 |
| ST | 20 | 0.47 | 0.53 | 0.41 | 0.41 | 0.37 | 0.33 |
| | 40 | 0.35 | 0.48 | 0.43 | 0.41 | 0.39 | 0.34 |
| | 60 | 0.32 | 0.46 | 0.43 | 0.42 | 0.38 | 0.37 |
| | 80 | 0.35 | 0.45 | 0.44 | 0.43 | 0.40 | 0.38 |
| SG | 20 | 0.37 | 0.48 | 0.42 | 0.36 | 0.34 | 0.31 |
| | 40 | 0.27 | 0.41 | 0.42 | 0.39 | 0.37 | 0.35 |
| | 60 | 0.26 | 0.37 | 0.41 | 0.39 | 0.36 | 0.36 |
| | 80 | 0.29 | 0.38 | 0.41 | 0.39 | 0.37 | 0.38 |
| SLC | 20 | 0.19 | 0.48 | 0.42 | 0.38 | 0.33 | 0.30 |
| | 40 | 0.19 | 0.43 | 0.40 | 0.37 | 0.34 | 0.31 |
| | 60 | 0.21 | 0.42 | 0.40 | 0.38 | 0.36 | 0.34 |
| | 80 | 0.23 | 0.42 | 0.42 | 0.39 | 0.37 | 0.34 |
| SS | 20 | 0.36 | 0.50 | 0.54 | 0.55 | 0.49 | 0.50 |
| | 40 | 0.27 | 0.46 | 0.51 | 0.53 | 0.49 | 0.50 |
| | 60 | 0.27 | 0.44 | 0.48 | 0.50 | 0.47 | 0.49 |
| | 80 | 0.30 | 0.43 | 0.47 | 0.50 | 0.48 | 0.48 |
| SDC | 20 | 0.25 | 0.47 | 0.40 | 0.38 | 0.33 | 0.34 |
| | 40 | 0.22 | 0.44 | 0.40 | 0.39 | 0.35 | 0.35 |
| | 60 | 0.23 | 0.42 | 0.40 | 0.38 | 0.36 | 0.37 |
| | 80 | 0.26 | 0.43 | 0.40 | 0.39 | 0.37 | 0.37 |
| HLC | 20 | 0.24 | 0.40 | 0.36 | 0.35 | 0.34 | 0.33 |
| | 40 | 0.23 | 0.38 | 0.37 | 0.35 | 0.34 | 0.34 |
| | 60 | 0.22 | 0.36 | 0.35 | 0.34 | 0.34 | 0.34 |
| | 80 | 0.24 | 0.36 | 0.36 | 0.35 | 0.35 | 0.34 |
| HG | 20 | 0.24 | 0.40 | 0.35 | 0.32 | 0.30 | 0.30 |
| | 40 | 0.23 | 0.38 | 0.35 | 0.33 | 0.31 | 0.32 |
| | 60 | 0.23 | 0.37 | 0.35 | 0.34 | 0.32 | 0.32 |
| | 80 | 0.25 | 0.37 | 0.36 | 0.34 | 0.32 | 0.32 |

## 5.5 International Friction Index and Skid Number Calculations

The DFT and texture measurements were used to calculate the IFI as given in Equation 5.2 (Masad et al. 2011). The IFI values were then used to estimate the skid number values measured at 50 mph (SN50) using a skid trailer with smooth tires (Equation 5.3).

$$IFI = 0.081 + 0.732 DFT_{20} \exp\left(\frac{-40}{S_p}\right)$$

$$S_p = 14.2 + 89.7 MPD$$

$$MTD = 0.947\ MPD + 0.069$$

Where:

*IFI* = International Friction Index
*$DFT_{20}$* = coefficient of friction at 20 km/h measured using DFT
*$S_p$* = speed constant
*MPD* = mean profile depth
*MTD* = mean texture depth

**Equation 5.2 IFI Calculation**

$$SN(50) = 1.41 + 143.19(IFI - 0.045)e^{\frac{-20}{S_p}}$$

Where:

*SN(50)* = skid number measured at 50 mph using skid trailer with smooth tires

**Equation 5.3 *SN(50)* Calculation**

Figure 5.7(a) shows the change in IFI with polishing cycles. The IFI is an index that combines both microtexture and macrotexture. The DFT measured at 20 km/h is used to present microtexture while MTD or MPD is used to represent macrotexture. The results of IFI and predicted skid number at 50 mph (SN50) shown in Figure 5.7(b) further demonstrated that SMA mixtures had higher friction compared to HMA mixtures. Also, SS had the highest friction followed by ST. SG, SLC and SDC had relatively comparable friction values but less than the control mixture ST; however, such difference is low at the terminal friction. The two HMA mixtures had lower friction compared to SMA mixtures and HLC had slightly higher friction compared to HG.

These results were consistent with the findings of previous studies (Kassem et al. 2012, 2013) where mixtures with coarser aggregate gradations such as SMA and porous friction course (PFC) had higher friction compared to dense graded HMA mixtures. In addition, the steel slag was reported to improve the friction in previous studies (Noureldin et al. 1990, Ji et al. 2023). The researchers noted that SS test slabs caused significant wear to the rubber tires of the three-

wheel polisher, and there was a residue of ground rubber at the surface of slabs as shown in Figure 5.8.

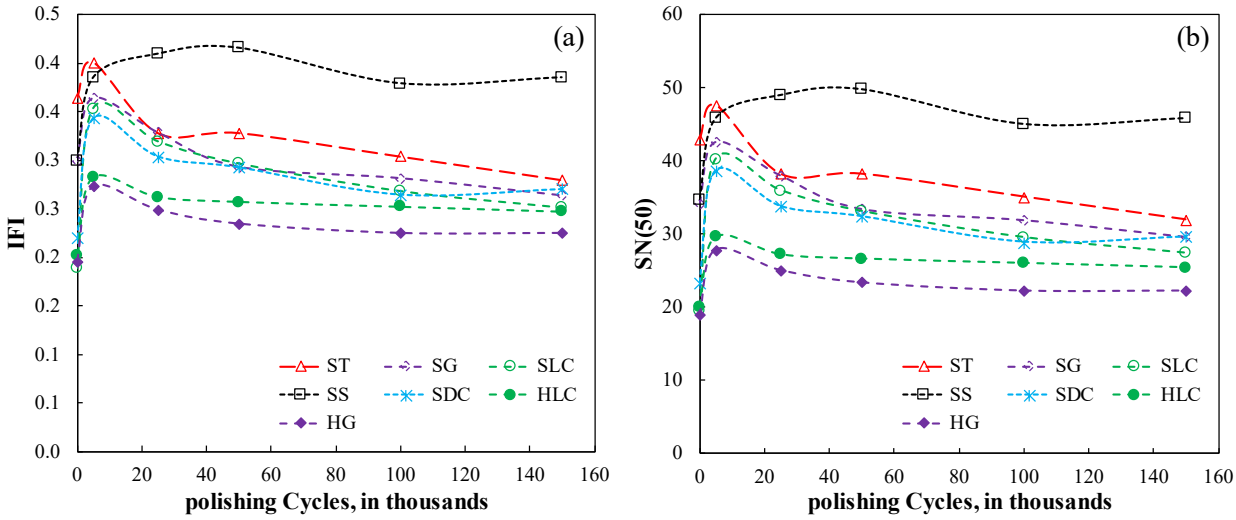


**Figure 5.7 Results at different polishing cycles: (a) change in IFI with polishing, and (b) predicted skid number at 50 mph (SN50).**

**Figure 5.8 Excessive wearing of rubber tires and gound rubber at the surface of the test SS.**

# CHAPTER 6 CONCLUSIONS AND RECOMMENDATIONS

The objective of this study was to identify and compare locally available, cost-effective, and durable crushed aggregates as alternatives to traprock (the current specified aggregate type for SMA in Missouri) for use in SMA and higher level Superpave mixes. Multiple well-distributed aggregates were evaluated in this study as candidate coarse aggregates, including traprock (control), chat, gravels, steel slag, limestone, and dolomite. A series of screening tests, including deleterious materials, LA abrasion test, angularity, flat and elongated aggregates, absorption, and sand equivalent, were conducted. Additionally, the Micro-Deval abrasion test, post-compaction degradation assessment, and soundness tests were also undertaken to assess their resistance to polishing, degradation, and freeze-thaw damage, respectively. After the screening tests, SMA and HMA mixtures with qualified candidate aggregates were designed in accordance with the AASHTO R 46 and R35, respectively. Following the volumetric design, performance tests, including the HWTT rutting tests and IDEAL-CT cracking tests, were conducted for performance verification. The design was finalized if it passed the performance requirements. Otherwise, more tests were conducted to identify the performance optimum binder content. To fully evaluate and compare the mix performance with different aggregates, cracking and rutting tests, AMPT and low-temperature IDT tests were also performed. Performance analysis on both the material and the structural level was also completed. DFT was also conducted to evaluate their resistance to polishing under traffic load and cost analyses were applied to mixes with these alternatives. The results of each candidate aggregates used in both SMA and HMA were concluded as follows:

**Steel Slag:**

Except for degradation, steel slag in both SMA and HMA met all the requirements in aggregate screening and durability tests. SMA with steel slag showed a 5.7% increase of aggregate on the #8 sieve in the degradation test, slightly exceeding the 4% limit in Kansas DOT's report. During the design of both SMA and HMA mixtures with steel slag, the mixtures passed the volumetric and moisture susceptibility tests but failed to meet the IDEAL-CT cracking threshold. After identifying the performance optimum binder content, the revised SMA and HMA mixtures with steel slag satisfied all the requirements in volumetric properties, moisture susceptibility, workability, and resistance to cracking and rutting.

Compared to the control mixture ST, SMA with steel slag exhibited lower cracking resistance at intermediate temperatures, though still within acceptable limits. It demonstrated enhanced rutting resistance, with comparable results in the HWTT and a 61.1% improvement in the AMPT SSR test. The difference in thermal cracking temperature was minimal, at 0.3 ℃. There was a 5.1% rise in moisture susceptibility, a 37.6% increase in friction, and a 10.1% reduction in fatigue resistance. Additionally, it showed a 14.4% decrease in the predicted life cycle cost.

Compared to the control mixture HLC, HMA with steel slag displayed a slight decline in both cracking resistance at intermediate temperatures and rutting resistance, yet it remained within acceptable performance levels. The difference in TSR (moisture susceptibility) was minimal, at 0.038. It showed a 5.16% improvement in thermal cracking resistance and a 26% enhancement in fatigue resistance. Additionally, the predicted life cycle cost rose slightly by 1.1%.

**Gravel:**

The angularity test results for gravel were determined as 98% for one face and 95% for two faces in SMA mixtures, and 98% for one face and 97% for two faces in HMA mixtures. These results were slightly below the required limit of 100% for both conditions. Given that this deviation is small, and the gravel met all other screening test criteria, it was included for further evaluation, including mix design and performance analysis. The mix designs for SMA and HMA with gravel achieved satisfactory volumetric properties and passed the BMD performance tests requirements.

Compared to the control mixture ST, SMA with gravel exhibited reduced cracking resistance at intermediate temperatures, although it still performed adequately. It demonstrated enhanced rutting resistance, with a 10.6% improvement in the HWTT and a 30.1% increase in the AMPT SSR test. The differences in TSR (moisture susceptibility) and thermal cracking temperature were minimal, at 0.003 and 0.4 ℃, respectively. There was a 5.7% reduction in friction and a 19% decrease in fatigue resistance. Additionally, the predicted life cycle cost was reduced by 4.3%.

Compared to the control mixture HLC, HMA with gravel exhibited a 22.5% improvement in cracking resistance at intermediate temperatures. It demonstrated reduced rutting resistance, with a 1.9% decrease in the HWTT and a 28.4% reduction in the AMPT SSR test, although still within acceptable levels. The difference in TSR was minimal, at 0.011. Thermal cracking resistance increased by 5.6%, while fatigue resistance improved by 26.7%, and friction decreased by 9%. Additionally, the predicted life cycle cost rose by 2.4%.

**Limestone, Dolomite, and Chat:**

Testing revealed that using limestone or dolomite alone as the coarse aggregate in both SMA and HMA mixtures could be challenging in meeting VMA requirements. The chat sampled in this study displayed remarkable durability in screening tests but was unsuitable as the sole coarse aggregate due to its small NMAS. To address these issues, researchers developed new blends by combining limestone or dolomite with chat.

**Limestone & Chat:**

Limestone and chat in SMA met all the requirements in aggregate screening and durability tests. The mix design for SMA with limestone & chat also achieved satisfactory volumetric properties and met the BMD performance tests.

Compared to the control mixture ST, SMA with limestone & chat exhibited reduced cracking resistance at intermediate temperatures, yet it still performed well. It showed enhanced rutting resistance, with results in the HWTT comparable and a 32.9% improvement in the AMPT SSR test. The TSR difference was minimal, at 0.004. Thermal cracking resistance decreased by 5.5%, friction was reduced by 10.4%, and fatigue resistance dropped by 12.8%. Additionally, the predicted life cycle cost was lowered by 13.8%.

**Dolomite & Chat:**

Dolomite & chat in both SMA and HMA met all the requirements in aggregate screening and durability tests. The mix design for SMA and HMA with dolomite & chat also achieved satisfactory volumetric properties and fulfilled the BMD performance tests.

Compared to the control mixture ST, SMA with dolomite & chat showed decreased resistance to cracking at intermediate temperatures and rutting, though it remained within required limits. The thermal cracking temperature difference was minimal, at 0.4 ℃. TSR was reduced by 9.1%, though still meeting the minimum requirement. Fatigue resistance decreased by 35.4%, and friction dropped by 3.4%. Additionally, the predicted life cycle cost was reduced by 7.6%.

Compared to the control mixture HLC, HMA with dolomite & chat demonstrated reduced cracking resistance at intermediate temperatures yet remained acceptable. Moisture susceptibility increased by 2.8%, while thermal cracking resistance improved by 4.2% and fatigue resistance saw a 2.5% enhancement. Additionally, the predicted life cycle cost remained consistent.

**Recommendations**

- Steel slag and crushed gravel can replace traprock in SMA mixtures and limestone & chat in HMA mixtures, meeting all aggregate requirements and providing satisfactory performance with a verified optimum performance binder content.

- Limestone or dolomite alone are challenging to use as coarse aggregates in both SMA and HMA mixtures due to difficulties in meeting the VMA requirement.

- The chat sampled in this study showed excellent durability in screening tests but was not used alone as coarse aggregate in mixtures due to its small NMAS.

- Blending limestone or dolomite with chat as coarse aggregate in SMA and HMA mixtures yielded acceptable results in aggregate tests, volumetric properties, and qualified performance in mixtures.

# REFERENCE


Al-Assi, M., Kassem, E., Kogbara, R.B., and Masad, E. 2018. "Improving pavement friction through aggregate blending." *Advances in Materials and Pavement Performance Prediction*. CRC Press (2018): 277-280.

Ale Mohammadi, M., Aghasoltan, A., & Kavusi, A. 2014. "An optimal grading model to improve the rut resistance of stone mastic asphalt." *Transportation Research Board. 93rd Annual meeting,* Paper #14-4633.

Ameli, A., Hossein Pakshir, A., Babagoli, R., Norouzi, N., Nasr, D., and Davoudinezhd, S. 2020. "Experimental investigation of the influence of nano $TiO_2$ on rheological properties of binders and performance of Stone Matrix Asphalt mixtures containing steel slag aggregate." *Construction and Building Materials*, Vol. 265, No. 120750.

Apeagyei, A. K., McGhee, K. K., Clark, T., & Clark, T. M. 2013. "Influence of aggregate packing and asphalt binder characteristics on performance of stone matrix asphalt." *Transportation Research Board. 92nd Annual meeting*, Paper #13-0622.

Bloem, D. L. 1971. Skid-Resistance: "The role of aggregates and other factors." *National Sand and Gravel Association Circular 109*, Silver Spring, Md.

Bonaquist R. 2011. *Characterization of Wisconsin mixture low temperature properties for the AASHTO MEPDG*. Report WHRP 11-12. Wisconsin Department of Transportation, Madison.

Celaya, B. J., Haddock, J. E. 2006. *Investigation of coarse aggregate strength for use in Stone Matrix Asphalt*. Final Report. FHWA/IN/JT2P-2006/4. Indiana Department of Transportation.

Christensen, D. 1998. "Analysis of creep data from indirect tension test on asphalt concrete." *Journal of the Association of Asphalt Paving Technologists*, 67(1998): 458-492.

Cross, S. A. 1999. *Aggregate specification for Stone Mastic Asphalt (SMA).* Final Report. K-TRAN: KU-97-5. Kansas Department of Transportation.

Crouch L. K., Gothard J. D., Head G., and Goodwin W. A. 1995. "Evaluation of textural retention of pavement surface aggregates". *Transportation Research Record 1486:* 124–129.

Dahir, S. H. 1979. "A review of aggregate selection criteria for improved wear resistance and skid resistance of bituminous surfaces." *Journal of Testing and Evaluation*, JTEVA, Vol. 7, No. 5: 254-253.

Feigenbaum, B., Bui, T., and Nguyen, T. *2023. Missouri ranks 11th in the nation in highway performance and cost-effectiveness.* Accessed April 20, 2023. https://reason.org/policy-study/27th-annual-highway-report/missouri/.

Hills, J.F. and Brien, D. 1966. “The fracture of bitumens and asphalt mixes by temperature induced stresses.” *Prepared Discussion, Proceedings, the Association of Asphalt Paving Technologists*, 35: 292-309.

Hogervorst, D. 1974. “Some properties of crushed stone for road surfaces.” *Bulletin of The International Association of Engineering Geology* 10: 59-64.

James, T., & Prowell, B. 2022. “Evaluation of high Los Angeles abrasion loss aggregate in Stone Matrix Asphalt.” *Transportation Research Record*, 2676(5): 116-131.

Ji, K., Shi, C., Jiang, J., Tian, Y., Zhou, X., Xiong, R. 2023. “Determining the Long-Term Skid Resistance of Steel Slag Asphalt Mixture Based on the Mineral Composition of Aggregates.” *Polymers*, 15: 807, doi: 10.3390/polym15040807.

Kandhal, P. S., and F. Jr. Parker 1998. *Aggregate tests related to asphalt concrete performance in pavements*. NCHRP Report 405, National Cooperative Highway Research Program, National Academy Press, Washington, D.C.

Kassem, E., Awed, A., Masad, E., and Little, D. 2013. “Development of a predictive model for skid loss of asphalt pavements.” *Journal of the Transportation Research Board*, 2372: 83–96.

Kassem, E., Masad, E., Awed, A., and Little, D. 2012. *Laboratory evaluation of friction loss and compactability of asphalt mixtures*. Texas Transportation Institute, Research Report SWUTC/12/476660-00025-1, Texas A&M University, College Station, TX

Kim, Y. R., Castorena, C., Wang, Y. D., Ghanbari, A., and Jeong, J. 2018. Comparing performance of full-depth asphalt pavements and aggregate base pavements in NC. Final Report. NCDOT Project 2015-02, FHWA/NC/2015-02. North Carolina Department of Transportation.

Kim, Y. R., Guddati, M., Choi, Y., Kim, D., Norouzi, A., Wang, Y. D., Keshavarzi, B., Ashouri, M., Ghabari, A., Wargo, A. D. 2022. *Hot-mix asphalt performance-related specification based on viscoelastoplastic continuum damage (VEPCD) models*. Final Report. Federal Highway Administration. Publication No. FHWA-HRT-21-093.

Kim, Y. R., J. Lee, and Y. Wang. 2015. *MEPDG inputs for Warm-Mix Asphalts*. Final Report. NCDOT Project 2012-01, FHWA/NC/2012-01.

Kowalski, K. J., McDaniel, R. S., & Olek, J. 2010. *Identification of laboratory technique to optimize Superpave HMA surface friction characteristics*.

Liu, J., Mullin, A., and Rein, J. 2012. *Use of the Micro-Deval test for assessing Alaska aggregates*. Final Report. FHWA-AK-RD-12-22. Alaska Department of Transportation.

Liu, J., and Wang, Y. D., 2023. Comprehensive data analysis for AMPT Tests on MO 740 and Hwy 54. Final Report. cmr 23-017. Missouri Department of Transportation.

Liu, J., Zhao, S., Li, L., Li, P., & Saboundjian, S. 2017. “Low temperature cracking analysis of asphalt binders and mixtures.” *Cold Regions Science and Technology*, 141: 78-85.

Liu, J., Zhou, F., Romero, P., Wang, Y. D., & Lin, B. 2022. *Development of holistic methodologies for improving asphalt mix durability,* Final Report. TriDurLE.

Liu, Y., Nair, H., Lane, S., Wang, L., & Sun, W. (2019). *Influence of aggregate morphology and grading on the performance of 9.5-mm Stone Matrix Asphalt mixtures*. Final Report. FHWA/VTRC 19-R15. Virginia Transportation Research Council.

Masad, E., Rezaei, A., Chowdhury, A. 2011. *Field evaluation of asphalt mixture skid resistance and relationship to aggregate characteristics*, Report 0-5627-3, Texas Transportation Institute, College Station, Texas

McDaniel, R. S., and Shah, A. 2012. *Maximizing the use of local materials in HMA surfaces*. Final Report. FHWA/IN/JTRP-2012/07. Indiana Department of Transportation.

Miao, Y., Wang, S., Sun, F., and Yang, J. 2022. “A laboratory investigation into the polishing behavior of Stone Matrix Asphalt with different lithology types of coarse aggregates.” *Journal of Testing and Evaluation*. Vol. 50(4): 1749-1762.

Mohammad, L., Zhang, X., Huang, B., and Tan, Z. 1999. “Laboratory performance evaluation SMA, CMHB, and dense graded asphalt mixtures.” *Journal of the Association of Asphalt Paving Technologists*. Vol. 68: 252-283.

National Asphalt pavement Association (NAPA). 2002. *Designing and constructing SMA Mixtures, state-of-the-practice.* Quality Improvement Series 122.

Noureldin, A. Samy, McDaniel, S. Rebecca 1990. “Evaluation of surface mixtures of steel slag and asphalt.” *Transportation Research Record*, 1269 (1990): 133-149.

Polaczyk, P., Ma, Y., Hu, W., Xiao, R., Jiang, X., & Huang, B. 2022. “Effects of mixture and aggregate type on over-compaction in hot mix asphalt in Tennessee.” *Transportation Research Record*, 2676(4): 448-460.

Smith, K. L., Pierce, L. M., Chang, G. K., & Nadkarni, A. A. 2023. *Lifecycle cost analysis RealCost user manual*. Final Report. No. FHWA-HRT-23-021. United States. Department of Transportation. Federal Highway Administration. Office of Infrastructure Research and Development.

Temperature Estimate Model for Pavement Structures (TEMPS). 2016. Asphalt Research Consortium, University of Nevada Reno (ARC-UNR). http://www.arc.unr.edu/Software.html# , TEMPS Accessed on July 31, 2016.

Wang, Y. D. Ghanbari, A., Underwood, B. S., and Kim, Y. R. 2021. “Development of performance-engineered mix design for asphalt concrete.” *International Journal of Pavement Engineering*. DOI: 10.1080/10298436.2021.1938044

Wang, Y. and Kim, Y. R. 2017. “Development of a pseudo strain energy-based fatigue failure criterion for asphalt mixtures.” *International Journal of Pavement Engineering*. DOI: 10.1080/10298436.2017.1394100

Wang, Y. D., Keshavarzi, B., and Kim, Y. R. 2018. “Fatigue performance analysis of pavements with RAP using viscoelastic continuum damage theory.” *KSCE Journal of Civil Engineering*, 22(6): 2118-2125. DOI: 10.1007/s12205-018-2648-0

Wang, Y. D., Liu, J. and Liu, J. 2023. “Integrating quality assurance in balance mix designs for durable asphalt mixtures: state-of-the-art literature review.” *ASCE Journal of Transportation Engineering Part B: Pavements*. 149(1). DOI: 10.1061/JPEODX.PVENG-957

Wang, Y. D., Underwood, B. S., and Kim, Y. R. 2020. “Development of fatigue index parameter, $S_{app}$, for asphalt mixes using viscoelastic continuum damage theory.” *International Journal of Pavement Engineering*. DOI: 10.1080/10298436.2020.1751844

Yin, F., West, R., Powell, B., & DuBois, C. J. 2023. “Short-term performance characterization and fatigue damage prediction of asphalt mixtures containing polymer-modified binders and recycled plastics.” *Journal of the Transportation Research Board. https://doi.org/10.1177/03611981221143119*.

Zhao X., Sheng, Y., Lv, H., Jia, H., Liu, Q., Ji, X., Xiong, R., and Meng, J. 2022. “Laboratory investigation on road performances of asphalt mixtures using steel slag and granite as aggregate.” *Construction and Building Materials*. Vol. 315(10).

Zhou, F. 2019. *Development of an IDEAL cracking test for asphalt mix design, quality control and quality assurance*. NCHRP-IDEA Program Project Final Report No. 195. Transport Research Board, National Research Council, Washington, DC, 2019.

# APPENDIX A QUARRIES INFORMATION

**Table A.1 List of Quarries and Aggregates**

| Quarry | Ledge/ Component Facility ID | Ledge Description | Mix Component Material | Type |
|---|---|---|---|---|
| **Willard Constr, Sleeper** | 1-2 | Jefferson City | | Chat |
| **Williams Divers Matl (WDM), Lawyer (Bingham #11)** | CHAT | Flint Chat | | Chat |
| **Williams Divers Matl (WDM), Skelton (Bingham #12)** | CHAT | Flint Chat | | Chat |
| **Flint Rock Products, Admiralty (Humble S&G)** | FLINT CHAT | Commerce | Mineral Filler Traditional | Chat |
| **Williams Divers Matl (WDM), Sooner (Bingham #10)** | CHAT | Chat | | Chat |
| **Ameren - Union Electric, Rush Island Power Plant** | - | Jefferson County, Mo. | Mineral Filler from Fly Ash | Coal waste |
| **Cane Creek Stone** | 1-2 | Eminence-Potosi | | Dolomite |
| **Capital Quarries #17, Sullivan** | 1-2 | Potosi | | Dolomite |
| **Williamsville Stone #1** | 14A-17A | Gasconade | | Dolomite |
| **Lead Belt, Desloge Stone** | 1-2 | Bonne Terre | | Dolomite |
| **Martin Marietta (Mill Creek Quarry), OK** | 1 | Troy Granite | | Granite |
| **Capital Sand #1, Wardsville (Osage Riv)** | GRAVEL | Wardsville, MO | | Gravel |
| **Norris Quarries, Breit Quarry, Savannah** | 8AZ | Amazonia | | Limestone |
| **Lafarge - Perryville Quarry (Martin Marietta #366)** | 3A/3-7 | Plattin | | Limestone |
| **Capital Materials, Sedalia (Snow Rd-Dresden)** | 5-11 | Chouteau | | Limestone |
| **Bailey (Roach) Quarry** | 6-7 | Jefferson City-Cotter | | Limestone |
| **Boone Quarries, Millersburg (Mid MO Mertens)** | 2-4 | Burlington | | Limestone |
| **Bussen #3, Antire Quarry** | 14-11 | Plattin | | Limestone |

| | | | | |
|---|---|---|---|---|
| **Bussen #3, Antire Quarry** | 15-21 | Plattin | | Limestone |
| **Bussen #3, Antire Quarry** | 19-21 | Plattin | | Limestone |
| **Carthage Crushed Limestone** | 3 | Warsaw | Mineral Filler Traditional | Limestone |
| **Central Stone #31, Florissant** | 3-9 | St. Louis | | Limestone |
| **Kerford Limestone Co., NE** | 1K-4P | Plattsmouth, NE | Mineral Filler Traditional | Limestone |
| **Mississippi Lime #2 Quarry Ste. Genevieve** | MF | Ste. Genevieve | Mineral Filler Traditional | Limestone |
| **New Frontier, New Melle Quarry** | 7-2 | Plattin | | Limestone |
| **New Frontier, New Melle Quarry** | 2-4,4-7 | Plattin | | Limestone |
| **Seminole Ag-Lime Company, Inc.** | 23 | Plattin | | Limestone |
| **Southeast Missouri Stone (SEMO)** | 15-5A | Plattin | | Limestone |
| **Southeast Missouri Stone (SEMO)** | 34-22 | Plattin | | Limestone |
| **Southeast Missouri Stone (SEMO)** | 34-24 | Plattin | | Limestone |
| **Southeast Missouri Stone (SEMO)** | 39-11 | Plattin | | Limestone |
| **Southeast Missouri Stone (SEMO)** | 39-23 | Plattin | | Limestone |
| **New Frontier, Alton Weber #8** | 1-7 | St. Louis | | Limestone |
| **Nucor Steel Slag, Sedalia** | SLAG | Sedalia | | Slag/Steel Slag |
| **New Frontier, Iron Mountain Quarry-Porphyry** | 1 | Porphyry | | Traprock |
| **New Frontier, Iron Mtn Trap Rock Pit #3- Porphyry** | 1 | Porphyry | | Traprock |
| **Trap Rock and Granite Quarries, LLC*** | 2 | Rhyolite | | Traprock |
| **City Utilities, Springfield, James River Power** | | Springfield | Mineral Filler from Fly Ash | |
| **EM Resources, Cincinnati (ThomasHill Headwaters)** | | Cincinnati,OH | Mineral Filler from Fly Ash | |
| **EM Resources, Springfield, MO** | | Springfield | | |
| **Fischer Bros Pit #2, Ste. Genevieve** | 21-25 | Salem | | |

**Table A.2 Locations of Quarries for Candidate Aggregates**

| Aggregate Type | Quarry | Location | Remark |
|---|---|---|---|
| **Traprock** | New Frontier, Iron Mountain Quarry-Porphyry | Ironton, Iron County | Control; Southeast |
| **Chat 1** | Flint Rock Products, Admiralty (Humble S&G) | Commerce, Ottawa County | Southwest, Oklahoma |
| **Chat 2** | Willard Asphalt Paving | Lebanon, Laclede County | Middle |
| **Gravel 1** | Norris Quarries Savannah Quarry-Breit | Savannah, Andrew County | Northwest |
| **Gravel 2** | Capital Sand #1, Wardsville (Osage Riv) | Jefferson, Cole County | Middle |
| **Steel Slag** | Nucor Steel Slag | Sedalia, Pettis County | Midwest |
| **Limestone 1** | Kerford Limestone Co., NE | Weeping Water, Cass County | Northwest, Nebraska |
| **Limestone 2** | Carthage Crushed Limestone | Carthage, Jasper County | Southwest |
| **Limestone 3** | Mid-Missouri Limestone, Inc.-Millersburg Quarry | Fulton, Callaway County | Middle |
| **Dolomite 1** | Cane Creek Stone | Poplar Bluff, Butler County | Southeast |
| **Dolomite 2** | Lafarge - Perryville Quarry (Martin Marietta #366) | Perryville, Perry County | Mideast |
| **Granite** | Williamsville Stone #1 | Poplar Bluff, Butler County | Southeast |

# APPENDIX B LITERATURE REVIEW

This literature review aimed to compile and present information on the comprehensive efforts involved in testing and screening qualified aggregates for both SMA and high-quality HMA mixtures. The review covers various aspects, including aggregate types, properties that may impact the mixture, mixture design, performance, and the methodologies used to evaluate both aggregates and mixtures, providing a summarized overview in this chapter.

## B.1 Aggregate

### B.1.1 Aggregate Types Specified by DOTs

As the strength and the durability of the coarse aggregates are critical to SMA and higher level Superpave mixes, many states have limited the types of aggregates that can be used in the specifications, and Table B.1 lists some examples. The current MoDOT standard specifications (Sec. 403.3.3) allow the coarse aggregates to be a combination of at least 40% of porphyry by total weight (without the usage of steel slag) and other aggregates.

While the specified high-quality aggregates have been proven to be effective, the associated costs and availability are of concern to transportation agencies. One approach to reduce initial construction costs is to maximize the use of locally available aggregates. However, although the local aggregates are cost-beneficial, their applications may be limited, due to their quality.

**Table B.1 Examples of Specified Coarse Aggregate Types for SMAs and High-Level Superpave Mixtures**

| States | Aggregate Requirements |
|---|---|
| **Missouri** | ≥ 40% porphyry by weight; ≥ 50% porphyry on specific sieves; or ≥ 45% steel slag and porphyry; when using limestone, ≥ 30% non-carbonate material. |
| **Kansas** | For BM-1T, ≥ 50% and 45% on No. 4 and No. 8 of primary aggregates, respectively; Primary aggregates: sandstone, porphyry, siliceous gravel chat, crushed steel slag. |
| **Illinois** | For SMA $N_{design}$ 80: aggregates allowed to be used alone: crystalline crushed stone, crushed sandstone, crushed slag, and crushed steel slag; no limestone, carbonate crushed stone, or crushed concrete; combination: ≤ 50% crushed gravel, or Dolomite with crushed sandstone, crushed slag, crushed steel lag, or crystalline crushed stone. |
| **Arkansas** | Crushed stone, crushed gravel, or crushed steel slag; ≥ 90% crushed aggregates and ≤ 5% novaculite. |
| **Iowa** | Crushed stone, gravel, slag; for 30 million ESALs, when >40% limestone, specific friction requirements are needed. |
| **Nebraska** | Crushed Rock; Quartzite, granite, Dolomite, crushed rock with limestone with requirement met; chat or coal sand shall not be used in any mix. |
| **Indiana** | Steel furnace slag, sandstone, crushed dolomite, polish resistant aggregates or any blend of these aggregates may be used provided the aggregates are in |

| | |
|---|---|
| | accordance with 904.03(a); Polish resistant aggregates or crushed dolomite may be used when blended with sandstone but shall not exceed 50% of the coarse aggregate by weight (mass) or shall not exceed 40% of the coarse aggregate by weight (mass) when blended with steel furnace slag. The aggregates shall be in accordance with 904.03(a). |
| **Alabama** | Coarse aggregate shall be aggregate retained on the No. 4 sieve. The virgin coarse aggregate shall be 100% crushed granite, quarried quartzite, limestone, sandstone, slag, or other 100% crushed manufactured stone meeting the requirements given in Standard Specifications for Highway Construction Section 801. |
| **Louisiana** | Crushed stone; Crushed gravel, slag can be used in SMA. RAP is not allowed in SMA. |
| **Georgia** | Crushed stone, gravel, slag, or synthetic aggregates with percent wear of each individual size not to exceed 45% based on the B grading of AASHTO T 96. The maximum ratio of RAP material to the recycled mixture is 15% for Stone Matrix Asphalt (SMA) mixes. |
| **Texas** | Aggregates from sources listed in the Department's Bituminous Rated Source Quality Catalog (BRSQC) are preapproved for use. Use only the rated values for HMA listed in the BRSQC. |
| **Colorado** | Aggregates for stone matrix asphalt (SMA) shall be of uniform quality, composed of clean, hard, durable particles of crushed stone, crushed gravel, or crushed slag. |

### B.1.2 Efforts in Exploring Alternative Aggregate Types

Several states have initiated research studies to identify locally available aggregates for SMA and higher-level Superpave mixtures. Celaya and Haddock (2006) developed testing methods to quantify aggregate qualities and evaluate local aggregates to be used in SMA for Indiana DOT (INDOT). Among the tested materials, two dolomite aggregates experienced extensive degradation during compaction, and two SMA mixtures containing dolomite failed to meet the minimum requirements. It is required that aggregate used for asphalt surface mixtures with high volume traffic should have high friction to be resistant to polishing, according to INDOT specifications. This would include aggregate such as steel slag, blast furnace slag, or sandstone. A follow-up research project (McDaniel and Shah 2012) suggested that some local polish-susceptible coarse aggregates (i.e., limestone) could be allowed to be blended with steel or blast furnace slags or sandstone, and the combination could provide adequate friction. Additional studies (Mohammad et al. 1999, Miao et al. 2022, Zhao et al. 2022) have also been conducted to evaluate the applicability of other aggregate sources, such as novaculite and sandstone for the use in SMA mixtures. The Illinois DOT (IDOT) is currently conducting a research project aiming to determine the applicability of local and relatively soft aggregates (e.g., limestone, dolomite, or gravel) in SMA mixtures. In South Dakota, local quartzite aggregate was used successfully in its first SMA, because of its great surface friction (MacDonald 2005). In addition to governmental institutions' interest in the exploration and

applicability of alternative aggregates, many researchers have also made efforts to study this area. Listed below are some potential alternative aggregates, and information on their performance, that could be used in SMA and Superpave mixtures.

#### B.1.2.1 Basalt

In SMA mixes, basalt is preferred over limestone because basalt is harder than limestone (Ibrahim et al. 2009). Miao et al. (2022) investigated the polishing behavior of SMA mixtures with three different coarse aggregates (basalt, red sandstone, and limestone) and found that the mixture with basalt exhibited the best polishing resistance while the mixture with limestone showed relatively low polishing resistance. Cao et al. (2015) also compared the performance of SMA blends with different aggregate types, including limestone, basalt, and combinations thereof. The researchers arrived at the same conclusion that the basalt mixture showed better rutting resistance while the limestone performed well in terms of moisture stability.

#### B.1.2.2 Limestone

Limestone is cheaper than basalt. Therefore, some researchers tried to replace basalt with a certain percentage of limestone. Moaveni (2014) evaluated limestone as a fine fraction and filler in SMA with basalt. Despite the reduction in rutting resistance, limestone was suggested as a substitute for fine and filler aggregates in SMA. Mixtures containing soft limestone exhibited lower friction than mixtures with hard limestone or dolomite (Kowalski et al. 2010). Mohammad et al. (1999) evaluated the effect of different types of aggregates (i.e., limestone, sandstone, and novaculite) on the properties of SMA mixtures. The mixture with sandstone exhibited the highest anti-rutting index value, and the mixture with novaculite showed a higher rutting resistance than the mixture with limestone. The mixture with limestone had the highest axial creep slope out of these three types of aggregate.

#### B.1.2.3 Granite

James et at. (2022) evaluated the rutting resistance, moisture susceptibility, drain down, and cracking potential of the mixtures using a high-loss granitic aggregate source in South Carolina. The results were equivocal because the performance metrics varied widely when different nominal maximum aggregate sizes were used. Brown and Manglorkar (1993) performed several mechanical tests (i.e., Marshall Stability, tensile strength, and resilient modulus) to compare silicious gravel and granite in the SMA mixtures and concluded that the gradation and aggregate type had a significant impact on the optimum asphalt content and the durability of mixtures. The mixtures with granite aggregates had a higher optimum asphalt content, resilient modulus, and static creep modulus than the mixtures with the silicious gravel.

#### B.1.2.4 Steel slag

Steel slag is a by-product of iron. Many researchers have been exploring the feasibility of replacing aggregate with steel slag in SMA mixtures. Compared to SMA with basalt, the SMA with steel slag exhibited better high-temperature performance, low-temperature cracking resistance, and roughness (Xue et al. 2006). Zhao et al. (2022) evaluated SMA mixtures containing granite and steel slag. The mixtures showed better road performance including high-temperature stability and low-temperature cracking resistance. However, its long-term

resistance to moisture damage required further study. Replacing a portion of coarse aggregates with steel slag could improve the rutting resistance of SMA mixtures while reducing resilient modulus, indirect tensile (IDT) strength, tensile strength ratio (TSR), and fatigue resistance of mixtures (Ameli et al. 2020). Similar conclusions were obtained by Hainin et al. (2013). They conducted resilient modulus, rutting, and creep deformation tests on SMA with steel slag and found that strength and rutting resistance improved when using steel slag. Kowalski et al. (2010) also found that blending steel slag and quartzite can improve the frictional properties of SMA mixtures. After conducting various performance tests on SMA mixtures with steel slag, Xue et al. (2006) recommended the utilization of steel slag in SMA mixtures. The SMA road surfacing using the rotating furnace slag (RFS) as fine aggregate demonstrated excellent resistance to cracking, deformation, and moisture-related damage, which were characterized by X-ray diffraction fluorescence (XRF) and the toxicity characteristic leachability procedure (TCLP) (Liu et al. 2021).

#### B.1.2.5 Recycled Materials

Studies were also conducted to evaluate the suitability of irregular aggregate sources. Considering the environmental and economic factors, researchers often used recycled materials as aggregate in the mixture. Numerous studies are concerned with recycling waste materials, evaluating the performance to ensure feasibility, and presenting a systematic approach to the design and application of recycled materials in pavement construction. The LCCA and life cycle assessment (LCA) are recommended to be used to evaluate the economic and environmental factors when replacing aggregates in SMA mixtures with waste materials (Babalghaith et al. 2022). Shivkumar et al. (2018) replaced part of the coarse aggregate with construction demolition waste and found that 10% of the replacement was suitable to be used for the SMA surface layer. They also evaluated the mechanical and volumetric properties and moisture susceptibilities of SMA mixtures to determine the maximum content of construction and demolition (C&D) waste that could be used. A mixture composed of ten percent C&D waste was concluded to be suitable for the SMA surface layer. Pourtahmasb et al. (2014) evaluated recycled concrete aggregates (RCA) as an alternative to SMA mixtures and HMA mixtures. They concluded that adding RCA in SMA mixtures would increase the required binder content but using a certain percentage of RCA substitution could still meet the requirement in specifications. Karakus (2011) evaluated basalt wastes as alternative aggregates in SMA. The properties of basalt waste characterized in the study include gradation, chemical properties, specific gravity, water absorption, Loss attrition value, aggregate soundness, flake index, and peel strength. The testing results indicated that basalt waste could be used as aggregate and mineral filler in SMA.

Reclaimed asphalt pavement (RAP) and recycled asphalt shingles (RAS) are commonly used recycled materials in asphalt pavement, but their application in SMA mixtures has been limited. The mixtures containing RAP are susceptible to fracture failure because of higher stiffness. Shen et al. (2017) compared the difference between preheating the RAP in a 110 ℃ oven for 2 hours with not heating before using the RAP in the SMA mixture and concluded that the methods of processing the RAP before mixing would affect rutting and stripping performance of SMA mixture. MoDOT is conducting a research project about the usage of RAP and RAS in SMA

mixtures. They used Micro-Deval and British Pendulum methods to evaluate the quality of RAP, such as its durability and friction. They also evaluated the effect of RAP on SMA mixture through conducting performance tests such as HWTT, IDEAL-CT and I-FIT (MoDOT 2020). Katla et al. (2021) conducted rheological testing to evaluate the miscibility and performance of SMA mixture by infusing different amount of RAP binder into virgin binders. They concluded that the rutting resistance would be increased, and the fatigue life would be decreased. The study recommended 20% as an optimum RAP content in SMA mixture. Riccardi et al. (2016) used the parameter $G^*sin\delta$ and linear amplitude sweep test to evaluate fatigue properties of virgin and RAP binders. It was found that the RAP content should be limited to 23% to converse the fatigue resistance of the mixture. Devulapalli et al. (2020) conducted semicircular bending (SCB) tests to evaluate the SMA mixtures with different RAP content and rejuvenators and suggested that 30% RAP content along with 6% waste vegetable oil (WVO) was suitable for SMA mixtures.

Palm oil clinker (POC) is a waste byproduct of palm oil mills. Tons of POC are produced when producing electricity through burning solid palm oil waste materials. Babalghaith et al. (2020) assessed the effect of POC as a substitute for fine aggregate on the mechanical properties of SMA mixtures. According to the results, the POC can be used as a 100% substitution of the fine aggregate in the SMA mixture because of the enhancement of mixture performance.

#### B.1.2.6 Other Aggregates Sources

Besides the regular aggregates mentioned above, some other aggregates sources were evaluated by scholars. Polaczyk et al. (2022) analyzed the effect of aggregate types (i.e., hard limestone, soft limestone, gravel, and granite) on compaction and concluded that gravel was the most resistant to compaction damage. Based on the cost analysis and performance evaluation, the aggregates from glacial deposits were suggested to be used in the structural layers of asphalt pavement including AC and SMA mixtures (Radziszewski et al. 2011). The stiffness of SMA mixtures were increased when the filler was replaced by diatomite (Atasaral 2008). Al-Kheetan et al. (2022) investigated using magnetite as a partial replacement for aggregate in SMA mixtures containing granite and gritstone. The results showed that magnetite led to better thermal conductivity, which could increase the interface bonding between asphalt layers. Cubical aggregates were tested and passed the criteria to be used in SMA (Brown et al. 1997). Barbosa et al. (2020) used the sintered aggregate of calcined clay as a coarse aggregate in SMA mixtures, and concluded that the tensile strength, resilient modulus, and dynamic modulus were increased significantly compared to separate research that used other kinds of coarse aggregate such as basalt, limestone, and high-quality dolomite in SMA mixtures for asphalt wearing layers, and that calcined clays produced good bitumen-aggregate adhesion properties.

## B.2 Properties of Aggregates

### B.2.1 Requirements for Coarse Aggregates

In addition to regulating the types of aggregates, DOTs have also specified the requirements of aggregate physical properties and durability for SMA and/or high-level Superpave mixes. These

properties include physical aspects needed for mix design such as gradation, specific gravity, absorption, loss in LA abrasion, sand equivalent, angularity, and percentage of flat and elongated particles. Tables B.2 to B.9 present examples from several DOTs.

**Table B.2 Requirements for Aggregates in HMA by MoDOT (Standard Specification Sec. 1002.2 and Sec. 403)**

| Property | Testing | Parameter | MoDOT Limits |
|---|---|---|---|
| **Deleterious Materials** | N/A | Max. percentage | 8.0, Deleterious Rock; 1.0, Shale; 0.5, Others |
| **LA Abrasion** | AASHTO T 96 | Max. percentage loss | 40 |
| **Angularity** | ASTM D5821 | Min. percentage of | 95/90[a]; 100/100[b] |
| **Flat and Elongated Aggregate** | ASTM D4791 | Max. percentage | 20[c] (3:1 ratio); |
| **Elongated Aggregates** | | | 5[d] (5:1 ratio) |
| **Absorption** | AASHTO T 85 | Max. percentage of | 3.5 |
| **Clay Content** | AASHTO T 176 | Sand Equivalent | 50[c,d] |

[a] Traffic volume between 3 and 30 million ESALs; [b] Traffic volume > 30 million ESALs; [c] on blended aggregate particles passing No. 4 sieve. [D] for >30 million EASLs, minimum sand equivalent. N/A = not applicable

**Table B.3 Requirements for Aggregates in HMA in Alabama DOT**

| Property | Testing | Parameter | ALDOT Limits |
|---|---|---|---|
| **Deleterious Materials** | AASHTO T 112 | Max. percentage | 0.25[a] |
| | | | 0.25[b] |
| | | | 2.0[c] |
| **LA Abrasion** | AASHTO T 96 | Max. percentage loss | Coarse |
| | | | 55[d] |
| **Flat and Elongated Aggregate** | ASTM D4791 | Max. percentage | 20 (3:1 ratio); |
| | | | 5 (5:1 ratio) |
| **Absorption** | AASHTO T 85 | Max. percentage of | 2[e] |
| **Soundness of coarse** | AASHTO T 104 | Max. percentage | 10 |

[a] Coal and Lignite (Visual); [b] Clay Lumps and Friable Particles; [c] Other local deleterious substances (Shale, Mica, Marcasite, etc. (Visual); [d] Sandstone and Blast Furnace Slag; [e] Materials passing the 19 mm sieve and retained on the 4.75mm sieve, applies to gravel aggregates only.

**Table B.4 Requirements for Aggregates in HMA in Colorado DOT**

| Property | Testing Specification | Parameter | CDOT Limits |
|---|---|---|---|
| **LA Abrasion** | AASHTO T 96 | Max. percentage loss | 30 |
| **Micro-Deval Abrasion** | CP-L 4211[a] | Max. percentage loss | 18[b] |
| | | | 20[c] |
| **Sodium sulfate** | AASHTO T104 | Max. percentage | 12 |

[a] Resistance of Coarse Aggregate to Degradation by Abrasion in the Micro-Deval Apparatus; [b] Combined aggregates (Mix design); [c] Combined aggregates (1/10000 tons, or fraction thereof during production).

**Table B.5 Requirements for Aggregates in HMA in Georgia DOT**

| Property | Testing Specification | Parameter | GDOT Limits |
|---|---|---|---|
| **Flat and Elongated Aggregate** | ASTM D4791 | Max. percentage | 20[a] |

[a] Flat and elongated piece is defined as a particle having a ratio of length to thickness greater than 3.

**Table B.6 Requirements for Aggregates in HMA in Illinois DOT**

| Property | Testing | Parameter | IDOT Limits |
|---|---|---|---|
| **Absorption** | ASTM D4791 | Max. percentage | 2.5 |
| **Sodium sulfate** | AASHTO T104 | Max. percentage | 15 |
| **LA Abrasion** | AASHTO T 96 [a] | Max. percentage loss | 40[b] |
| **Deleterious Materials** | N/A | Max. percentage | Shale; 2.0 |
| | | | Clay Lumps; 0.5 |
| | | | Soft & Unsound |
| | | | Other deleterious; 2.0 |
| | | | Total deleterious; 6.0 |

[a] Illinois modified ITP 203; [b] Does not apply to crushed slag or crushed steel slag; N/A = not applicable

**Table B.7 Requirements for Aggregates in HMA in Indiana DOT**

| Property | Testing Specification | Parameter | INDOT Limits |
|---|---|---|---|
| **Flat and Elongated Aggregate** | ASTM D4791 | Max. percentage | 10[a] |

[a] Flat and elongated piece is defined as a particle having a ratio of length to thickness greater than 5.

**Table B.8 Requirements for Aggregates in HMA in Louisiana DOT**

| Property | Testing Specification | Parameter | LaDOTD Limits |
|---|---|---|---|
| **Flat and Elongated Aggregate** | ASTM D4791 | Max. percentage | 25 (3:1 ratio); |
| | | | 5 (5:1 ratio) |

**Table B.9 Requirements for Aggregates in HMA in Texas DOT**

| Property | Testing | Parameter | TxDOT Limits |
|---|---|---|---|
| **Deleterious Materials** | Tex-217-F Part I | Max. percentage | 1 |
| **Decantation** | Tex-217-F Part II | Max. percentage | 1.5 |
| **LA Abrasion** | Tex-410-A | Max. percentage loss | 30 |
| **Magnesium sulfate soundness** | Tex-411-A | Max. percentage | 20 |
| **Crushed face count** [a] | Tex-460-A, Part I | Min. percentage | 95 |
| **Flat and elongated particles** | Tex-280-F | Max. percentage | 10(5:1 ratio) |

[a] For crushed gravel.

### B.2.2 Physical Properties

The physical properties of aggregates, such as the shape, size, texture, and angularity affect the quality of asphalt mixtures directly. Using more spherical (equivalent), equidimensional, angular, or rough-textured aggregates particles in SMA mixtures can improve the resistance of the SMA to rutting (Cross 1999, Liu et al. 2017). Holleran (2008) confirmed the conclusion by evaluating three similar SMA mixtures with different primary aggregates through performance tests including indirect modulus, wheel tracking, and retained tensile strength.

Mohammadi et al. (2014) concluded that the appropriate texture depth for SMA was affected by angularity, aggregate size, asphalt percentage, voids, and density of the mixture. They also concluded that the contact area between the tire and the road surface could be optimized based on a stepwise regression analysis. SMA mixtures blended with more angular fillers were compacted more easily and exhibited more air voids.

The percentage of flat and elongated aggregates in a mixture has a significant impact on the performance of the mixture. Watson et al. (2017) evaluated the effect of the percentage of flat and elongated particles on SMA performance and concluded that SMA mixtures could use the same flat and elongated ratio requirements as Superpave mixes. However, Liu et al. (2017) suggested that flat and elongated aggregates should only be used in limited amounts. Brown et al. (1997) found that the percentage of flat and elongated particles had a good correlation with the degree of aggregate breakdown. Additionally, it was found that aggregates with fewer flat and elongated particles could improve the rutting resistance of SMA mixtures (Liu et al. 2019). It has also been found that flat and elongated aggregates are more likely to cause aggregate degradation than cubical aggregates. Therefore, the percentage of flat and elongated aggregates should be limited in the specification (Aho et al. 2001, Xie et al. 2004). Cubical

particles can increase aggregate internal friction and improve the rutting resistance of SMA mixtures while flat and elongated aggregates have lower compatibility and higher breakage (Chen et al. 2013).

Many technologies have been applied to determine the morphology of aggregates, including Aggregate Imaging System (AIMS), X-Ray Computed Tomography, and Scanning Electron Microscopy (SEM). AIMS has good reproducibility and repeatability in characterizing the shape characteristics (i.e., angularity, form, texture, and three-dimensional shape) of aggregates (Gatchalian et al. 2006). Texture was found to be associated with permanent deformation using AIMS measurements. However, AIMS is labor-intensive in characterizing the shape of coarse aggregates (Fletcher et al., 2003). X-Ray Computed Tomography can be used to analyze the internal structure of the SMA mixture and to verify the stone-on-stone contact in SMA mixtures (Watson et al. 2004). Masad et al. (2005) evaluated the shape, angularity, and texture characteristics of three different aggregates including traprock, limestone, and crushed river gravel using the X-ray CT method. The study concluded that X-ray was a reliable method for analyzing the shape characteristic in granular materials. Tashman et al. (2012) utilized X-ray CT and image analysis techniques to characterize the microstructure of SMA mixtures, and the stone-on-stone coarse aggregate skeleton was confirmed by the CT. Xue et al. (2006) used X-ray Diffraction (XDR), SEM, and Mercury Intrusion Porosimetry (MIP) to determine the composition, structure, and morphology of steel slag, and the porous microstructure of the steel slags was verified.

Friction in aggregate is another important factor that can affect the safety of the pavement. Kowalski et al. (2010) performed IFI to measure the frictional characteristics of SMA mixtures and proposed that the high friction aggregate could be replaced by polish-susceptible coarse aggregates, but the content should be no more than 20% of the total aggregate. Also, blending with steel slag and quartzite could improve the frictional properties of SMA mixtures. McDaniel et al. (2012) also found through a screening test that the high friction aggregates in SMA mixtures could be replaced partially with local polish-susceptible aggregates. The sample blends of polish-susceptible and high friction aggregates were polished by a circular polishing machine to simulate the action of traffic. Then the IFI was calculated by the Dynamic Friction Tester (DFT) and texture measured by the Circular Track Meter (CTM) as per ASTM E1911 and E2157, respectively. The IFI was used to assess the effects of adding local aggregate on overall friction resistance. This procedure could be used to ascertain the potential of new materials or new types of mixtures.

### B.2.3 Durability of Aggregates

Aggregates used in asphalt mixtures, especially in SMA, need to have resistance to degradation, polishing, and freeze-thaw damage. In addition to aggregates tests mentioned above (i.e., physical properties needed for mix design and properties detailed in the current specification – gradation, specific gravity, absorption, loss in LA abrasion, sand equivalent, angularity, and percentage of flat and elongated particles), the following aggregate parameters for durability assessment can be utilized on the selected aggregates.

### B.2.3.1 Abrasion of Aggregate

The resistance to abrasion should be considered because the aggregates in SMA should avoid crushing, degradation and disintegration from any associated activities including manufacturing, stockpiling, production, placing, and compaction (Roberts et al. 1996).

LA Abrasion Test

The LA abrasion test is a common test method used to indicate aggregate toughness and abrasion characteristics. European specifications require SMA aggregates to have no more than 30% LA abrasion loss (AASHTO T 96) and no more than 40% is required by MoDOT. However, some researchers have concluded that the LA abrasion test was not sufficient to determine aggregate quality. As the drum rotates, the load between the steel spheres and the abrasion of the aggregates can both lead to the breakdown of aggregates. Therefore, the breakdown may be caused by steel spheres loading rather than the abrasion. Senior et al. (1991) found that granite and gneiss performed well in service but had a high level of loss in the LA Abrasion test. A similar finding was presented by Wu et al. (1998). They concluded that some aggregates such as slag and limestone tend to have high LA Abrasion loss but perform adequately in the field.

Micro-Deval Abrasion Test

The Micro-Deval Abrasion test was proposed to complement the LA Abrasion test (Celaya and Haddock 2006). In contrast to the LA Abrasion test, the Micro-Deval abrasion test uses a much smaller drum and spheres, and occurs in the presence of water, rather than under a completely dry condition like in the LA Abrasion test. It takes degradation into account due to mechanical abrasion and weathering to better simulate field performance during construction as well as in traffic and under adverse environmental conditions. Gatchalian et al. (2006) conducted the Micro-Deval Abrasion test to determine aggregate resistance to abrasion. The experience of this study's research team also supports that the Micro-Deval abrasion test may serve as a more reliable alternative to predict the abrasion resistance of aggregate, since it tends to "polish" the aggregate particles while the LA Abrasion test tends to break them (Liu et al. 2012).

### B.2.3.2 Degradation after Compaction

Degradation after compaction is considered an important durability indicator for the coarse aggregates in SMA mixtures (Series 2002, Celaya and Haddock 2006). The degradation test has been used in selecting aggregates for high-level HMAs in several states (Cross 1999, Celaya and Haddock 2006). Unlike tolerance tests such as the LA Abrasion and Micro-Deval tests, the degradation test directly examines the aggregate durability and behavior in the mixture.

Testing results have indicated that aggregate that pass the abrasion tests may not necessarily have high resistance to the compaction force. Xie et al. (2005) evaluated the breakdown of aggregate caused by different compaction methods by comparing gradation before and after compaction. They suggested that it is important to consider aggregate degradation when selecting aggregates used in SMA. Gatchalian et al. (2006) evaluated the resistance to degradation of SMA by comparing the results of sieve analysis and X-ray before and after

compaction. Cross (1999) designed a SMA mixture with the local limestone, but the mixture didn't pass the specification limit associated with the amount of degradation after compaction. Cross (1999) also evaluated the percent degradation of the SMA mixture using Kansas-sourced aggregates during laboratory compaction and performance tests. It can be concluded that the aggregates, which degraded extensively on the 9.5 mm sieve, would cause the excess material remains that were found on the 2.36 mm and 1.18 mm sieves. A low LA Abrasion value, finer gradation, and a limited percent of flat and elongated aggregates would be beneficial for decreasing aggregate degradation. Since the strength of the aggregate skeleton structure is critical to SMA, aggregates that exhibit high degradation on the primary sieves should not be used in SMA mixtures.

#### B.2.3.3 Soundness

The soundness test has been required by several states (e.g., Kansas, Illinois, Arkansas, Iowa, and Nebraska) to assess an aggregate's resistance to disintegration by weathering and freeze-thaw cycles, according to AASHTO T 104. The Magnesium sulfate soundness test in conjunction with the Micro-Deval test was recommended in lieu of the LA abrasion and impact test and other soundness tests (Cooley et al. 2003). Ioannou et al. (2013) conducted the soundness test to investigate the extent of weathering inflicted on aggregates by magnesium sulphate salt solutions. They found that the loss in mass for coarse aggregates increased as the fraction size was reduced. Karakus (2011) evaluated the feasibility of basalt waste as aggregates and filler in SMA based on several parameters, such as soundness of aggregate, sieve analysis, and LA abrasion. The results indicated that the properties of basalt waste and the SMA produced were all within the specified limits.

## B.3 Mixture Design

The goal of the SMA mix design is to keep the gradation consistent, ensure an adequate coarse aggregate skeleton and satisfactory mixture volume, while changing the percentages of different types of aggregates and meeting the desired aggregate content (McDaniel et al 2012). Brown et al. (1997) suggested the parameters, including aggregate toughness, flat and elongated particle ratio, mixture aggregate gradation, percent passing 0.02 mm sieve, stone-on-stone contact, voids in the total mixture (VTM), VMA, asphalt binder content, compactive effort, and asphalt binder draindown, that should be considered in the mix design procedure. In SMA mixture design, the effect of the gradation, asphalt-aggregate ratio, and fiber content on overall performance is ranked from most to least influential: gradation, asphalt-aggregate ratio, and fiber contents (Ai et al. 2016).

### B.3.1 Gradation

The design of aggregate gradation varies from institution to institution, considering the location, climatic condition, availability, and cost of the aggregates. The performance of SMA and Superpave mixtures in the laboratory is significantly affected by the aggregate gradation, suggesting that very tight control of the aggregate gradation is required during construction (Brown 1992). Roque et al. (1997) compared the shear strength of 18 different mixtures with

different gradations and concluded that the coarse aggregate gradation controlled the shear performance of SMA mixtures.

Proper aggregate gradation allows easier stone-on-stone contact in the mixtures. Brown et al. (1997) proposed a method to check stone-on-stone contact in SMA mixtures by controlling the *VCA* for coarse aggregates only and the entire SMA mixture.

SMA mixtures with a low percentage (no more than 30%) of particles passing the 4.75 mm sieve (the critical sieve size for the mixes) more easily formed a good stone-on-stone contact structure and were less sensitive to low air void content (Brown et al. 1995,1997). The contact energy index, representing the ability of asphalt mixtures to develop aggregate contact and resist shear deformation, can be calculated by shear force and deformation during compaction (Dessouky et al. 2003, 2004).

Verification of stone-on-stone contact with *VCA* is essential because it has a direct impact on the aggregates contact in SMA (Gatchalian et al. 2006). The values for *VCA* are determined by using the equation in the AASHTO T 19 as shown in Equations B.1 and B.2.

$$VCA_{DRC} = \left[\frac{G_{CA}\gamma_W - \gamma_s}{G_{CA}\gamma_W}\right] * 100$$

Where:

$G_{CA}$ = bulk specific gravity of the coarse aggregate
$\gamma_W$ = unit weight of water (998 kg/m$^3$)
$\gamma_s$ = unit weight of the coarse aggregate fraction of the aggregate blend

**Equation B.1 *VCA* in Dry-Rodded Condition**

$$VCA_{MIX} = 100 - \left[\frac{G_{MB}}{G_{CA}} P_{CA}\right]$$

Where:

$G_{MB}$= bulk specific gravity of mix
$G_{CA}$= bulk specific gravity of coarse aggregate
$P_{CA}$ = percent of coarse aggregate (retained on breakpoint sieve) by weight of total mix

**Equation B.2 *VCA* in Mixture**

The size of aggregates also has a significant effect on the performance of SMA mixtures and Superpave mixtures. A higher percentage of SMA-9.5 mixtures passing through the No. 4 sieve can be observed in poor field performance (Apeagyei et al. 2013). The use of larger size aggregates in SMA mixtures improved rutting resistance and stiffness but reduced fatigue life (Hafeez et al. 2015). Kowalski et al. (2010) claimed that larger nominal maximum aggregate size (NMAS) had better overall friction properties than smaller-sized mixtures. Two aggregate gradations with NMAS of 16 mm and 13 mm were compared and concluded that the mixture with the larger coarse aggregate size performed better (Sarang et al. 2014). Qiu et al. (2006) adapted the Bailey method in the mix design to quantify contact between stones, which improved the rutting resistance of SMA mixtures.

### B.3.2 Mixture Compaction

The compaction method has a significant impact on the aggregate quality and structure created by the SMA non-continuous gradation. Different compaction methods can lead to differences in air voids, different levels of aggregate breakdown, and different performance of the designed SMA mixture in the laboratory and in the field. Several compaction methods have been considered for SMA mixture compaction by researchers and agencies, such as Texas gyratory, rolling wheel, kneading, SHRP gyratory, Marshall hammer compactor, Superpave gyratory compactor (SGC), and California Kneading compactor (Sousa et al. 1995).

Some U.S. highway agencies now use the SGC method for lab compaction for SMA. Maryland, which has been at the forefront of SMA use in the U.S., has been using 100 gyrations for its SMA mixtures for several years (Michael et al. 2003). The resultant density of SMA samples fabricated by 100 revolutions of the SGC method is close to that of a Marshall hammer method at 50 blows, and the SGC method could cause less aggregate breakdown than the Marshall hammer method (Brown et al. 1997). A similar conclusion was made by West et al. (2005). They found that compaction with the SGC method caused less aggregate breakdown than with the Marshall hammer method by comparing changes in percent passing the 4.75 mm sieve and the 0.075 mm sieve before and after the compaction. Smit et al. (2011) suggested designing SMA mixtures with local aggregates and utilizing the SGC method with the capability of measuring the shear stress of the mix during compaction. Hainin et al. (2013) found that the SGC method could reduce degradation and represent a field roller well. Miranda (2019) evaluated the effect of different aggregate skeleton matrices performed by different compaction methods on permanent deformation. The results demonstrated that proctor and steel roller compaction could optimize higher content of coarse aggregates and binder, which meant better cracking resistance and durability. He also proposed new parameters, such as the ratio between binder film thickness and porosity and the ratio between Marshall stability and flow, which were related to permanent deformation. Qiu (2007) found a positive correlation between the different degrees of internal aggregate packing in SMA and rutting resistance.

As shown in the Table B.10 below, the SMA mixture specifications refer to specimens compacted by the SGC method at 100 gyrations, as seen in AASHTO M 325 design standards.

**Table B.10 SMA Mixture Specification for SGC**

| Property | Requirement |
|---|---|
| **Asphalt Binder Content, %** | 6 minimum |
| **Air Voids, %** | 4 |
| ***VMA*, %** | 17 minimum |
| ***VCA* of Compacted SMA ($VCA_{mix}$), %** | Less than *VCA* in dry-rodded condition ($VCA_{DRC}$) |
| **TSR, %** | 80 minimum |
| **Draindown at Production Temperature, %** | 0.3 Maximum |

### B.3.3 Additives in the Mixtures

Traditionally, stabilizing additives are used to maintain the binder in the mixture at high temperatures, preventing drainage during production, transportation, and construction. The additives include cellulose fiber, rock wool fiber, or polymer, which can also reduce the age hardening of the binder (Stuart et al. 1994). In addition, the fibers can reduce the drainage of asphalt so that the permanent deformation would be reduced as well (Woodside et al. 1997).

Coconut fiber is a suitable replacement for cellulose fiber used in SMA mixtures (Vale et al. 2014). Raghuram et al. (2013) claimed that low-cost fibers can also be used as stabilizers to improve the performance of SMA mixtures by retarding the drain down of asphalt from the SMA mixtures to a greater extent. 0.3 % of cellulose fiber is a suitable content to stabilize the mixture even without conducting drain-down tests (Devulapalli et al. 2022).

### B.3.4 Mixture Design

For SMA mix design, five basic steps are required to obtain a satisfactory SMA mixture: 1) select materials; 2) determine optimum aggregate gradation yielding stone-on-stone contact; 3) determine optimum asphalt binder content that provides the desired air void level; 4) evaluate asphalt draindown potential; and 5) evaluate moisture susceptibility using AASHTO T 283 (Brown et al.1997).

The SMA mixtures that met the criterion of $VCA_{mix} < VCA_{DRC}$ indicate good stone-on-stone contact and a denser coarse aggregate fraction (Liu et al. 2019). West et al. (2005) examined Lock Point in the SMA mix design. Lock point was defined by Alabama Department of Transportation (ALDOT) as the second of two consecutive gyrations, which have the same recorded sample height. This is the limit of gyrations where the aggregate has locked together to reduce aggregate breakdown, indicating that good stone-on-stone contact has been achieved and that further gyrations may only degrade the aggregate. Comparing the results from the lab and field, 70 gyrations with the SGC method are recommended to replace the 50 blow Marshall hammer method for SMA mix designs in Alabama.

Miranda et al. (2019) developed a new analytical approach for SMA mix design for the optimization of the stone-on-stone effect. In addition to volumetric characteristic of SMA test sample, they evaluated the characteristic of coarse aggregates prepared using different aggregate compaction method, such as *VCA*, $VCA_{mix}$, air void content, void filler with bituminous

binder (VFB) and workability of SMA. Compared to pre-established grading, the SMA mixture with aggregates compacted using Proctor compaction resulted in an air void and particle breakage more similar to field results. Qiu and Lum (2006) proposed a mix design procedure based on and adapted from the Bailey method, which can quantify aggregate stone-on-stone contact in SMA.

## B.4 Mixture Performance Evaluation

Performance tests of SMA mixtures with different aggregate sources have been conducted for aggregate selection. The main performance criteria considered for a SMA mixture, by researchers and agencies, are rutting resistance, cracking resistance, moisture susceptibility, fatigue, drain down, and friction and polishing resistance.

### B.4.1 Rutting Resistance

Various tests have been used to evaluate the rutting performance of SMA mixtures, including wheel tracking, Marshall, creep, HWTT, AMPT, Flow Number (FN), and Asphalt Pavement Analyzer (APA) (Mohammad et al. 1999, Tayfur et al 2007, Taher et al. 2011, Apeagyei et al. 2013, Liu et al. 2019).

Binder stiffness, binder content, and aggregate structure (gradation and *VCA*) were the main factors affecting the rutting resistance of a SMA mixture based on the results from the FN test (Apeagyei et al. 2013). Cross (1999) evaluated the rutting resistance of an SMA sample to check the feasibility of Kansas-sourced aggregate used in the SMA mixture using APA tests. Liu et al. (2017) conducted an APA test to assess the effect of coarse aggregate morphology on the rutting resistance of SMA, which can be improved by using more angular coarse aggregates with rougher texture.

Compared to the APA test, the HWTT test which combines the evaluation of rutting and moisture susceptibility is more comprehensive for rutting resistance evaluation (James et al. 2022). Qiu, et al. (2006) conducted the Creep test and Wheel Tracking test to determine the effect of asphalt content and gradation on resistance to rutting and permanent deformation of SMA mixtures in the mixtures' design. Babalghaith et al. (2020) used the Wheel Tracking test to determine the failure susceptibility of SMA mixtures due weakness in aggregate structure, insufficient binder coating, and weak adhesion between binder and aggregates. Brown et al. (1997) evaluated the effect of the type of stabilizer used in a mixture on the rutting resistance of the SMA mixture, using the Wheel Tracking test, and found that polymer stabilizers could produce better rutting resistance, while fiber stabilizers showed a better resistance to drain down in SMA mixtures.

Based on the results from HWTT tests of SMA mixtures with different contents of coarse aggregates, decreasing the coarse aggregate content from 80 to 60% had no significant effect on the rutting resistance of a SMA mixture (Mogawer et al.1995). Ameli et al. (2020) conducted HWTT tests, four-point beam fatigue (FPBF) tests, resilient modulus tests, and moisture susceptibility tests, as per AASHTO T 283, and found that replacing a coarse portion of the

aggregate skeleton with steel slag aggregate in SMA resulted in improved rutting resistance of mixtures but might decrease the stripping and cracking resistance.

### B.4.2 Cracking Resistance

Low-temperature cracking is one of the major pavement distresses in asphalt pavement, and the mixture performance at low temperatures should be evaluated when new materials are introduced (Buttlar et al. 2019, Liu et al. 2021).

Liu et al. (2019) performed the Texas Overlay test to assess the cracking resistance of SMA mixes with different aggregates. They confirmed that more spherical (equant), angular, or better-crushed rough coarse aggregate particles in SMA mixtures would yield better cracking and rutting resistance. The Indirect Tension Test (IDT), according to AASHTO T 322, can fully characterize the complex behaviors of asphalt mixture at low temperatures (Liu and Li 2012, Liu et al. 2017, Liu et al. 2021).

The IDEAL-CT procedure, developed by Zhou et al. (2017), is a relatively new and simple method that is used to determine the cracking resistance of asphalt mixtures. James et al. (2022) conducted the IDEAL-CT tests to evaluate the cracking resistance of SMA mixtures with high LA Abrasion (44%, 53%, and 56%) aggregate loss, and concluded that high LA abrasion and smaller NMAS produced a lower CT index value and therefore worse cracking performance.

### B.4.3 Moisture Susceptibility

The moisture susceptibility of SMA can be affected highly by the physical properties and proportion of coarse aggregates (Stuart and Mogawer 1995, Chen et al. 2013). The Moisture Induced Stress Tester (M.i.S.T) could evaluate moisture susceptibility and stripping resistance of mixtures, which is believed to be typically more aggressive than the regular AASHTO T 283 conditioning without any freeze-thaw cycles (Tayebali et al. 2017). The test can successfully rank the field performance of mixtures (Tavassoti and Baaj 2020), yielding lower variability and requiring a shorter conditioning time than conventional water bath conditioning, which makes it a promising test for quality assurance.

The TSR is another common way to evaluate asphalt mixtures' resistance to moisture damage. Liu et al. (2021) used the value of TSR to confirm that the SMA mixture with RFS rotating furnace slag showed less sensitivity to moisture damage than the SMA mixture with natural gravel based on the SMA-RFS, showing a higher TSR.

### B.4.4 Fatigue Resistance Evaluation

The property of fatigue should be considered when evaluating SMA mixtures' performance, in the long term, when new aggregates are used in the SMA mixtures. Liu et al. (2017) tested the fatigue resistance of SMA mixtures containing aggregates with different morphology using a modal mobile load simulator in conjunction with a portable seismic pavement analyzer. The results showed that using more spherical and less flaky coarse aggregates could improve fatigue performance of a SMA mixture. Three-point beam fatigue tests were conducted to analysis the fatigue resistance of the SMA mixture with alternative aggregates. The results demonstrated

that the SMA mixtures with RFS aggregates exhibited better fatigue resistance than the mixtures with natural materials (Liu et al. 2021). The fatigue life of diatomite-added SMA was determined using the four-point bending beam fatigue test and it is slightly lower than the conventional SMA mixture. Atasaral et al. (2008) performed the four-point bending beam fatigue test of SMA mixtures at different strain levels and found that the fatigue life is sensitive to the strain level, with the increase in strain level from 700 to 800 microns leading to an approximately 70% reduction in the fatigue life of the SMA mixture (Alinezhad et al. 2019).

### B.4.5 Draindown

Draindown is a major concern in SMA mixtures, as it may affect the overall performance of the mixture. Compared to conventional HMA, SMA mixtures generally have a higher asphalt content and more coarse aggregate, which is more sensitive to drain down.

As a result of this impact, suitable stabilizing additives are necessary for SMA mixtures to retain asphalt during production and placement. Brown et al. (1997) evaluated the effect of stabilizer type on the mixture and concluded that fibers act to prevent drain down better than polymers. Decreasing the coarse aggregate content would be helpful for the drain down of the SMA mixture as well (Mogawer et al. 1995). Both chemically treated aggregates with normal bitumen, which shows better moisture resistance properties, and Crum Rubber Modified Bitumen (CRMB) with normal aggregates, which is superior in performance, can be used in SMA to meet the drain down requirements (Sarang et al. 2014).

### B.4.6 Friction and Resistance to Polish

The friction and resistance to polish were also investigated for alternative aggregate usages in SMA (Kowalski et al. 2010, McDaniel and Shah 2012). For the conventional British Pendulum Test, only friction at low speeds is assessed and the results are highly affected by the orientation of aggregate particles in the aggregate coupons (Fwa et al. 2003, Liu et al. 2004). The AFT measure both the coefficient of friction and mean profile depth under different speeds at different polishing levels to obtain more accurate assessment of friction of test mixtures (Kassem et al. 2013), and it was found to simulate and correlate well with the skid performance of asphalt pavements in the field (Chowdhury et al. 2017). Kowalski et al. (2010) performed AFT and calculated the IFI. While they demonstrated that hard limestone or dolomite provided higher friction than soft limestone in mixes, steel slag and quartzite were found to improve SMA frictional properties greatly.

## B.5 Summary

The literature review provides a comprehensive overview of efforts in testing and screening qualified aggregates for SMA and high-quality HMA mixtures. It summarizes research on aggregate types specified by DOTs, aggregate properties influencing mixtures, mixture design, performance, and evaluation methodologies. The summary is stated as follows.

**Efforts in Exploring Alternative Aggregate Types:**

- Specific aggregate requirements from various states are listed, highlighting limitations and considerations. MoDOT allows the coarse aggregates to be a combination of at least 40% traprock by total weight (without the usage of steel slag) and other aggregates.
- Alternative aggregate types such as basalt, limestone, granite, steel slag, and some other irregular aggregate sources such as glacial deposits, diatomite, magnetite, and calcined clay are explored in other studies for their performance in SMA and Superpave mixtures.
- Studies on the use of recycled materials like RAP, RAS, and POC are discussed, emphasizing economic and environmental factors.
- Ongoing research in other states focuses on identifying locally available aggregates and evaluating their suitability for SMA and Superpave mixtures.

**Aggregate Requirements:**

- DOTs specify physical and durability criteria for aggregates in SMA and high-level Superpave mixes, including gradation, specific gravity, absorption, LA abrasion loss, sand equivalent, angularity, and flat/elongated particle percentage.
- Specific characteristics like spherical or angular particles can enhance SMA resistance to rutting.
- Tests such as L.A. and Micro-Deval abrasion tests simulate wear and tear.
- Degradation after compaction is vital, as aggregates may not resist both abrasion and compaction.
- Soundness tests assess resistance to weathering and freeze-thaw cycles, crucial for long-term performance.

**Mix Design Considerations:**

- SMA mix design should focus on optimizing stone-on-stone contact, considering volumetric characteristics, compaction methods, and workability for enhanced performance.
- Mixture design steps include material selection, determining optimal gradation and binder content based on the volumetric parameters such *VMA* and *VCA*, evaluating draindown, and assessing moisture susceptibility.
- The gradation of the SMA mixture can directly impact stone-on-stone contact, shear strength, and overall performance.
- Methods such as the dilation concept, lock-up concept, and Bailey method were used for optimizing the gradation of SMA mixtures used for aggregate gradation.
- After comparing different compaction methods, the SGC method was determined to be preferred method due to its consistency and minimal aggregate breakdown.
- Stabilizing additives like cellulose fiber or polymers maintain binder integrity and improve performance of SMA.

**Performance Evaluation for Mixture with New Components:**

- Various tests were conducted to assess rutting resistance, cracking resistance, moisture susceptibility, fatigue, draindown, friction, and polishing resistance for SMA.

- Rutting resistance was evaluated using wheel tracking, Marshall, creep, HWTT, AMPT, FN, and APA tests, with influencing factors such as binder stiffness, content, and aggregate structure.
- Cracking resistance was assessed via Texas Overlay, IDT, and IDEAL-CT tests.
- M.i.S.T and TSR were used to evaluate moisture susceptibility of mixtures.
- Draindown was a concern for SMA mixtures due to higher asphalt content, and it was addressed through stabilizing additives and aggregate content adjustments.
- Friction and resistance to polish were investigated through the British Pendulum Test and AFT. Steel slag and quartzite improved frictional properties of mixtures.
- Aggregate morphology, types and properties have significant impact on mixture performance such as cracking resistance, moisture susceptibility, and friction and resistance to polish.

## B.6 Reference


Aho, B. D., Vavrik, W. R., & Carpenter, S. H. 2001. "Effect of flat and elongated coarse aggregate on field compaction of hot-mix asphalt." *Transportation Research Record*, 1761(1): 26-31.

Ai, C., Qiu, S., Xin, C., Yang, E., & Qiu, Y. 2016. "Evaluation and optimization of stone matrix asphalt (SMA-13) mix design using weight-matrix method." *Road Materials and Pavement Design*, 17(4): 958-967.

Ale Mohammadi, M., Aghasoltan, A., & Kavusi, A. 2014. "An optimal grading model to improve the rut resistance of stone mastic asphalt." *Transportation Research Board. 93rd Annual meeting,* Paper #14-4633.

Alinezhad, M., & Sahaf, A. 2019. Investigation of the fatigue characteristics of warm stone matrix asphalt (WSMA) containing electric arc furnace (EAF) steel slag as coarse aggregate and Sasobit as warm mix additive. *Case Studies in Construction Materials, 11*, e00265.

Al-Kheetan, M. J., Azim, T., Byzyka, J., Ghaffar, S. H., & Rahman, M. M. 2022. "Performance of magnetite-based stone mastic asphalt (SMA) as a superior surface course material." *Construction and Building Materials*, Vol. 322, No. 126463.

Ameli, A., Hossein Pakshir, A., Babagoli, R., Norouzi, N., Nasr, D., and Davoudinezhd, S. 2020. "Experimental investigation of the influence of nano $TiO_2$ on rheological properties of binders and performance of Stone Matrix Asphalt mixtures containing steel slag aggregate." *Construction and Building Materials*, Vol. 265, No. 120750.

Apeagyei, A. K., McGhee, K. K., Clark, T., & Clark, T. M. 2013. "Influence of aggregate packing and asphalt binder characteristics on performance of stone matrix asphalt." *Transportation Research Board. 92nd Annual meeting*, Paper #13-0622.

Atasaral, M., Gungor, A. G., Orhan, F., Kasak, S., & Cubuk, M. K. 2008. “The use of diatomite in the stone mastic asphalt mixture.” *In Proceedings of the 4th Eurasphalt and Eurobitume Congress* Held May 2008, Copenhagen, Denmark.

Babalghaith, A. M., Koting, S., Sulong, N. H. R., Karim, M. R., & AlMashjary, B. M. 2020. Performance evaluation of stone mastic asphalt (SMA) mixtures with palm oil clinker (POC) as fine aggregate replacement. *Construction and building materials*, Vol. 262, No. 120546.

Babalghaith, A. M., Koting, S., Sulong, N. H. R., Karim, M. R., Mohammed, S. A., & Ibrahim, M. R. 2020. “Effect of palm oil clinker (POC) aggregate on the mechanical properties of stone mastic asphalt (SMA) mixtures.” *Sustainability*, 12(7): 2716.

Babalghaith, Ali Mohammed, et al. 2022. “A systematic review of the utilization of waste materials as aggregate replacement in stone matrix asphalt mixes.” *Environmental Science and Pollution Research* 29(24): 35557-35582.

Barbosa CA, Monteiro AK, Frota CA. 2020. "SMA mix with sintered aggregate of calcinated clay (SACC) and curauá fiber". *European Academic Research*, 8(1):256269.

Brown, E.R. 1992. *Evaluation of SMA used in Michigan (1991)*. NCAT Report No. 93-03, NCAT, Auburn University, Alabama, US.

Brown, E. R., & Haddock, J. E. 1997. “Method to ensure stone-on-stone contact in stone matrix asphalt paving mixtures.” *Transportation Research Record*, 1583(1): 11-18.

Brown, E. R., & Manglorkar, H. 1993. *Evaluation of laboratory properties of stone of matrix asphalt (SMA) mixtures*. NCAT Report No. 93-05, NCAT, Auburn University, Alabama, US.

Brown ER, Haddock JE, Mallick RB, Lynn TA. 1997. *Development of a mixture design procedure for stone matrix asphalt (SMA)*. Report No. 97-3. Auburn (AL): National Center for Asphalt Technology.

Buttlar W., Meister J., Jahangiri B., Majidifard H.2019. *Performance characteristics of modern recycled asphalt mixes in Missouri, including ground tire rubber, recycled roofing shingles, and rejuvenators*. Report no. cmr 19-002. Missouri Department of Transportation.

Cao, L., Li, X., & Lei, X. 2015. “Preliminary investigation of adhesion failure mechanisms of crack sealant to pavement crack walls.” *Transportation Research Board. 94th Annual meeting*, Paper #15-4191.

Celaya, B. J., Haddock, J. E. 2006. *Investigation of coarse aggregate strength for use in Stone Matrix Asphalt*. Final Report. FHWA/IN/JT2P-2006/4. Indiana Department of Transportation.

Chen, J., Hsieh, W., and Liao, M. 2013. “Effect of coarse aggregate shape on engineering properties of Stone Mastic Asphalt applied to airport pavements.” *International Journal of Pavement Research and Technology*, Vol. 6 (5): 595-601.

Chowdhury, A., Kassem, E., Aldagari, S., & Masad, E. 2017. *Validation of asphalt mixture pavement skid prediction model and development of skid prediction model for surface treatments*. Final Report. FHWA/TX-17/0-6746-01-1. Texas. Dept. of Transportation. Research and Technology Implementation Office.

Cooley Jr, L. A., & James, R. S. 2003. "Micro-Deval testing of aggregates in the southeast." *Transportation Research Record*, 1837(1): 73-79.

Cross, S. A. 1999. *Aggregate specification for Stone Mastic Asphalt (SMA).* Final Report. K-TRAN: KU-97-5. Kansas Department of Transportation.

Dessouky, S., Masad, E., & Bayomy, F. 2003. "Evaluation of asphalt mix stability using compaction properties and aggregate structure analysis." *International Journal of Pavement* Engineering, 4(2): 87-103.

Dessouky, S., Masad, E., & Bayomy, F. 2004. "Prediction of hot mix asphalt stability using the Superpave gyratory compactor. " *Journal of Materials in Civil Engineering*, 16(6): 578-587.

Devulapalli, L., Kothandaraman, S., & Sarang, G. 2020. "Effect of rejuvenating agents on stone matrix asphalt mixtures incorporating RAP." *Construction and Building Materials*, Vol. 254, No. 119298.

Devulapalli, L., Sarang, G., & Kothandaraman, S. 2022. "Characteristics of aggregate gradation, drain down and stabilizing agents in stone matrix asphalt mixtures: A state of art review." *Journal of Traffic and Transportation Engineering*, 9(2): 167-179.

Fletcher, T., Chandan, C., Masad, E., & Sivakumar, K. 2003. "Aggregate imaging system for characterizing the shape of fine and coarse aggregates." *Transportation Research Record*, 1832(1): 67-77.

Fwa, T. F., Choo, Y. S., & Liu, Y. 2003. "Effect of aggregate spacing on skid resistance of asphalt pavement. " *Journal of transportation engineering*, 129(4): 420-426.

Gatchalian, D., Masad, E., Chowdhury, A., & Little, D. 2006. "Characterization of aggregate resistance to degradation in stone matrix asphalt mixtures." *Transportation Research Record*, 1962(1): 54-63.

Hafeez, I., Kamal, M. A., & Mirza, M. W. 2015. "An experimental study to select aggregate gradation for stone mastic asphalt." *Journal of the Chinese Institute of Engineers*, 38(1): 1-8.

Hainin, M. R., Rusbintardjo, G., Aziz, M. A. A., Hamim, A., & Yusoff, N. I. M. 2013. "Laboratory evaluation on steel slag as aggregate replacement in stone mastic asphalt mixtures." *Jurnal Teknologi*, 65(2): 13-19.

Holleran G., Mccaffrey L., and Wilson D. 2023. “The effect of particle shape and angularity on SMA mix characteristics,” *ARRB Conference, 23rd*, 2008, Adelaide, South Australia, Australia, Jul. 2008. Accessed: Feb. 06, 2023. https://trid.trb.org/view/885958

Ibrahim, A., Faisal, S., & Jamil, N. 2009. “Use of basalt in asphalt concrete mixes.” *Construction and Building Materials*, 23(1): 498-506.

Ioannou, I., Fournari, R., & Petrou, M. F. 2013. “Testing the soundness of aggregates using different methodologies.” *Construction and Building Materials*, 40: 604-610.

James, T., & Prowell, B. 2022. “Evaluation of high Los Angeles abrasion loss aggregate in Stone Matrix Asphalt.” *Transportation Research Record*, 2676(5): 116-131.

Karakus, A. 2011. “Investigating on possible use of Diyarbakir basalt waste in Stone Mastic Asphalt.” *Construction and Building Materials*, 25(8): 3502-3507.

Kassem, E., Awed, A., Masad, E., and Little, D. 2013. “Development of a predictive model for skid loss of asphalt pavements.” *Journal of the Transportation Research Board*, 2372: 83–96.

Kassem, E., Masad, E., Awed, A., and Little, D. 2012. *Laboratory evaluation of friction loss and compactability of asphalt mixtures*. Texas Transportation Institute, Research Report SWUTC/12/476660-00025-1, Texas A&M University, College Station, TX

Katla, B., Ravindra, W. A., Kota, S. K., & Raju, S. 2021. “RAP-added SMA mixtures: How do they fare? ” *Journal of Materials in Civil Engineering*, 33(8): 04021199.

Kowalski, K. J., McDaniel, R. S., & Olek, J. 2010. *Identification of laboratory technique to optimize Superpave HMA surface friction characteristics*.

Liu, H., Ai, Z., Yang, G., Wang, C., Xing, C., Li, M., & Liu, G. 2021. “The suitability of rotating furnace slag for use as aggregates and powders in SMA-10 road surfacing.” In *CICTP 2021*, 2021: 863-873.

Liu, J., and Li, P. 2012. “Low temperature performance of sasobit-modified Warm-Mix Asphalt.” *Journal of Materials in Civil Engineering*, vol 24(1): 57-63.

Liu, J., Liu, J., & Hao, G. 2021. “Characterization of highly polymerized Alaskan asphalt binders and mixtures.” *Journal of Transportation Engineering*, Part B: Pavements, 147(4): 04021047.

Liu, J., Liu, J., Shi, X., & Honarvarnazari, M. 2021. *Snow and ice treatment products evaluation.* No. cmr 21-009, TR202002. Missouri. Department of Transportation. Construction and Materials Division.

Liu, J., Mullin, A., and Rein, J. 2012. *Use of the Micro-Deval test for assessing Alaska aggregates*. Final Report. FHWA-AK-RD-12-22. Alaska Department of Transportation.

Liu, J., Zhao, S., Li, L., Li, P., & Saboundjian, S. 2017. “Low temperature cracking analysis of asphalt binders and mixtures.” *Cold Regions Science and Technology*, 141: 78-85.

Liu, Y., Fwa, T. F., & Choo, Y. S. 2004. “Effect of surface macrotexture on skid resistance measurements by the British Pendulum Test.” *Journal of Testing and Evaluation*, 32(4): 304-309.

Liu, Y., Huang, Y., Sun, W., Nair, H., Lane, D. S., & Wang, L. 2017. “Effect of coarse aggregate morphology on the mechanical properties of stone matrix asphalt.” *Construction and Building Materials*, 152: 48-56.

Liu, Y., Nair, H., Lane, S., Wang, L., & Sun, W. (2019). *Influence of aggregate morphology and grading on the performance of 9.5-mm Stone Matrix Asphalt mixtures*. Final Report. FHWA/VTRC 19-R15. Virginia Transportation Research Council.

Liu, Y., Sun, W., Nair, H., Stephen Lane, D., & Wang, L. 2016. “Quantification of aggregate morphologic characteristics as related to mechanical properties of asphalt concrete with improved FTI system.” *Journal of Materials in Civil Engineering*, 28(8): 04016046.

MacDonald, C. 2005. “South Dakota project succeeds with SMA.” *HMAT: Hot Mix Asphalt Technology*, 10(4).

Masad, E., Saadeh, S., Al-Rousan, T., Garboczi, E., & Little, D. 2005. “Computations of particle surface characteristics using optical and X-ray CT images.” *Computational Materials Science*, 34(4): 406-424.

McDaniel, R. S., and Shah, A. 2012. *Maximizing the use of local materials in HMA surfaces*. Final Report. FHWA/IN/JTRP-2012/07. Indiana Department of Transportation.

Miao, Y., Wang, S., Sun, F., and Yang, J. 2022. “A laboratory investigation into the polishing behavior of Stone Matrix Asphalt with different lithology types of coarse aggregates.” *Journal of Testing and Evaluation*. Vol. 50(4): 1749-1762.

Michael, L., Burke, G., & Schwartz, C. W. 2003. “Performance of stone matrix asphalt pavements in Maryland.” *Asphalt paving technology*, 72: 287-314.

Miranda, H. M. B., Batista, F. A., Lurdes Antunes, M. D., & Neves, J. 2019. “A new SMA mix design approach for optimization of stone-on-stone effect.” *Road Materials and Pavement Design*, 20(sup1): S462-S479.

Moaveni, M., Tutumluer, E., & Yılmaz, A. 2014. “Laboratory characterization of compaction and damping properties of Stone Matrix Asphalt.” *International Journal of Pavement Research & Technology*, 7(1):1.

Mogawer, W. S., & Stuart, K. D. 1995. “Effect of coarse aggregate content on stone matrix asphalt rutting and draindown.” *Transportation research record*, 1492: 1-11.

Mohammad, L., Zhang, X., Huang, B., and Tan, Z. 1999. “Laboratory performance evaluation SMA, CMHB, and dense graded asphalt mixtures.” *Journal of the Association of Asphalt Paving Technologists*. Vol. 68: 252-283.

Polaczyk, P., Ma, Y., Hu, W., Xiao, R., Jiang, X., & Huang, B. 2022. “Effects of mixture and aggregate type on over-compaction in hot mix asphalt in Tennessee.” *Transportation Research Record*, 2676(4): 448-460.

Pourtahmasb, M. S., & Karim, M. R. 2014. “Performance evaluation of stone mastic asphalt and hot mix asphalt mixtures containing recycled concrete aggregate.” *Advances in Materials Science and Engineering,* 2014: 1-12.

Qiu, Y. 2007. “Design and performance of stone mastic asphalt in Singapore conditions.” Doctoral dissertation, Nanyang Technological University.

Qiu, Y. F., & Lum, K. M. 2006. “Design and performance of stone mastic asphalt.” *Journal of transportation engineering*, 132(12): 956-963.

Radziszewski, P., Piłat, J., Kowalski, K. J., & Król, J. 2012. “Use of aggregate from glacier deposits in high-traffic asphalt pavements: a Polish experience.” *The Baltic Journal of Road and Bridge Engineering*, 7(1): 5-12.

Raghuram, K. B., & Chowdary, V. 2013. “Performance evaluation of stone matrix asphalt (SMA) using low-cost fibres.” *Journal of The Indian Roads Congress*, Vol. 2: 159.

Riccardi, C., Falchetto, A. C., Losa, M., & Wistuba, M. 2016. “Back-calculation method for determining the maximum RAP content in Stone Matrix Asphalt mixtures with good fatigue performance based on asphalt mortar tests.” *Construction and Building Materials*, 118: 364-372.

Roberts, F.L.; Kandhal, P.S.; Brown, E.R.; Lee, D.Y. and Kennedy, T.W. 1996. *Hot mix asphalt materials, mixture design, and construction*. National Asphalt Pavement Association Education Foundation. Lanham, MD, 603.

Roque, R., Huang, S. and Ruth, B. E. 1997. “Maximizing shear resistance of asphalt mixtures by proper selection of aggregate gradation.” *International Society for Asphalt Pavements*, Volume I: 249-268.

Sarang, G., Lekha, B. M., & Shankar, A. R. 2014. “Stone matrix asphalt using aggregates modified with waste plastics.” *Pavement Materials, Structures, and Performance*, 2014: 9-18.

Senior S. A., and Rogers C. A. 1991. “Laboratory tests for predicting coarse aggregate performance in Ontario.” *Transportation Research Record 1301*, TRB, National Research Council, Washington, D.C., 1991:97–106.

Shen, Junan, Sungun Kim, and M. Myung Jeong. *Evaluation of Georgia asphalt mixture properties using a Hamburg wheel-tracking device*. No. GDOT Research Project No. 15-03. Georgia Institute of Technology. School of Civil and Environmental Engineering, 2017.

Shivkumar, Harish, N., Mandal, S., & Prabhakara, R. 2018. "Investigations on Stone Matrix Asphalt using construction demolition waste as partial replacement to coarse aggregates for sustainable roads." *Urbanization Challenges in Emerging Economies: Resilience and Sustainability of Infrastructure,* pp. 345-353. Reston, VA: American Society of Civil Engineers.

Smit, A., Prasad, S., Prozzi, J., & Tahmoressi, M. 2011. *CAM mix design with local aggregates* Final Report. No. FHWA/TX-12/0-6435-1. Texas Department of Transportation.

Sousa, J. B., Way, G., Harvey, J. T., & Hines, M. 1995. "Comparison of mix design concepts." *Transportation Research Record*, Vol 1492: 151.

Stuart, K. and Mogawer, W. 1995. "Effect of coarse aggregate content on Stone Matrix Asphalt durability and low-temperature cracking." *Transportation Research Record*, Vol 1492: 26-35.

Stuart, K. D., & Malmquist, P. 1994. "Evaluation of using different stabilizers in the US route 15 (Maryland) stone matrix asphalt. "*Transportation Research Record*, Vol 1492: 48).

Taher, B. M., Mohamed, R. K., & Mahrez, A. 2011. "A review on fatigue and rutting performance of asphalt mixes." *Scientific Research and Essays*, 6(4): 670-682.

Tashman, L., & Pearson, B. 2012. "Characterization of stone matrix asphalt mixtures." *International Journal of Pavement Engineering,* 13(4): 297-309.

Tavassoti, P., and Baaj, H. 2020. "Moisture damage in asphalt concrete mixtures: state of the art and critical review of the test methods." *Soils and Materials Session, Transportation Association of Canada (TAC) Conference*.

Tayebali A. A., Guddati M., Yadav S., LaCroix A. 2017. *Use of Moisture Induced Stress Tester (M.i.S.T) to determine moisture sensitivity of asphalt mixtures*. Report No. FHWA/NC/2017-01. North Carolina. Department of Transportation, Raleigh.

Tayfur, S., Ozen, H., & Aksoy, A. 2007. "Investigation of rutting performance of asphalt mixtures containing polymer modifiers." *Construction and Building Materials*, 21(2): 328-337.

Vale, A. C. D., Casagrande, M. D. T., & Soares, J. B. 2014. "Behavior of natural fiber in stone matrix asphalt mixtures using two design methods." *Journal of materials in civil engineering*, 26(3): 457-465.

Watson, Donald E., and Grant Julian.2017. *Effect of flat and elongated aggregate on Stone Matrix Asphalt performance*. No. NCAT Report 17-03. NCAT Report.

Watson, D. E., Masad, E., Ann Moore, K., Williams, K., & Cooley Jr, L. A. 2004. "Verification of voids in coarse aggregate testing: Determining stone-on-stone contact of hot-mix asphalt mixtures. "*Transportation Research Record*, 1891(1): 182-190.

West, R. C., & James, R. S. 2005. *Determining $N_{Design}$ for SMA mixtures in Alabama. Report* No. ALDOT Research Project 930-584. Auburn University. National Center for Asphalt Technology.

Woodside, A. R., Woodward, W. D. H., Clements, H. W., Sikich, J., & RUSSELL, T. 1997. "The use of fabrics to inhibit reflective cracking in porous asphalt." *European conference on porous asphalt*, Madrid, March 12-14, Volume 1.

Wu, Y.; Parker, F. and Kandhal, K. 1998. *Aggregate toughness/abrasion resistance and durability/soundness tests related to asphalt concrete performance in pavements*. NCAT Report 98-4. National Center for Asphalt Technology. Auburn, AL.

Xie, H., & Watson, D. E. 2004. Lab study on degradation of stone matrix asphalt (SMA) mixtures. In *83rd Annual Meeting of the Transportation Research Board*, Washington DC.

Xie, H., Watson, D. E., & Brown, E. R. 2005. "Evaluation of two compaction levels for designing stone matrix asphalt." *Transportation research record*, 1929(1): 149-156.

Xue, Y., Wu, S., Hou, H., & Zha, J. 2006. "Experimental investigation of basic oxygen furnace slag used as aggregate in asphalt mixture." *Journal of hazardous materials*, 138(2): 261-268.

Zhao X., Sheng, Y., Lv, H., Jia, H., Liu, Q., Ji, X., Xiong, R., and Meng, J. 2022. "Laboratory investigation on road performances of asphalt mixtures using steel slag and granite as aggregate." *Construction and Building Materials*. Vol. 315(10).

Zhou, F., Im, S., Sun, L., & Scullion, T. (2017). "Development of an IDEAL cracking test for asphalt mix design and QC/QA." *Road Materials and Pavement Design*, 18(sup4): 405-427.

# APPENDIX C VOLUMETRIC MIX DESIGN

## C.1 SMA Volumetric Mix Design

### C.1.1 Verification of JMF (Control, ST)

Traprock served as a control in SMA mixtures and was initially utilized in mix design verification with identical aggregates, specific proportions, combined gradation, and binder content as outlined in the JMF. However, verification results revealed a notable deviation from the data in the JMF.

The properties of the sampled aggregates such as specific gravity and absorption between the tested data of traprock and other aggregates were compared to the data provided in the JMF, as shown in Table C.1. For the three traprock stockpiles, the average absorption ratios measured at around 0.67%, which is 2.5 times greater than those listed in the JMF, at around 0.27%. Additionally, the average specific gravities measured from the three traprock stockpiles were 0.06 lower compared to the values provided in the JMF. Similarly, for the three stockpiles, the average absorption ratios, measured at around 4.3%, were 1.7 times greater than those in the JMF, at around 2.6%. The average specific gravities measured were lower compared to the values listed in the JMF. Such variations could potentially lead to the failure of the volumetric parameter *VMA* to meet the 17% limit. The comparison of volumetric parameters between testing results and JMF is illustrated in Table C.2. Therefore, the ST was redesigned to meet the volumetric requirements of AASHTO M 325.

**Table C.1 Aggregate Properties Comparison between Testing Results and JMF**

| Aggregates | Stockpiles | Absorption | | Bulk Specific Gravity | |
|---|---|---|---|---|---|
| | | Test Data | JMF | Test Data | JMF |
| | | % | % | - | - |
| Traprock | 1/2''M | 0.7 | 0.3 | 2.585 | 2.645 |
| | 1/2'' | 0.7 | 0.2 | 2.591 | 2.628 |
| | 3/8''#4 | 0.6 | 0.3 | 2.594 | 2.629 |
| Remaining Aggregates in JMF | 1/2''C | 4.1 | 2.6 | 2.517 | 2.573 |
| | 3/8''C | 4.3 | 2.4 | 2.508 | 2.57 |
| | 3/8''M | 4.5 | 2.8 | 2.476 | 2.531 |

**Table C.2 Volumetric Parameters Comparison Between Testing Results and JMF**

| Volumetric Parameters | JMF | Test Data |
|---|---|---|
| $G_{mb}$ | 2.299 | 2.276 |
| $G_{sb}$ | 2.606 | 2.557 |
| $P_{s,}$ % | 93.5 | 93.5 |
| $G_{ca}$, % | N/A | 2.552 |
| $P_b$, % | 6.2 | 6.2 |
| PCA, % | 68.1 | 67.2 |
| $G_{mm}$ | 2.394 | 2.423 |
| VMA, ≥17% | 17.3 | 16.8 |
| $VCA_{mix}$, % | 39.8 | 40.1 |
| $P_a$ , % | 4.0 | 6.1 |

N/A: Data is not provided in the JMF

### C.1.2 Volumetric Mix Design for ST

To meet the volumetric design criteria, the coarse aggregate proportion was increased from the original JMF portion given the low measured *VMA* during mix design verification. An asphalt content of 6.5% for the trial mixtures was determined based on the bulk specific gravity of coarse aggregate ($G_{ca}$) following AASHTO R 46.

Figure C.1 and Table C.3 display the gradations and volumetric parameters of ST mixtures from the three trial designs, all exceeding the required 17% *VMA* in AASHTO M 325. Considering potential VMA reduction for other candidate aggregates, Design 3, with *VMA* close to 17%, was deemed less favorable than the other two trial designs. Design 1, with a lower proportion of coarse aggregate, was preferred over Design 2, despite comparable *VMA*. Design 1, with $VCA_{DRC}$ of 41.54% exceeding $VCA_{mix}$ of 37.3%, was chosen as the desired gradation. Finally, Design 1 with 7.5% binder content was selected as the optimal design for ST after measuring the volumetric parameters for the optimum Design 1 with varying binder contents.

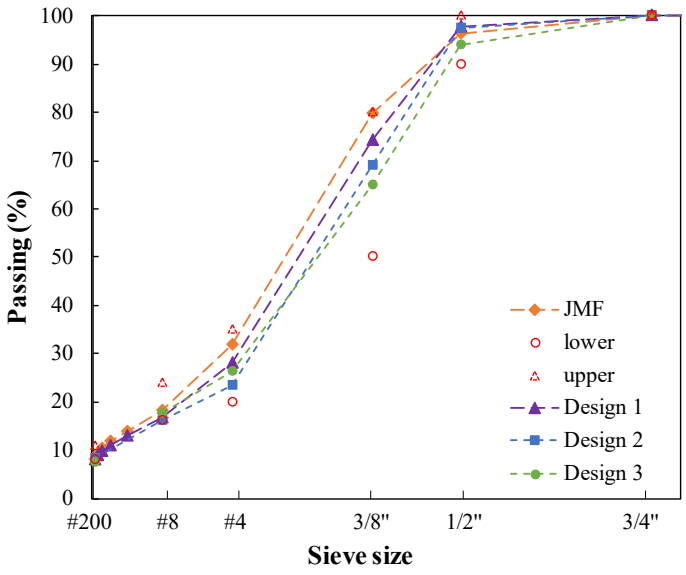


**Figure C.1 Trial gradations for ST.**

**Table C.3 Volumetric Parameters of Trial Mixtures for ST**

| Volumetric Parameters | Design 1 | Design 2 | Design 3 |
|---|---|---|---|
| $G_{mb}$ | 2.236 | 2.223 | 2.270 |
| $G_{sb}$ | 2.579 | 2.571 | 2.557 |
| $P_s$, % | 93.2 | 93.2 | 93.2 |
| $P_b$, % | 6.5 | 6.5 | 6.5 |
| $G_{ca}$, % | 2.566 | 2.558 | 2.556 |
| *PCA*, % | 71.9 | 76.6 | 79.1 |
| $G_{mm}$ | 2.404 | 2.387 | 2.400 |
| *VMA*, ≥17% | 19.2 | 19.4 | 17.2 |
| $VCA_{mix}$, % | 37.3 | 33.4 | 29.7 |
| $P_a$, % | 7.0 | 6.9 | 5.4 |

### C.1.3 Volumetric Mix Design for SS

As illustrated in Figure C.2, the gradation of the SMA mixture containing 65% steel slag initially matched that of ST. Additionally another gradation with a lower proportion of steel slag (31%) was also evaluated. This analysis helped to understand the correlation between steel slag content and relative volumetric parameters. The binder content for SS was determined to be 6.0% based on the $G_{ca}$ of the blended aggregates.

Table C.4 presents the volumetric parameters of SS mixtures from the two trial designs, both surpassing the required 17% *VMA* in accordance with AASHTO M 325. Design 1, exhibiting a

higher *VMA* and $VCA_{DRC}$ of 45.82% exceeding $VCA_{mix}$ of 34.5%, was preferred over Design 2. Design 1, with 6.5% binder content, was selected as the optimal mix design for SS after comparing the volumetric parameters for the optimal gradation with varying binder contents.

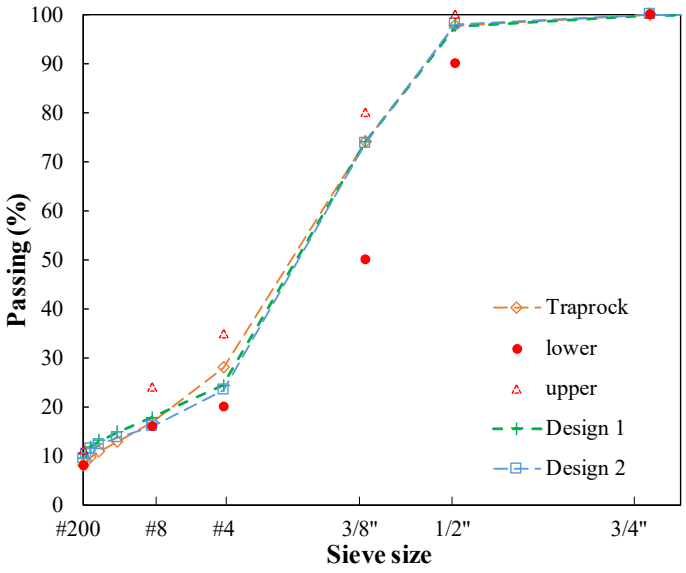


**Figure C.2 Trial gradations for SS.**

**Table C.4 Volumetric Parameters of Trial Mixtures for SS**

| Volumetric Parameters | Design 1 | Design 2 |
|---|---|---|
| $G_{mb}$ | 2.641 | 2.448 |
| $G_{sb}$ | 3.027 | 2.768 |
| $P_{s,}$ %` | 93.7 | 93.7 |
| $P_b$, % | 6.0 | 6.0 |
| $G_{ca}$, % | 3.048 | 2.769 |
| *PCA, %* | 75.6 | 76.7 |
| $G_{mm}$ | 2.801 | 2.558 |
| *VMA, ≥17%* | 18.2 | 17.1 |
| $VCA_{mix}$, % | 34.5 | 32.2 |
| $P_a$, % | 5.7 | 4.3 |

### C.1.4 Volumetric Mix Design for SG

As depicted in the Figure C.3, the gradation of the SG mixtures initially aligned with that of ST. The binder content was 6.6%, determined based on the $G_{ca}$ of the blended aggregates. Table C.5 presents volumetric parameters for SG mixtures across various designs. The *VMA* was 20.4% while the air voids of the sample measured 8.6%. Although the *VMA* exceeds the

specified limit of 17%, the air voids are too high to reach the target value of 4% by adjusting the binder content within a reasonable range.

To reduce air voids, Design 2 incorporated more fine aggregates and fewer coarse aggregates. However, altering the coarse aggregate percentage from 69.9% to 65.9%, which was close to the minimum limit of 65%, did not yield the desired outcome.

After multiple mix design trials, the research team discovered that the percentage of aggregate retained on or passing the #8 sieve significantly influences *VMA* when the total amount of fine aggregate remains constant. As shown in Table C.5, the total amount of coarse aggregates remained consistent from Design 3 to Design 6, with the crucial factor being the #8 sieve. The relationship between the percentage remaining on the #8 sieve and the *VMA* of the sample, compacted under the design gyrations, is illustrated in Figure C.4. Linear relationships highlight the efficacy of the #8 sieve in adjusting *VMA* of the SMA sample. Ultimately, Design 6 achieved a qualified *VMA* of 17.9% and $VCA_{DRC}$ of 42.36% exceeding $VCA_{mix}$ of 41.8%, and an air voids value of 3.9% with a 7.5% binder content.

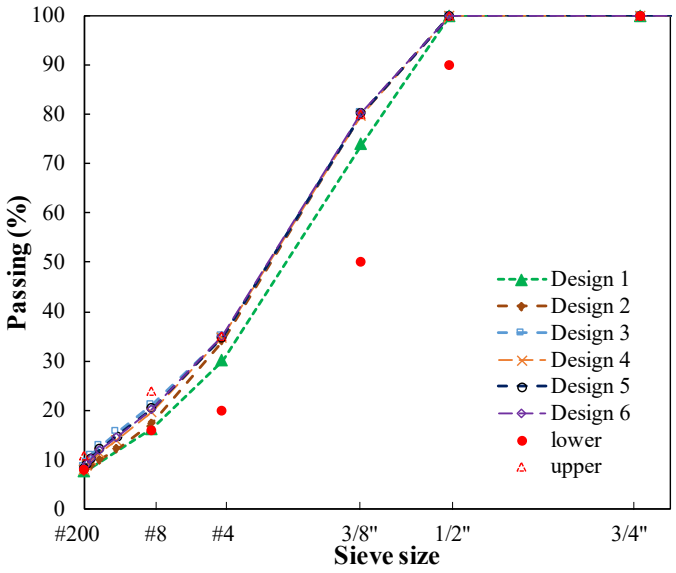


**Figure C.3 Trial gradations for SG.**

**Table C.5 Volumetric Parameters of Trial Mixtures for SG**

| Volumetric Parameters | Design 1 | Design 2 | Design 3 | Design 4 | Design 5 | Design 6 |
|---|---|---|---|---|---|---|
| $G_{mb}$ | 2.127 | 2.129 | 2.262 | 2.189 | 2.250 | 2.219 |
| $G_{sb}$ | 2.489 | 2.489 | 2.494 | 2.491 | 2.491 | 2.490 |
| $P_{s,}$ % | 93.1 | 93.1 | 93.1 | 92.2 | 92.2 | 92.2 |
| $P_b$, % | 6.6 | 6.6 | 6.6 | 7.5 | 7.5 | 7.5 |
| $G_{ca}$, % | 2.470 | 2.470 | 2.475 | 2.472 | 2.472 | 2.471 |
| PCA, % | 69.851 | 65.851 | 65.059 | 65.177 | 65.851 | 64.858 |
| $G_{mm}$ | 2.327 | 2.325 | 2.352 | 2.301 | 2.312 | 2.310 |
| VMA, ≥17% | 20.4 | 20.4 | 15.6 | 19.0 | 16.7 | 17.9 |
| $VCA_{mix}$, % | 39.835 | 43.219 | 40.527 | 42.288 | 40.053 | 41.760 |
| $P_a$, % | 8.6 | 8.4 | 3.8 | 4.9 | 2.7 | 3.9 |

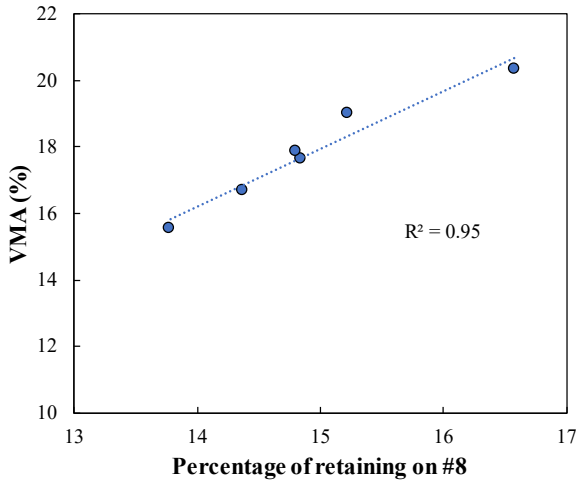


**Figure C.4 The percent of retaining on the #8 sieve vs. *VMA*.**

## C.1.5 Volumetric Mix Design for SL

Figure C.5 and Tables C.6 and C.7 illustrate 13 different designs conducted for SMA mixtures with limestone alone. The Bailey method was employed to ascertain a qualified gradation, yet none of the designs met the *VMA* requirement. Subsequently, to resolve the issue, the research team created new stockpiles by blending limestone with chat, which exhibited relatively fine gradation and excellent durability during the screening tests.

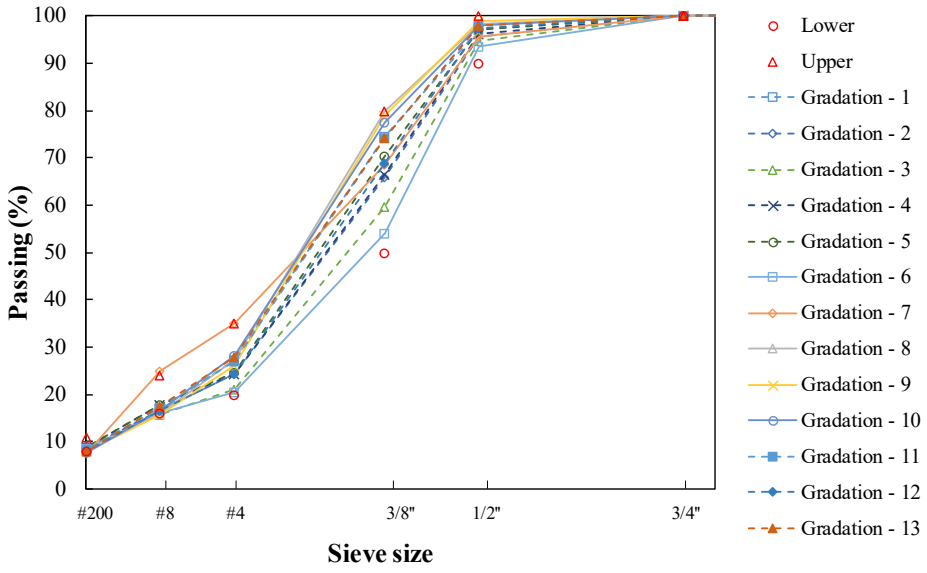


**Figure C.5 Trial gradations for SL.**

**Table C.6 Volumetric Parameters of Trial Mixtures for SL (Designs 1-7)**

| Volumetric Parameters | Design 1 | Design 2 | Design 3 | Design 4 | Design 5 | Design 6 | Design 7 |
|---|---|---|---|---|---|---|---|
| $G_{mb}$ | 2.374 | 2.366 | 2.376 | 2.353 | 2.373 | 2.366 | 2.373 |
| $G_{sb}$ | 2.599 | 2.599 | 2.596 | 2.595 | 2.581 | 2.570 | 2.610 |
| $P_s$, % | 93.2 | 92.7 | 93.7 | 93.7 | 93.7 | 93.7 | 93.7 |
| $P_b$, % | 6.8 | 7.3 | 6.3 | 6.3 | 6.3 | 6.3 | 6.3 |
| $G_{mm}$ | 2.408 | 2.384 | 2.435 | 2.428 | 2.424 | 2.414 | 2.424 |
| VMA, ≥17% | 14.9 | 15.6 | 14.2 | 15.0 | 13.8 | 13.8 | 14.8 |
| $P_a$, % | 1.4 | 0.8 | 2.4 | 3.1 | 2.1 | 2.0 | 2.1 |

**Table C.7 Volumetric Parameters of Trial Mixtures for SL (Designs 8-13)**

| Volumetric Parameters | Design 8 | Design 9 | Design 10 | Design 11 | Design 12 | Design 13 |
|---|---|---|---|---|---|---|
| $G_{mb}$ | 2.420 | 2.342 | 2.309 | 2.305 | 2.322 | 2.306 |
| $G_{sb}$ | 2.586 | 2.574 | 2.569 | 2.568 | 2.588 | 2.585 |
| $P_s$, % | 93.7 | 93.7 | 93.7 | 93.7 | 93.7 | 93.7 |
| $P_b$, % | 6.3 | 6.3 | 6.3 | 6.3 | 6.3 | 6.3 |
| $G_{mm}$ | 2.435 | 2.421 | 2.409 | 2.410 | 2.407 | 2.405 |
| VMA, ≥17% | 12.3 | 14.7 | 15.8 | 15.9 | 15.9 | 16.4 |
| $P_a$, % | 0.6 | 3.2 | 4.2 | 4.4 | 3.5 | 4.1 |

### C.1.6 Volumetric Mix Design for SLC

To design a durable mixture with limestone, the sampled chat, with a NMAS of #4—smaller than other candidate aggregates—was introduced as a candidate aggregate in this research. The blending of chat with limestone was then evaluated as a new candidate aggregate.

Figure C.6 displays the gradation of mix designs for SLC. Drawing on experience from the gravel, Design 1 for SLC commenced with the same gradation as gravel, incorporating an additional gradation with a different passing ratio on the #8 sieve. The determined binder content for both designs was 7.0%, based on the $G_{ca}$ of the blended aggregates. Table C.8 reveals that both designs met the VMA requirements and exhibited reasonable air voids in the samples. However, in comparison to Design 1, Design 2 had a lower air void, closer to the target of 4%, making it the preferred optimum design.

Subsequently, the $VCA_{DRC}$ was measured at 42%, exceeding the $VCA_{mix}$ of 41.6%. Consequently, the optimum binder content was adjusted to 7.4% using Design 2 to achieve the desired air voids of 3.9%.

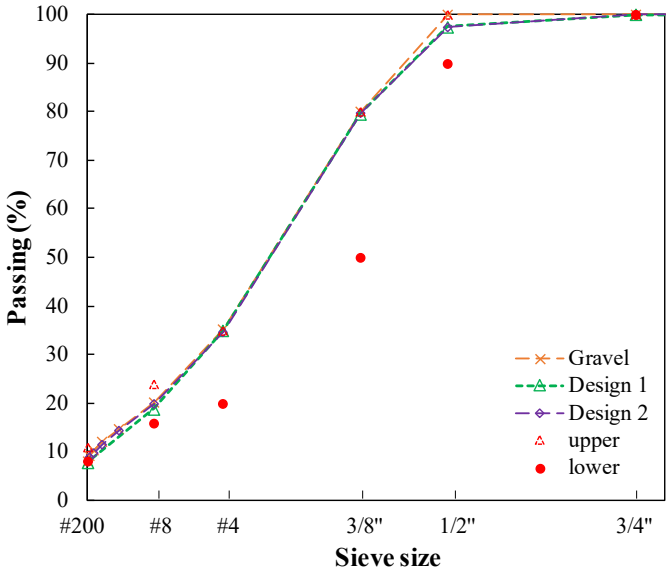


**Figure C.6 Trial gradations for SLC.**

**Table C.8 Volumetric Parameters of Trial Mixtures for SLC**

| Volumetric Parameters | Design 1 | Design 2 |
|---|---|---|
| $G_{mb}$ | 2.236 | 2.275 |
| $G_{sb}$ | 2.564 | 2.563 |
| $P_{s,}$ % | 92.7 | 92.7 |
| $P_b$, % | 7.0 | 7.0 |
| $G_{ca}$, % | 2.550 | 2.549 |
| PCA, % | 65.0 | 65.4 |
| $G_{mm}$ | 2.371 | 2.390 |
| VMA, ≥17% | 19.2 | 17.7 |
| $VCA_{mix}$, % | 43.0 | 41.6 |
| $P_a$, % | 5.7 | 4.8 |

### C.1.7 Volumetric Mix Design for SD

Mix Designs 1 and 2 utilized dolomite exclusively, with the trial gradations referencing the optimum gradation of SMA mixtures using traprock and gravel respectively. An additional gradation with a higher proportion of coarse aggregate was evaluated at the same time, drawing insights from the results of designing SL. The binder content for the trial designs featuring the new candidate aggregate was determined to be 6.4%. Figure C.7 displays all gradations, while Table C.9 presents the calculated volumetric parameters for the mix designs.

Despite Design 3 having a relatively high percentage of coarse aggregates, the *VMA* began around 13%, significantly below the 17% threshold, reminiscent of the situation with limestone. Subsequently, as the solution used for SL, the researchers created new stockpiles by blending dolomite with chat.

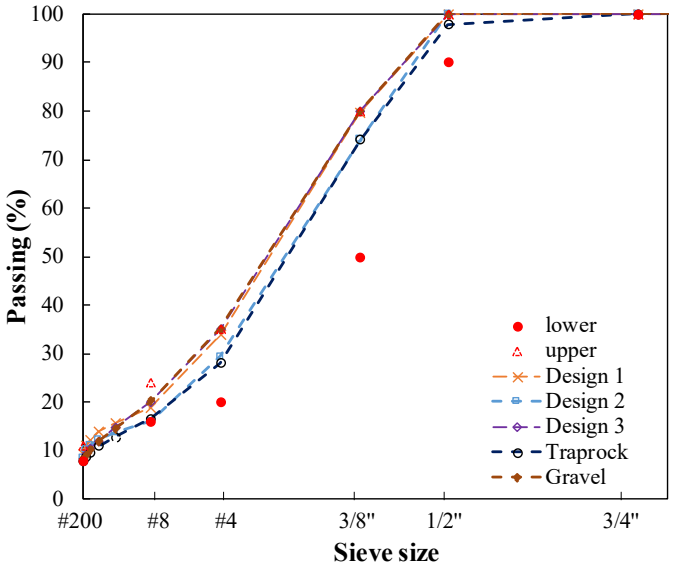


**Figure C.7 Trial gradations for SD.**

**Table C.9 Volumetric Parameters of Trial Mixtures for SD**

| Volumetric Parameters | Design 1 | Design 2 | Design 3 |
|---|---|---|---|
| $G_{mb}$ | 2.373 | 2.348 | 2.357 |
| $G_{sb}$ | 2.543 | 2.549 | 2.563 |
| $P_s$, % | 92.7 | 93.3 | 93.3 |
| $P_b$, % | 7 | 6.4 | 6.4 |
| $G_{ca}$, % | 2.530 | 2.539 | 2.551 |
| PCA, % | 66.0 | 70.7 | 74.1 |
| $G_{mm}$ | 2.391 | 2.409 | 2.397 |
| VMA, ≥17% | 13.5 | 14.1 | 14.2 |
| $VCA_{mix}$, % | 38.1 | 34.6 | 31.6 |
| $P_a$, % | 0.8 | 2.5 | 1.7 |

### C.1.8 Volumetric Mix Design for SDC

Drawing from experience in SL, mix design for dolomite introduced blending with chat as a new candidate aggregate, still referencing the gradation of SLC. As shown in Figure C.8, Design 1 met all volumetric parameter requirements, indicating that blending with another qualified candidate aggregate, such as chat, can enhance the usability of the relatively weak aggregate.

Nevertheless, the gradation of Design 1 approached the upper limits stipulated by standards. Considering the MODOT specification, a 2% tolerance on gradation, both upper and lower limits, was considered in the mix design to accommodate errors during construction. Designs 2

to 5 were subsequently conducted, and the gradations are shown in Figure C.8. The key factor was the adjustment of passing or remaining aggregate particles on the #8 sieve.

Figure C.10 presents the calculated volumetric parameters for the mix designs. Ultimately, Design 5 emerged as the optimum gradation, meeting all requirements for volumetric parameters, and achieving reasonable air voids. The optimal binder content was determined to be 6.9% for SDC.

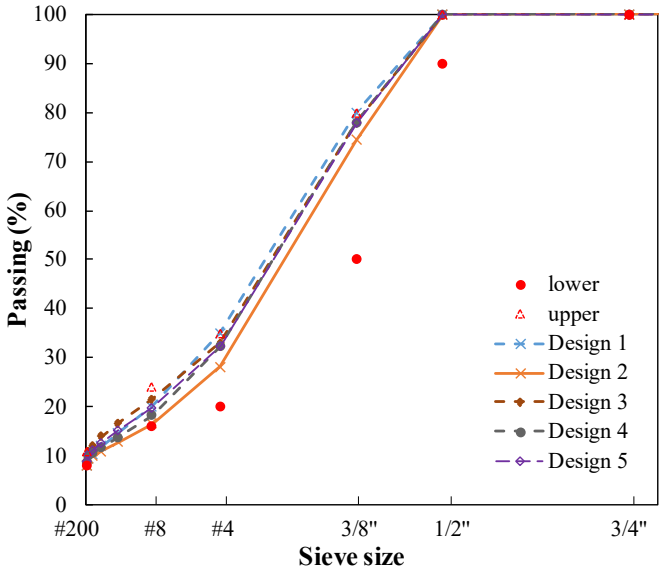


**Figure C.8 Trial gradations for SDC.**

**Table C.10 Volumetric Parameters of Trial Mixtures for SDC**

| Volumetric Parameters | Design 1 | Design 2 | Design 3 | Design 4 | Design 5 |
|---|---|---|---|---|---|
| $G_{mb}$ | 2.266 | 2.174 | 2.299 | 2.196 | 2.248 |
| $G_{sb}$ | 2.546 | 2.554 | 2.551 | 2.551 | 2.550 |
| $P_s$, % | 93.3 | 93.3 | 93.3 | 93.3 | 93.3 |
| $P_b$, % | 6.4 | 6.4 | 6.4 | 6.4 | 6.4 |
| $G_{ca}$, % | 2.533 | 2.542 | 2.536 | 2.536 | 2.535 |
| PCA, % | 65.0 | 71.8 | 67.0 | 67.7 | 67.7 |
| $G_{mm}$ | 2.386 | 2.381 | 2.389 | 2.381 | 2.386 |
| VMA, ≥17% | 17.0 | 20.6 | 15.9 | 19.7 | 17.8 |
| $VCA_{mix}$, % | 41.8 | 38.6 | 39.2 | 41.4 | 40.0 |
| $P_a$, % | 5.0 | 8.7 | 3.7 | 7.8 | 5.8 |

### C.1.9 SMA Final Volumetric Mix Design

For each SMA mixture, the coarse aggregate traprock was replaced with other candidate aggregates, while the proportions of the remaining components in the JMF varied. The final gradations and volumetric parameters required in the standards for the SMA mixtures with candidate aggregates are presented in Figure C.9 and Table C.11. Ultimately, all mixtures with candidate aggregates met the 17% limit of *VMA* and 4% air voids under design gyrations (100). Furthermore, the $VCA_{mix}$ of all SMA mixtures was lower than $VCA_{DRC}$, indicating effective contact among coarse aggregates and the formation of an aggregate skeleton in the SMA mixtures.

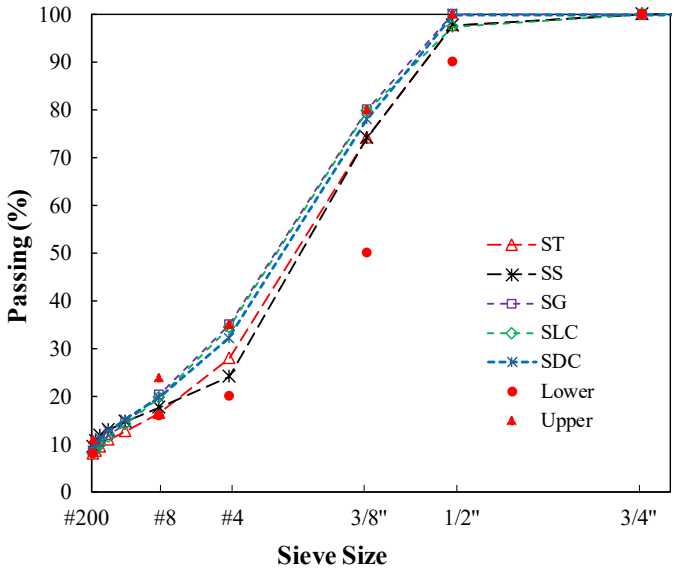


**Figure C.9 Final gradation of SMA mixtures.**

**Table C.11 Volumetric Parameters of SMA Mixtures**

| Volumetric Parameters | ST | SS | SG | SLC | SDC |
|---|---|---|---|---|---|
| $G_{mb}$ | 2.261 | 2.656 | 2.219 | 2.274 | 2.282 |
| $G_{sb}$ | 2.579 | 3.027 | 2.49 | 2.563 | 2.55 |
| $P_{s,}$ % | 92.2 | 93.2 | 92.2 | 92.3 | 92.8 |
| $G_{ca}$, % | 2.566 | 3.048 | 2.471 | 2.549 | 2.535 |
| $P_b$, % | 7.5 | 6.5 | 7.4 | 7.4 | 6.9 |
| *PCA, %* | 71.9 | 75.6 | 64.9 | 65.4 | 67.7 |
| $G_{mm}$ | 2.362 | 2.764 | 2.310 | 2.367 | 2.371 |
| *VMA, ≥17%* | 19.1 | 18.2 | 17.9 | 18.1 | 17.0 |
| $VCA_{mix}$, % | 37.3 | 34.5 | 41.8 | 41.6 | 39.1 |
| $VCA_{DRC}$, % | 41.5 | 45.8 | 42.3 | 42.0 | 42.3 |

As depicted in Figure C.10(a), the draindown percentage for SMA mixtures ranged between 0.14% and 0.21%, well within the limit of 0.3%. Figure C.10(b) indicates that the TSR values spanned from 0.83 to 0.96, all exceeding the minimum requirement of 0.8. Except for SDC, the SMA mixtures with other candidate aggregates demonstrated moisture resistance comparable to the control mixture ST.

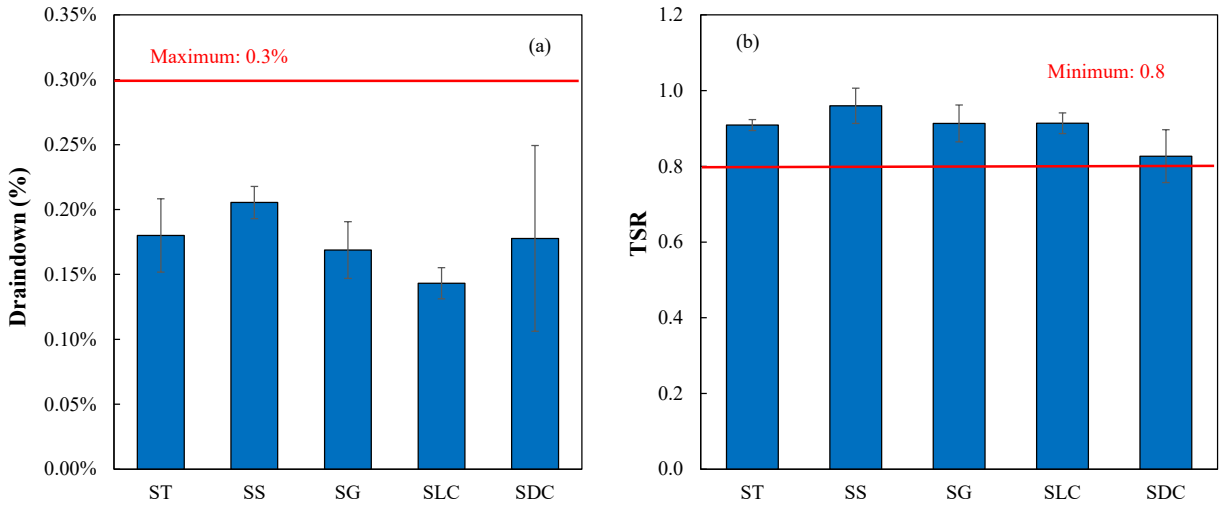


**Figure C.10 Performance test results of SMA mixtures with all candidate aggregates: (a) draindown, and (b) moisture susceptibility.**

## C.2 HMA Volumetric Mix Design

### C.2.1 Verification of JMF (HLC)

Limestone & chat (Blend H1) served as the control in HMA mixtures and underwent initial mix design verification using identical aggregates, specific proportions, combined gradation, and binder content outlined in the JMF. Figure C.11 displays both gradations while Table C.12 presents the calculated volumetric parameters for the verification. The results for HLC closely matched the JMF data, with all volumetric parameters meeting the limits required in AASHTO R 35.

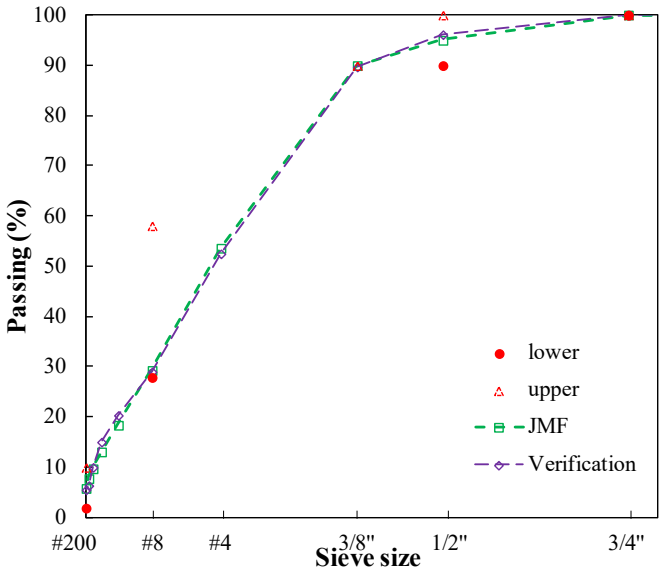


**Figure C.11 Verification of gradation for HLC.**

**Table C.12 Verification of Volumetric Parameters of HLC**

| Volumetric Parameters | JMF | Verification HLC |
|---|---|---|
| $G_{mb}$ | 2.310 | 2.332 |
| $G_{sb}$ | 2.556 | 2.557 |
| $P_s$, % | 94.2 | 94.2 |
| $P_b$, % | 5.8 | 5.8 |
| $G_{mm}$ | 2.407 | 2.419 |
| *VMA, ≥14%* | 14.87 | 14.09 |
| $V_a$, % | 4.03 | 3.59 |
| *VFA, 65%-75%* | 72.9 | 74.5 |
| $G_{se}$ | 2.623 | 2.638 |
| $P_{0.075}$, % | 5.70 | 5.40 |
| $P_{ba}$, % | 1.03 | 1.23 |
| $P_{be}$, % | 4.8 | 4.6 |
| Dust-to-Binder Ratio, *0.8-1.6* | 1.18 | 1.16 |

### C.2.2 Volumetric Mix Design for HS

As depicted in Figure C.12, initially, the gradation of the HMA mixture containing 33% steel slag aligned closely with that of HLC. Table C.13 lists the volumetric parameters of HS from the initial design phase. The *VMA* started at 13.85%, slightly below the 14% threshold. Subsequently, adjustments to the percent remaining on #8 sieve were made to Design 2 for HS. The resulting gradation and volumetric parameters are presented in Figure C.12 and Table C.13 accordingly.

The percent remaining on #8 sieve increased from 25.5% to 23.0%, leading to a significant elevation in *VMA* values to 14.55%, surpassing the specified requirement. All volumetric parameters met the specified limits in AASHTO R 35. The optimum binder content of 5.4% was determined following a comparative examination of volumetric parameters across different binder contents.

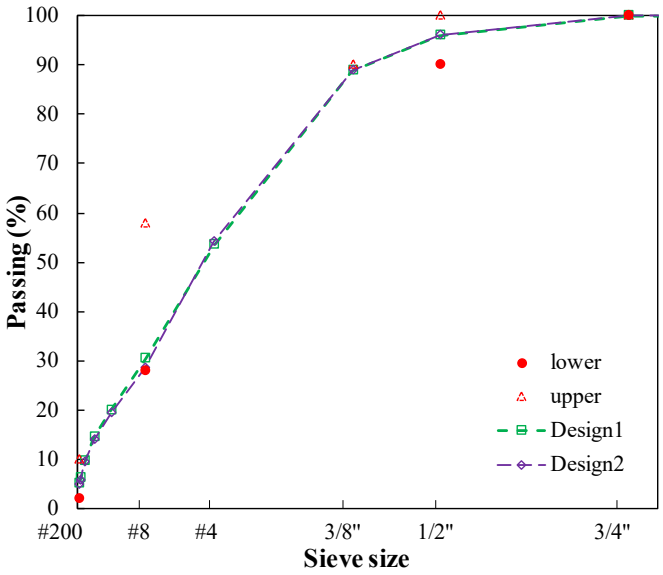


**Figure C.12 Trial gradations for HS.**

**Table C.13 Volumetric Parameters of Trial Mixtures for HS**

| Volumetric Parameters | Design 1 | Design 2 |
|---|---|---|
| $G_{mb}$ | 2.574 | 2.552 |
| $G_{sb}$ | 2.814 | 2.814 |
| $P_s$, % | 94.2 | 94.2 |
| $P_b$, % | 5.8 | 5.8 |
| $G_{mm}$ | 2.611 | 2.631 |
| *VMA, ≥14%* | 13.85 | 14.55 |
| $V_a$, % | 1.44 | 2.98 |
| *VFA, 65%-75%* | 89.6 | 79.5 |
| $G_{se}$ | 2.884 | 2.909 |
| $P_{0.075}$, % | 5.20 | 4.90 |
| $P_{ba}$, % | 0.89 | 1.20 |
| $P_{be}$, % | 5.0 | 4.7 |
| Dust-to-Binder Ratio, *0.8-1.6* | 1.05 | 1.05 |

### C.2.3 Volumetric Mix Design for HG

As illustrated in Figure C.13, initially, the gradation of the HMA mixture containing 38% gravel closely mirrored that of HLC. Table C.14 outlines the calculated volumetric parameters for HG Design 1. All volumetric parameters met the specified limits in AASHTO R 35. The optimum binder content of 6.4% was determined following a comparative examination of volumetric parameters across different binder contents for the optimal gradation.

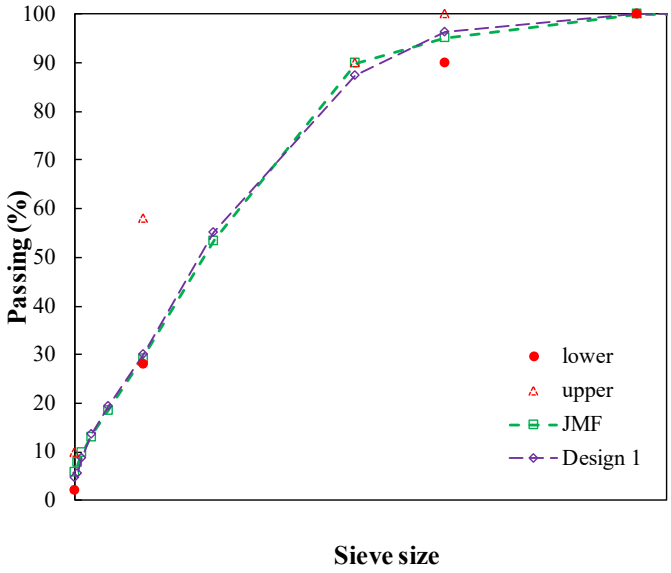


**Figure C.13 Trial gradation for HG.**

**Table C.14 Volumetric Parameters of Trial Mixture for HG**

| Volumetric Parameters | Design 1 |
|---|---|
| $G_{mb}$ | 2.266 |
| $G_{sb}$ | 2.528 |
| $P_{s,}$ % | 94.2 |
| $P_b$, % | 5.8 |
| $G_{mm}$ | 2.390 |
| *VMA, ≥14%* | 15.56 |
| $V_a$, % | 5.19 |
| *VFA, 65%-75%* | 66.7 |
| $G_{se}$ | 2.602 |
| $P_{0.075}$, % | 5.40 |
| $P_{ba}$, % | 1.15 |
| $P_{be}$, % | 4.7 |
| Dust-to-Binder Ratio, *0.8-1.6* | 1.15 |

### C.2.4 Volumetric Mix Design for HL

Initially, the gradation of HL closely paralleled that of HLC by substituting the chat with limestone in HLC. Table C.15 exhibits the volumetric parameters of HL from the initial design phase. The VMA commenced at 13.11%, falling below the 14% threshold. Consequently, adjustments to the percentage remaining on #8 sieve were implemented in Design 2 for HL. The resulting gradation and volumetric parameters are depicted in Figure C.14 and Table C.15 respectively. The percentage remaining on #8 sieve increased from 25.6% to 22.3%. However, there was no change observed in the VMA, reminiscent of the situation with limestone used in SMA. Therefore, the limestone was recognized as challenging to use alone in both SMA and HMA mixtures.

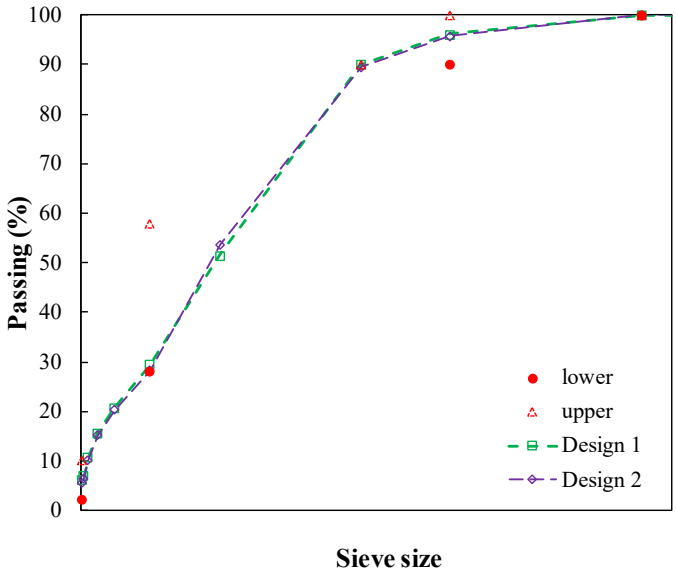


**Figure C.14 Trial gradations for HL.**

**Table C.15 Volumetric Parameters of Trial Mixtures for HL**

| Volumetric Parameters | Design 1 | Design 2 |
|---|---|---|
| $G_{mb}$ | 2.385 | 2.384 |
| $G_{sb}$ | 2.58526 | 2.586 |
| $P_{s,}$ % | 94.2 | 94.2 |
| $P_b$, % | 5.8 | 5.8 |
| $G_{mm}$ | 2.433 | 2.443 |
| *VMA, ≥14%* | 13.11 | 13.13 |
| $V_a$, % | 1.99 | 2.38 |
| *VFA, 65%-75%* | 84.8 | 81.9 |
| $G_{se}$ | 2.656 | 2.428 |
| $P_{0.075}$, % | 5.40 | 5.40 |
| $P_{ba}$, % | 1.06 | 0.00 |
| $P_{be}$, % | 4.8 | 5.8 |
| Dust-to-Binder Ratio, *0.8-1.6* | 1.12 | 0.93 |

## C.2.5 Volumetric Mix Design for HD

As illustrated in Figure C.15, initially, the gradation of the HMA mixture containing 33% dolomite closely matched that of HLC. Table C.16 displays the volumetric parameters of HS from the initial design phase. The VMA began at 12.46%, notably below the 14% threshold. Dolomite was then deemed challenging to be used alone, similar to limestone. Drawing from past experiences with SMA and HMA designs, the new stockpiles by blending dolomite with chat was employed.

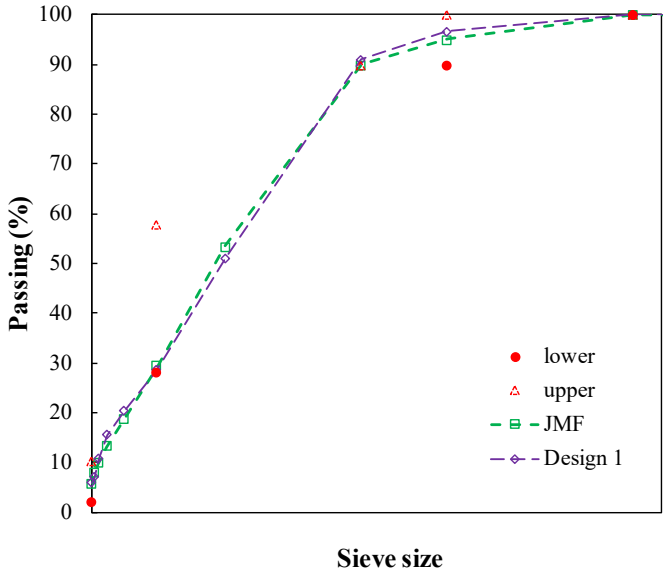


**Figure C.15 Trial gradation for HD.**

**Table C.16 Volumetric Parameters of Trial Mixture for HD**

| Volumetric Parameters | Design 1 |
|---|---|
| $G_{mb}$ | 2.372 |
| $G_{sb}$ | 2.552 |
| $P_{s,}$ % | 94.2 |
| $P_b$, % | 5.8 |
| $G_{mm}$ | 2.430 |
| *VMA, ≥14%* | 12.46 |
| $V_a$, % | 2.40 |
| *VFA, 65%-75%* | 80.7 |
| $G_{se}$ | 2.652 |
| $P_{0.075}$, % | 6.00 |
| $P_{ba}$, % | 1.52 |
| $P_{be}$, % | 4.4 |
| **Dust-to-Binder Ratio**, *0.8-1.6* | 1.4 |

## C.2.6 Volumetric Mix Design for HDC

Drawing from experience in SMA, mix design for dolomite introduced blending with chat as a new candidate aggregate, still referencing the gradation of HLC. As indicated in Figure C.16, the VMA rose from 12.5 to 14.5 through the substitution of some dolomite with chat. Design 1 fulfilled all volumetric parameter criteria as shown in Table C.17, demonstrating that blending with another qualified candidate aggregate, like chat, could improve the suitability of the relatively weak aggregate.

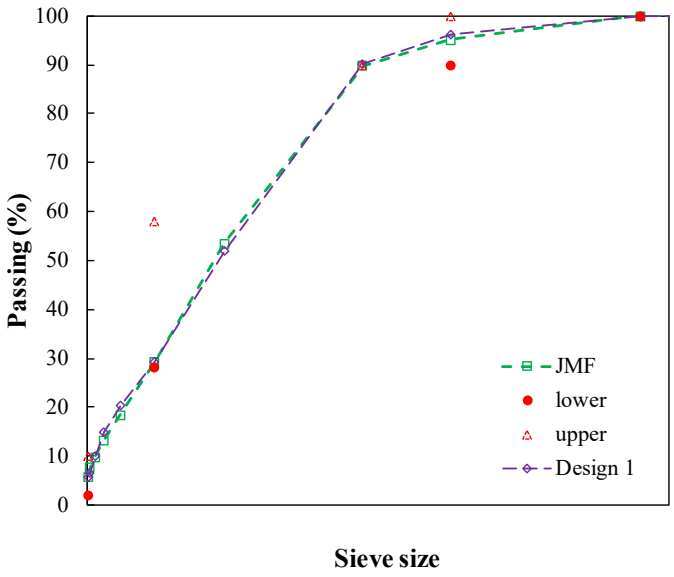


**Figure C.16 Trial gradation for HDC.**

**Table C.17 Volumetric Parameters of Trial Mixture for HDC**

| Volumetric Parameters | Design 1 |
|---|---|
| $G_{mb}$ | 2.323 |
| $G_{sb}$ | 2.560 |
| $P_{s,}$ % | 94.2 |
| $P_b$, % | 5.8 |
| $G_{mm}$ | 2.419 |
| *VMA, ≥14%* | 14.5 |
| $V_a$, % | 4.0 |
| *VFA, 65%-75%* | 72.6 |
| $G_{se}$ | 2.638 |
| $P_{0.075}$, % | 5.7 |
| $P_{ba}$, % | 1.19 |
| $P_{be}$, % | 4.68 |
| Dust-to-Binder Ratio ,*0.8-1.6* | 1.18 |

## C.2.7 HMA Final Volumetric Mix Design

For each HMA mixture, the combination of limestone & chat was replaced with other candidate aggregates, while the proportions of the remaining components in the JMF varied. The final gradations and volumetric parameters required in the standards for HMA mixtures with candidate aggregates are presented in Figure C.17 and Table C.18. Ultimately, all mixtures incorporating the updated candidate aggregates fulfilled the specified criteria, including

maintaining a *VMA* limit of 14%, falling within the range of 65% to 75% for *VFA*, maintaining a dust-to-binder ratio between 0.8 and 1.6, and achieving 4% air voids under design gyrations (125).

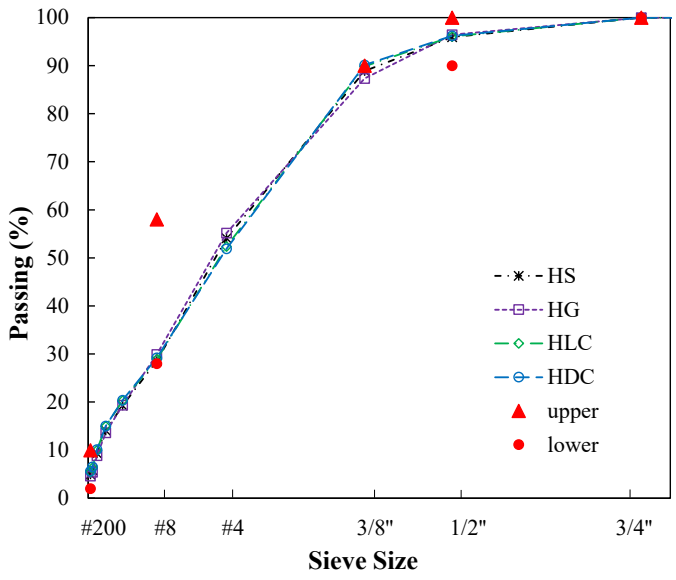


**Figure C.17 Final gradation of HMA mixtures.**

**Table C.18 Volumetric Parameters of HMA Mixtures**

| Volumetric Parameters | HS | HG | HLC | HDC |
|---|---|---|---|---|
| $G_{mb}$ | 2.540 | 2.276 | 2.332 | 2.323 |
| $G_{sb}$ | 2.814 | 2.528 | 2.557 | 2.560 |
| $P_s$, % | 94.6 | 93.7 | 94.2 | 94.2 |
| $P_b$, % | 5.3 | 6.4 | 5.8 | 5.8 |
| $G_{mm}$ | 2.633 | 2.378 | 2.419 | 2.419 |
| *VMA, ≥14%* | 14.6 | 15.6 | 14.1 | 14.5 |
| $V_a$, % | 3.9 | 4.2 | 3.8 | 4.0 |
| *VFA, 65%-75%* | 74.8 | 72.7 | 74.5 | 72.6 |
| $G_{se}$ | 2.890 | 2.607 | 2.638 | 2.638 |
| $P_{0.075}$, % | 4.9 | 5.4 | 5.4 | 5.7 |
| $P_{ba}$, % | 0.96 | 1.23 | 1.23 | 1.19 |
| $P_{be}$, % | 4.49 | 5.15 | 4.64 | 4.68 |
| Dust-to-Binder Ratio, *0.8-1.6* | 1.09 | 1.05 | 1.16 | 1.18 |

After obtaining the qualified volumetric parameters, the moisture susceptibility of HMA mixtures was evaluated. As shown in Figure C.18, the TSR values were determined as 0.96, 0.92, 0.95, and 0.89 for HS, HG, HLC, and HDC, respectively. All test results exceeded the TSR requirement of 0.8. Except HDC, HMA mixtures with other candidate aggregates exhibited moisture resistance comparable to the control mixture HLC.

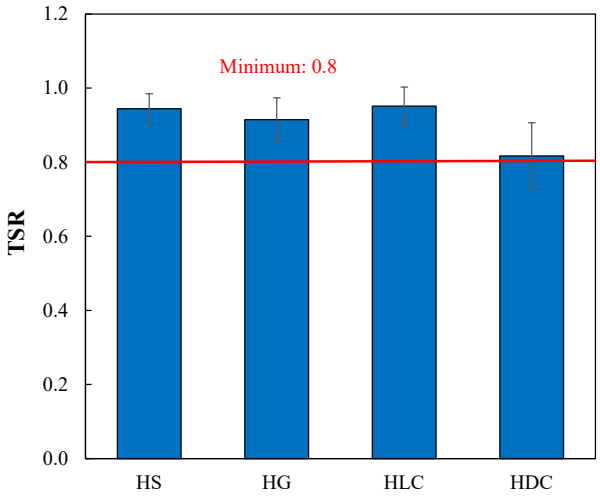


**Figure C.18 Moisture susceptibility results of HMA mixtures.**

# APPENDIX D AMPT DATA QUALITY

**Table D.1 AMPT Dynamic Modulus Data Quality_Dynamic Modulus $|E^*|$**

| Sample ID | Temp. | \|E*\|_ Rep.1 | \|E*\|_ Rep.2 | \|E*\|_ Rep.3 | \|E*\|_ Rep.4 | Average \|E*\| | Repeatability Coefficient of Variation for \|E*\| | Limit of Sr% | Acceptable Range for 4 Specimens | |
|---|---|---|---|---|---|---|---|---|---|---|
| | ˚C | MPa | MPa | MPa | MPa | MPa | % | % | MPa | MPa |
| ST | 4.0 | 11063.0 | 9873.0 | 8894.0 | 9115.0 | 9736.3 | 4.7 | 7 | 7399.6 | 12073.0 |
| | 20.0 | 3956.0 | 3200.0 | 3070.0 | 3006.0 | 3308.0 | 6.0 | 8 | 2381.8 | 4234.2 |
| | 40.0 | 602.5 | 392.2 | 299.5 | 391.1 | 421.3 | 9.4 | 14 | 210.7 | 632.0 |
| SS | 4.0 | 12472.0 | 11876.0 | 13082.0 | 12985.0 | 12603.8 | 4.5 | 6 | 9830.9 | 15376.6 |
| | 20.0 | 4984.0 | 5008.0 | 5408.0 | 4768.0 | 5042.0 | 5.5 | 7 | 3781.5 | 6302.5 |
| | 40.0 | 721.6 | 817.6 | 969.5 | 744.3 | 813.3 | 8.2 | 12 | 471.7 | 1154.8 |
| SG | 4.0 | 10268.0 | 9968.0 | 10178.0 | 10544.0 | 10239.5 | 4.7 | 6 | 7986.8 | 12492.2 |
| | 20.0 | 3554.0 | 3543.0 | 3966.0 | 3458.0 | 3630.3 | 5.9 | 7 | 2722.7 | 4537.8 |
| | 40.0 | 414.5 | 432.6 | 454.7 | 427.2 | 432.3 | 9.4 | 14 | 216.1 | 648.4 |
| SLC | 4.0 | 10803.0 | 10122.0 | 11645.0 | 11083.0 | 10913.3 | 4.6 | 6 | 8512.3 | 13314.2 |
| | 20.0 | 3613.0 | 3439.0 | 4250.0 | 4070.0 | 3843.0 | 5.8 | 7 | 2882.3 | 4803.8 |
| | 40.0 | 441.3 | 407.6 | 584.9 | 563.3 | 499.3 | 9.1 | 14 | 249.6 | 748.9 |
| SDC | 4.0 | 10791.0 | 10060.0 | 10693.0 | 9962.0 | 10376.5 | 4.7 | 6 | 8093.7 | 12659.3 |
| | 20.0 | 3628.0 | 3361.0 | 3977.0 | 3351.0 | 3579.3 | 5.9 | 7 | 2684.4 | 4474.1 |
| | 40.0 | 596.8 | 456.1 | 647.1 | 441.3 | 535.3 | 8.9 | 12 | 310.5 | 760.2 |
| HS | 4.0 | 15458.0 | 15352.0 | 15527.0 | 14655.0 | 15248.0 | 4.3 | 6 | 11893.4 | 18602.6 |
| | 20.0 | 6867.0 | 6318.0 | 6748.0 | 6500.0 | 6608.3 | 5.1 | 7 | 4956.2 | 8260.3 |
| | 40.0 | 1705.0 | 1326.0 | 1424.0 | 1283.0 | 1434.5 | 7.2 | 10 | 918.1 | 1950.9 |

| | | | | | | | | | | |
|---|---|---|---|---|---|---|---|---|---|---|
| **HG** | 4.0 | 14276.0 | 13142.0 | 13351.0 | 13361.0 | 13532.5 | 4.4 | 6 | 10555.4 | 16509.7 |
| | 20.0 | 5765.0 | 5215.0 | 5294.0 | 5403.0 | 5419.3 | 5.4 | 7 | 4064.4 | 6774.1 |
| | 40.0 | 1100.0 | 1029.0 | 963.4 | 1056.0 | 1037.1 | 7.7 | 10 | 663.7 | 1410.5 |
| **HLC** | 4.0 | 13836.0 | 13660.0 | 14517.0 | 13412.0 | 13856.3 | 4.4 | 6 | 10807.9 | 16904.6 |
| | 20.0 | 6074.0 | 6385.0 | 6538.0 | 6242.0 | 6309.8 | 5.2 | 7 | 4732.3 | 7887.2 |
| | 40.0 | 1410.0 | 1448.0 | 1671.0 | 1467.0 | 1499.0 | 7.1 | 10 | 959.4 | 2038.6 |
| **HDC** | 4.0 | 15841.0 | 13859.0 | 13846.0 | 14236.0 | 14445.5 | 4.3 | 6 | 11267.5 | 17623.5 |
| | 20.0 | 6834.0 | 6612.0 | 5938.0 | 6488.0 | 6468.0 | 5.2 | 7 | 4851.0 | 8085.0 |
| | 40.0 | 1547.0 | 1441.0 | 1441.0 | 1253.0 | 1420.5 | 7.2 | 10 | 909.1 | 1931.9 |

**Table D.2 AMPT Dynamic Modulus Data Quality_Phase Angle δ**

| **Sample ID** | **Temp.** | **δ_Rep.1** | **δ_Rep.2** | **δ_Rep.3** | **δ_Rep.4** | **Average δ** | **Repeatability Coefficient of Variation for δ** | **Limit of Sr°** | **Acceptable Range for 4 Specimens** | |
|---|---|---|---|---|---|---|---|---|---|---|
| | °C | Degrees | Degrees | Degrees | Degrees | Degrees | % | % | Degrees | Degrees |
| **ST** | 4.0 | 12.6 | 13.8 | 14.9 | 14.4 | 13.9 | 0.7 | 0.8 | 11.1 | 16.7 |
| | 20.0 | 25.8 | 28.5 | 29.2 | 29.2 | 28.2 | 0.9 | 0.9 | 24.8 | 31.6 |
| | 40.0 | 33.9 | 35.1 | 39.3 | 37.2 | 36.4 | 1.5 | 1.6 | 32.6 | 40.2 |
| **SS** | 4.0 | 12.9 | 13.5 | 12.8 | 14.1 | 13.3 | 0.7 | 0.7 | 10.9 | 15.7 |
| | 20.0 | 25.8 | 24.9 | 24.7 | 27.4 | 25.7 | 0.8 | 0.8 | 22.9 | 28.5 |
| | 40.0 | 36.7 | 33.9 | 35.5 | 35.9 | 35.5 | 1.3 | 1.3 | 30.7 | 40.3 |
| **SG** | 4.0 | 14.6 | 14.2 | 19.1 | 13.5 | 15.4 | 0.7 | 0.7 | 13.0 | 17.8 |
| | 20.0 | 29.9 | 29.5 | 29.2 | 29.3 | 29.5 | 0.8 | 0.8 | 26.7 | 32.3 |
| | 40.0 | 39.5 | 42.5 | 41.1 | 39.6 | 40.7 | 1.5 | 1.6 | 35.0 | 46.4 |

| | | | | | | | | | | |
|---|---|---|---|---|---|---|---|---|---|---|
| **SLC** | 4.0 | 14.8 | 14.7 | 13.8 | 13.2 | 14.1 | 0.7 | 0.7 | 11.7 | 16.5 |
| | 20.0 | 29.6 | 27.7 | 27.2 | 27.2 | 27.9 | 0.8 | 0.8 | 25.1 | 30.7 |
| | 40.0 | 39.5 | 36.0 | 37.3 | 36.1 | 37.2 | 1.5 | 1.6 | 31.5 | 42.9 |
| **SDC** | 4.0 | 10.3 | 13.1 | 13.1 | 14.4 | 12.7 | 0.7 | 0.7 | 10.3 | 15.1 |
| | 20.0 | 28.1 | 30.2 | 29.3 | 29.7 | 29.3 | 0.8 | 0.8 | 26.5 | 32.1 |
| | 40.0 | 38.9 | 39.1 | 37.1 | 41.0 | 39.0 | 1.3 | 1.3 | 34.2 | 43.8 |
| **HS** | 4.0 | 10.0 | 10.4 | 10.4 | 10.0 | 10.2 | 0.7 | 0.7 | 7.8 | 12.6 |
| | 20.0 | 21.6 | 22.8 | 22.6 | 21.8 | 22.2 | 0.8 | 0.8 | 19.4 | 25.0 |
| | 40.0 | 32.5 | 34.0 | 34.2 | 33.9 | 33.6 | 1.1 | 1.1 | 29.5 | 37.7 |
| **HG** | 4.0 | 10.8 | 11.7 | 11.2 | 10.9 | 11.2 | 0.7 | 0.7 | 8.8 | 13.6 |
| | 20.0 | 23.9 | 24.9 | 24.4 | 23.9 | 24.3 | 0.9 | 0.8 | 21.5 | 27.1 |
| | 40.0 | 34.2 | 33.4 | 34.2 | 35.4 | 34.3 | 1.1 | 1.1 | 30.2 | 38.4 |
| **HLC** | 4.2 | 10.8 | 10.3 | 10.0 | 10.8 | 10.4 | 0.7 | 0.7 | 8.0 | 12.8 |
| | 20.2 | 22.2 | 21.5 | 21.5 | 21.6 | 21.7 | 0.8 | 0.8 | 18.9 | 24.5 |
| | 40.1 | 33.3 | 33.0 | 31.7 | 32.9 | 32.7 | 1.1 | 1.1 | 28.6 | 36.8 |
| **HDC** | 4.2 | 9.1 | 9.9 | 9.7 | 9.4 | 9.5 | 0.7 | 0.7 | 7.1 | 11.9 |
| | 20.2 | 20.6 | 20.4 | 22.0 | 20.6 | 20.9 | 0.8 | 0.8 | 18.1 | 23.7 |
| | 40.1 | 33.1 | 33.5 | 33.2 | 33.8 | 33.4 | 1.1 | 1.1 | 29.3 | 37.5 |